PERFORMANCE STUDY OF TREPANNING TOOL FOR DEEP ANNULAR GROOVING

Ph.D. THESIS

by

GAIKWAD SHARAD VASANTRAO

DEPARTMENT OF MECHANICAL AND INDUSTRIAL ENGINEERING
INDIAN INSTITUTE OF TECHNOLOGY ROORKEE
ROORKEE-247667 (INDIA)
SEPTEMBER, 2019

PERFORMANCE STUDY OF TREPANNING TOOL FOR DEEP ANNULAR GROOVING

A THESIS

Submitted in partial fulfillment of the requirements for the award of the degree

of

DOCTOR OF PHILOSOPHY

in

MECHANICAL ENGINEERING

by

GAIKWAD SHARAD VASANTRAO

DEPARTMENT OF MECHANICAL AND INDUSTRIAL ENGINEERING
INDIAN INSTITUTE OF TECHNOLOGY ROORKEE
ROORKEE-247667 (INDIA)
SEPTEMBER, 2019

INDIAN INSTITUTE OF TECHNOLOGY ROORKEE
ROORKEE

STUDENT'S DECLARATION

I hereby certify that the work presented in the thesis entitled "**PERFORMANCE STUDY OF TREPANNING TOOL FOR DEEP ANNULAR GROOVING**" is my own work carried out during a period from July, 2014 to September, 2019 under the supervision of Dr. Rahul S. Mulik, Associate Professor, Indian Institute of Technology Roorkee, Roorkee.

The matter presented in the thesis has not been submitted for the award of any other degree of this or any other Institute.

Dated: 16.09.2019 **(GAIKWAD SHARAD VASANTRAO)**

SUPERVISOR'S DECLARATION

This is to certify that the above mentioned work is carried out under my supervision.

Dated: 16.09.209 (Rahul S. Mulik)

Acknowledgements

The work presented in this thesis would not have been possible without my close association with many people. I take this opportunity to extend my sincere gratitude and appreciation to all those who made this Ph.D thesis possible. First and foremost, I would like to extend my sincere gratitude to my research guide *Dr. Rahul S. Mulik* for introducing me to this exciting field of research and for his dedicated help, advice, inspiration, encouragement and continuous support, throughout my Ph.D. His enthusiasm, integral view on research and his mission for providing high-quality work, has made a deep impression on me. During our course of interaction during the last five and half years, I have learnt extensively from him. I owe him lots of gratitude for having me shown this way of research. I am really glad to be associated with a person like *Dr. Rahul S. Mulik* in my life.

My special words of thanks should also go to my internal examiner *Dr. Manas Mohan Mahapatra* for his continuous support, guidance, cooperation, encouragement and for facilitating all the requirements, going out of his way. His constant guidance, cooperation, motivation and support have always kept me going ahead.

I gratefully acknowledge the financial support provided by AICTE – QIP scheme, New Delhi, and QIP centre of I.I.T. Roorkee for the opportunity provided to me for carrying out this research work.

I take the opportunity to thank to *Dr. B. K. Gandhi*, Professor and Head, Department of Mechanical and Industrial Engineering, Indian Institute of Technology Roorkee for providing the basic infrastructural facilities for carrying out this research work. I am very thankful to my SRC members; *Dr. Dinesh Kimar* (Chairman), *Dr. P.K. Jha* (Internal expert, MIED), *Dr. Bimal Kumar* (External expert, Chemical Engg.) for their constructive criticism and valuable guidance during course of presentations. I wish to express my sincere thanks to all faculty members of the Department of Mechanical and Industrial Engineering, I.I.T. Roorkee. I am thankful to staff members, *Mr. Jasbir Singh, Mr. Pardeep Kumar, Mr. Mishra, Mr. Mohd. Idrish and Mr. Kapil* for helping me in my setup and experiments.

A special mention of thanks to my friends and well-wishers from Walchand College of Engineering, Sangli, specially *Dr. M.Y. Khire, Dr. S.P. Chavan, Dr.U.A. Dabade, Dr. B.S. Gawali, Dr. Ravindra Rathod, Dr. Sachin Kadam, Dr. Nitin Gawankar, Mr. J.G. Kulkarni and Mr. Babaso Naik.*

I am thankful to my co-researchers at IITR, *Dr. Nav Rattan, Mr. Ankit Saxena, Mr. Santhosh Dubba, Mr. Jayant Thakare, Mr. Uma Shankar Tripathi*, Mr. *Anup Kulkarni*, *Mr. Jasbirsingh* and *Mr. Harshal Kulkarni*. Their presence made my stay in Roorkee very pleasant.

I owe my life to my parents, *Aai* and *Dada*. I can imagine how happy my late mother *Kamal* would have been to see this day, but I am sure she will be very pleased in heaven. Also my late mother in law and father in law *Mrs. Suman and Shri. Krishna Shirke* would have been very happy. My deepest gratitude towards my better half, *Sou. Bharati* for her eternal support and understanding of my goals and aspirations. Her patience and sacrifice will remain my inspiration throughout my life. Without her help, I would not have been able to complete much of what I have done. I am thankful to my son *Peeyush* and daughter *Shourika* for giving me happiness throughout my life. Special thanks to my brothers *Dileep* and *Ganesh* and their families for their love and affection. I am also very much grateful to all my family members for their constant inspiration and encouragement.

I am also grateful to God, the almighty, for having blessed me to rise and take up this challenge.

Sharad Vasantrao Gaikwad

Abstract

Drilling is one of the most commonly used machining process in manufacturing industry. In drilling, the entire volume of hole is converted to chips. If the holes produced have diameter larger than 30 mm, a lot of material is converted into chips and wasted. The present study focuses on design and development of a trepanning tool for drilling of 40 mm diameter holes in stainless steel 304 steel, by cutting material in annular ring form and saving solid central disk shaped core.

Literature review available in the field of trepanning and drilling reveals that, most of the researchers studied the effect of various process parameters on the thrust force and torque developed while machining and surface roughness and material removal rate of the holes produced. A few researchers made attempt to design and develop a trepanning tool for machine composite materials to reduce the delamination of fibers. However, not much work is available on design of trepanning tool for stainless steel machining. The need for designing dynamometer for measurement of cutting forces and a new tool for trepanning of stainless steel 304 has been achieved by using finite element analysis of octagonal rings of dynamometer and trepanning tool.

Finite element analysis using ANSYS software was used to increase the sensitivity of the dynamometer by finding the accurate positioning of the strain gauges on octagonal rings of the dynamometer. A new design for two insert trepanning tool with 4 mm insert thickness was proposed. Simulation of the trepanning operation of 40 mm thick stainless steel 304 plate with this new tool was carried out using smoothed particle hydrodynamics (SPH) – a mesh free method in LS DYNA software. The structural analysis of the tool body was carried out using ANSYS software for validating the design. Three different insert coating grades were used in experimentation. Statically designed experimentation was carried out using three insert grades and three levels of cutting sped and feed rate.

Further experimentation can be conducted by choosing insert coating grades suitable for other difficult to cut materials like aerospace materials to analyze the performance of this new trepanning tool. Also insert mounting arrangement can be modified to make it more rigid. In future, the tool can be modified to incorporate a provision of finishing the drilled hole further to avoid need of any subsequent finishing processes.

Contents

List of Figures

List of Tables

Chapter 1

INTRODUCTION

1.1 Introduction

Manufacturing of products involves producing products that meet customer's requirements by converting raw materials, components, or parts into finished goods. Manufacturing processes are broadly classified into four major categories as casting, forming, machining and joining (Kalpakjian and Schmid 2009). Machining consists of different processes used to convert raw materials into a desired form by a material-removal or material addition processes. Most commonly used material removal processes are turning, milling, drilling and related operations.

1.2 Drilling

Producing a hole in a component is one of the most commonly used machining operation, and a large majority of these holes are made by drilling. Drilling process makes up about 25 % of total machining operations performed (Heinemann & Hinduja 2009). Drilling is very old technique and looks to be a simple process. However, in reality, it is a complex process (Kalpakjian and Schmid 2009, Stephonson and Agapiou 2016). Drilling mostly involves a tool having two cutting edges, or lips and the tool is termed as a twist drill. The cutting edges are at the end of the drill. The rotating tool is fed against the work-piece. The cutting edge of the drill is forced against the work-piece, thereby material is converted to chips from the hole volume. Cutting action takes place inside the work piece. The chips produced are made to exit through the drill flutes. The use of lubrication and coolant is difficult as the chips are coming out from the drill flutes (DeGarmo 2008, Kalpakjian and Schmid 2009).

The drilling processes can be further classified based on various aspects. The broader classification of various drilling related operations is given in Table 1.1 below. The various hole drilling / enlarging techniques are also shown in Fig. 1.1. As the application of methods mentioned below is different, some tools may have a design / geometry different than the conventional twist drill. The basic geometrical features of twist drills are more or less standardized.

Table 1.1 Classifications of various drilling related processes (Kalpakjian and Schmid 2009)

Process	Definition/purpose/characteristics
Spot drilling	Used for drilling guide hole for drilling the bigger final hole.
Centre drilling	Used for drilling a small centering hole in work piece for supporting further operations.
Deep hole drilling	Drilling of holes with Length / Diameter ratio > 10. Requires special equipment.
Micro drilling	Used for producing holes smaller than 0.5 mm diameter.
Vibration drilling	Combination of axial vibrations or oscillations in addition to the feed movement of the drill for easy chip removal from the cutting zone.
Circle interpolating	Drill rotates about its own axis and about machine center axis simultaneously. These axes are offset with each other.
Trepanning	Hole is produced by cutting an annular groove, keeping a solid core intact.

.

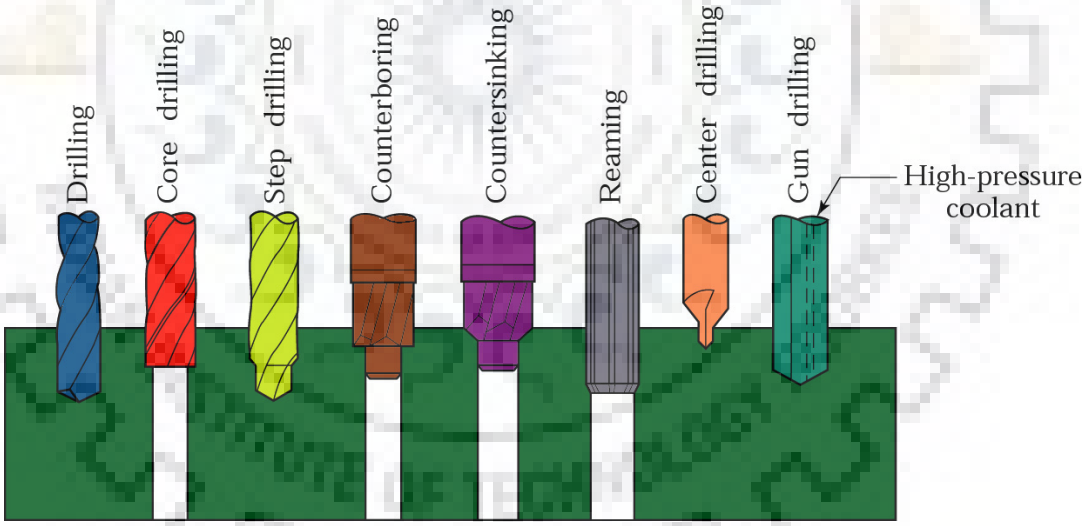

Fig. 1-1 Schematic representation of various drilling operations (Kalpakjian and Schmid 2009)

1.3 Limitations of conventional drilling process

Though drilling is one of the oldest and most commonly used techniques for production or enlargement of a hole, it has following limitations.

- The entire volume of drilled hole is converted to chips.
- Large diameter drills require high cutting forces and heavy set up.
- Drilling large diameter holes, may involve step drilling, increasing the machining time and reducing the material removal rate.

- Generally, it is not advisable for drilling of holes larger than 40 mm diameter.

To increase the productivity of process, it is important to recover the material from drilled hole especially for holes with large diameter (about 40 mm and above). Converting all the removed material in chips is not advisable. A special type of drilling technique called trepanning is very useful in such cases.

1.4 Trepanning process

Trepanning is the process of drilling a hole through solid metal work-piece, by cutting an annular groove and removing solid central core. In trepanning, a hole is produced by removing disk shaped piece of material (core), from the work piece. Thus, entire hole volume is not converted into chips (KalpakJian and Schmid 2009). The working principle of trepanning operations is shown in Fig. 1.2.

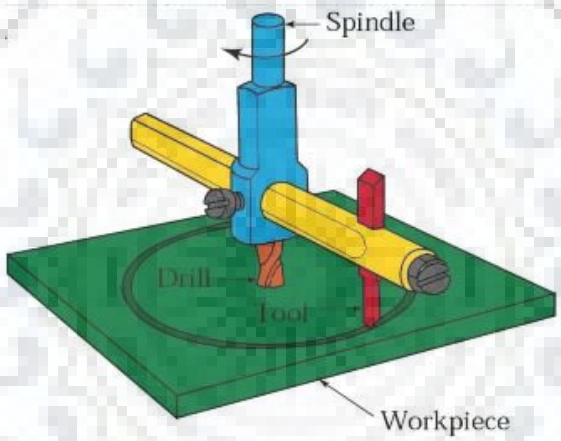

Fig. 1-2 Principle of trepanning operation (Kalpakjian and Schmid 2009)

The important process parameters in trepanning operations – cutting speed, feed rate and are briefly explained below.

1.4.1 Cutting speed

Cutting speed is one of the most important factors that determine the life of a tool. Too less cutting speed may result in tool chipping or breaking. On the other hand, a higher cutting speed rapidly dulls the cutting lips of the tool. Cutting speed employed depend on the following different variables (KalpakJian and Schmid 2009).

- The mechanical properties of work material (slower speeds are recommended for harder materials).
- The tool material (higher cutting speeds can be used with hard tool materials).
- Drill diameter (slower cutting speeds are preferred with increase in tool diameter).
- Higher cutting speeds can be used if cutting fluids are used in machining.

- More rigid machine set up permits use of higher cutting speeds.
- The rigidity of the drill (Shorter length of drills is preferred).
- Higher rigidity of the work set-up, permits use of higher cutting speeds.
- The speed setting also depends upon the desired quality of the hole to be drilled.

1.4.2 Feed rate

Feed rate in trepanning is selected to maximize productivity while maintaining chip control. Feed in trepanning operations is expressed in mm per revolution. The feed may be defined as the distance traveled by the tool in a single minute (Kalpakjian and Schmid 2009, Stephonson and Agapiou 2016). Selection of feed rate depends on other important parameters like work piece material, the hole diameter and depth required, tool holder and size, shape and coating of the inserts used in tool.

1.4.3 Tool holder and insert geometry

The design of the cutter body, number of inserts used, the geometry of the inserts including their key dimensions, mounting arrangement for the inserts and the coating used on the inserts are very important parameters influencing the success of trepanning operation. Proper selection these parameters and their integration in designed tool, affects the cutting performance of the tool. These factors influence the torque and thrust forces developed, surface finish of the holes produced, material removal rate, roundness of the hole, burr formation and tool life.

1.5 Trepanning tool configurations

In case of making large diameter holes, it is not necessary to convert all the material to chips, but conversion of material in the annular ring to chips is sufficient. In trepanning, a central core can be easily removed (for through holes), in solid cylindrical form and can be used for some other purpose.

Different variations of tool design are available for trepanning operation. Some of the commonly used tools configurations are shown in Fig. 1.3.

Fig. 1-3 Trepanning tools - Rotabroach, SANDVIK tool and single tube tool (Stephonson and Agapiou 2016 pp 234, SANDVIK, Mathew *et al.* 1999)

The rotabroach shown in Fig. 1.3 is a tool having a centering drill and spiral teeth on periphery as shown. This tool is suitable for drilling sheet metals and pipes. SANDVIK T-Max U cutters family uses triangular inserts for trepanning as shown in Fig. 1.3. Other specially developed tools like single tube tool shown in Fig. 1.3.are suitable for trepanning / drilling of composite materials like glass and or carbon fiber reinforced plastics, to avoid exit damage of the sheet when conventional twist drills are used.

1.6 Advancements in trepanning process applications

With the development in technology, the conventional trepanning operation has evolved with time. The need for overcoming various issues, researchers have used new energy sources for trepanning operations (Jain and Chak 2000, Chak 2007, Noh *et al*., Ashkenasi *et al*. 2011, Jahns *et al*. 2013). Modern machining techniques involving use of lasers, electrochemical energy etc. are preferred to gain superior quality of trepanned holes.

A brief overview of a few of the advanced trepanning techniques is discussed below:

1.6.1 Electrochemical discharge trepanning operation

The ceramic materials have high strength and hardness and corrosion resistance at high temperatures. These materials are used in tool inserts, in electronic components and as aerospace materials.

Chak (2007) has combined Electro chemical machining (ECM) and Electro discharge machining (EDM) to develop Electro Chemical Discharge Machining (ECDM). Chak used ECDM process successfully and economically, in drilling large diameter holes with orbital motion of small size electrodes for drilling of high strength, electrically non conducting ceramics. Working principle of ECDM process is shown in Fig. 1.4.

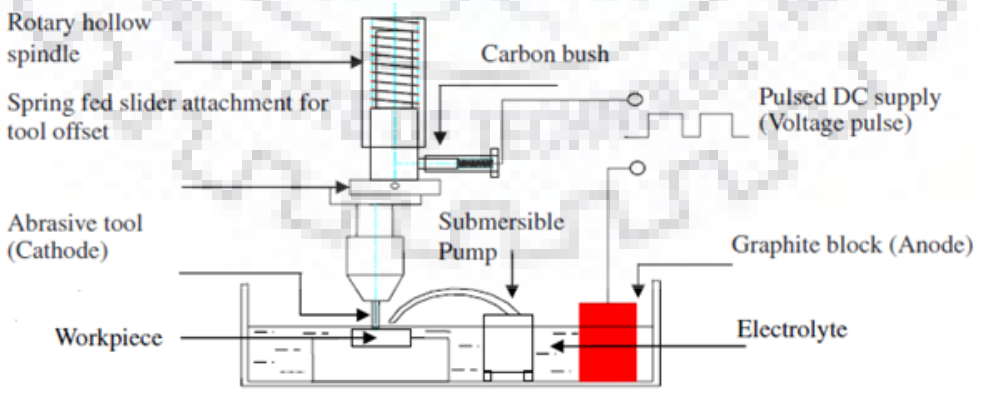

Fig. 1-4 Schematic set up of electrochemical discharge trepanning (Chak 2007)

Chak (2007) reported the success in producing straight as well engineered tapered holes in ceramic materials by providing orbital motion to tool, similar to

conventional trepanning. He concluded that by providing inclination to tool, tapered or reverse tapered holes can be produced in work-pieces.

1.6.2 Laser Beam Trepanning Operation

Precise and reproducible through holes can be machined using a process called as core drilling. In this technique, focused laser beam of suitable intensity is made to follow a perfect circular motion or profile onto the work piece. This produces a perfect circular hole. By providing a predetermined amount of inclination to laser beam, engineered taper holes were successfully machined by Ashkenasi *et al*. (2011) in tungsten and glass. This laser assisted trepanning is being used for machining of variety of materials. This method is used for drilling through holes of different sizes by making the path of different sizes for the focused laser beam. The schematic arrangement is shown in Fig. 1.5.

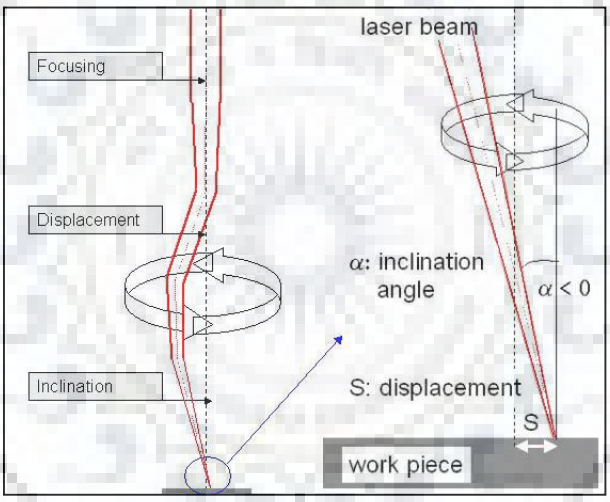

Fig. 1-5 Optical arrangement of laser trepanning system (Ashkenasi *et al*. 2011)

Conventional trepanning is generally used for producing large diameter holes in work pieces. Trepanning can be done on lathe machine, drill presses and milling machines, as well as other machines.

1.7 Advantages of trepanning

The trepanning process, compared to conventional drilling offers following advantages.

- Large diameter holes which are very difficult / impossible to produce by twist drill can be produced by trepanning (Kalpakjian and Schmid 2009).
- Since only annular material is removed in trepanning, this produce holes faster than conventional tooling.

- The cutting forces in this process are considerably lower than conventional drilling, increasing the tool life (Mathew *et al*. 1999).
- Since only periphery is cut and core remains intact, which can be reused. This leads to saving of material, increasing the process yield.
- Tolerance achievable is comparable to gun drilling process.
- This process can be carried out on horizontal boring mills, engine lathe, turret lathes, deep hole drilling machine and other machines (Mathew *et al*. 1999).
- Basic principle of trepanning can be implemented in advanced manufacturing process like laser beam trepanning, electrochemical discharge trepanning, ultrasonic trepanning etc. (Jain and Chak 2000, Chak & Rao 2007, Noh *et al*. 2009, Ashkenasi *et al*. 2011, Jahns *et al*. 2013).

1.8 Limitations of trepanning

The trepanning process, though have certain advantages over conventional drilling, it also has certain limitations as mentioned below.

- Trepanning is suitable for through hole production only and generally it is not used for blind hole drilling.
- Chip disposal is a problem for machining of materials prone to continuous chip formation and this restricts depth of hole to be drilled.
- Alike conventional drill-bit, trepanning tool also maintains compatibility to the pre-specified hole diameter.
- Manufacturing is difficult than that on twist drills.

1.9 Applications of trepanning

Trepanning process has many industrial applications. Trepanned holes find its applications in areas like:

- Weight reduction in certain finished parts and machine structures
- Fluid flow passages
- Working cavities
- Machining of blanks
- Piston and cylinder Features
- Seats for circular seals

Trepanning is very useful in machining of costly materials due to material savings it offers. Also it is very useful in nuclear and defense sector as the solid core can be used for mechanical and chemical testing for critical performance and safety specifications.

1.10 Motivation

During the study of the present work and available literature, it has been observed that there are a few commercial trepanning tool designs available, but they have limitation such as, large lip thickness, thus more wastage of materials, they require high pressure coolant application in large quantities and very rigid machine tools. Extensive study of conventional drilling, and some studies of trepanning of composite materials is available, but not much research is available on metal / steel trepanning. Literature on effects of various coating materials of drill on the forces encountered, tool wear etc. is available, however it appears that not much literature is available on effect of forces while using coated multi teeth trepanning tool. It has also been observed that research on surface finish obtained by drilling is available, however almost no literature is available for surface finish of trepanned hole.

There are several factors which must be considered before designing the trepanning tool. They are available resources, used technology, facility available during product design and manufacturing and economy of the production.

- Limitation of larger annular ring diameter succeeding to heavy material loss, due to larger width of the triangular inserts.
- Requirement of high pressure cutting fluid in large quantities and very rigid machine tools.
- Almost no earlier investigations trepanning of large sized holes to thick metallic sheets, no earlier results on the requirement of cutting forces for the operation and the surface finish resulted thereby.

This research work attempts economic development of simple cutting tool for trepanning of 40 mm thick stainless steel plate. Compliance to comment 1 suggests potential commercial application of the trepanning operation, and justifies the material selection. Advantages of this operation over equivalent drilling are also stated in the thesis in section 1.7, which suffice to describe the industrial benefits. Furthermore, this research work can be extended to verify compatibility of the tool (and insert grade) for trepanning of other materials like aluminum, carbon steels, alloy steels, titanium, Inconel etc.

1.11 Thesis overview

The thesis work has been presented in six chapters which are discussed as follows in brief:

Chapter 1: This chapter presents an introduction, variations of the drilling process, basic principle of trepanning with its advantages and limitations. Also overview of

advancements in conventional trepanning process is discussed in brief. At the last, motivation of the research with thesis overview has been discussed in brief.

Chapter 2: This chapter provides study of the literature review on the trepanning process. The research gaps have been highlighted at the end of the review and the possible opportunities have also been identified. Based on the literature review and research gaps, a suitable problem has been formulated.

Chapter 3: In this chapter, the finite element analysis and simulation of trepanning process is discussed in detail. The comparison of results of simulation and actual trials is also discussed in this chapter. The overall reduction in cutting forces i.e. thrust and torque for a conventional twist drill and newly developed trepanning tool is presented.

Chapter 4: In this chapter, the methodology followed for design of trepanning tool is discussed. This chapter also discusses the development of the tool and experimental setup in detail. The various subsystem of the setup with schematic diagram has been explained clearly.

Chapter 5: In this chapter, the effect of the various input process parameters on the thrust force and torque and surface roughness of the trepanned SS 304 work piece has been discussed. The experimental findings of effect of cutting speed and feed rate and their optimized values are compared with simulated results. The optimization of multiple responses has also been conducted with the help of response optimizer utility in Minitab 19 software.

Chapter 6: The overall conclusions drawn from the present work and future scope of work is discussed in this chapter.

Chapter 2

LITERATURE REVIEW

The brief review of literature on drilling process, trepanning, advancements in trepanning methods, simulation of machining in general and drilling and trepanning specifically, effect of various types of tool coatings on machining performance etc. has been presented in this chapter.

This literature review is organized according to various aspects. This review is organized under various categories such as: the research on effect of tool geometry on torque and thrust in trepanning tools (Mathew *et al.* 1999), analysis of damage investigation of drilled holes by twist drills compared to trepanning tool, by finite element method and its experimental validation (Hossainy *et al.* 2001, Saunders 2003, Bagci 2011, Rakesh *et al.* 2011, Pantel *et al.* 2012, Hongbing *et al.* 2012, Wu *et al.* 2012, Gyliene 2013, Lautre *et al.* 2014, Abdelhafeez *et al.* 2016 and Sara 2018), advancements in conventional trepanning or sometimes referred as assisted trepanning (Drake and McGEOUGH 1982, Chak and Rao 2007, Noh *et al.* 2009 and Jahns *et al.* 2013), various types of tool coatings and their effects (Audy *et al.* 2003, Benga 2008, Kusinski *et al.* 2009, Pathak *et al. 2011*) These categories are discussed in details below.

2.1 Effect of tool geometry on torque and thrust forces

Mathew *et al.* (1999) designed a tool for trepanning of glass fiber reinforced plastics (GFRP) aimed at reducing the delamination and generation of exit burr produced while using conventional drill. They reported about 50% reduction in thrust and about 10% reduction in torque, while trepanning of GFRP compared to twist drills. They also reported significant reduction in exit damage of the hole with new tool design.

Derflinger *et al.* (1999) studied the effect of new hard (TiAlN) / lubricant (WC) coated cemented carbide inserts in drilling of alloy steel and cast iron. The tool was coated with hard TiAlN layer first and then with a second lubricant layer of WC on the hard layer. They observed significant reduction in cutting forces due to lower friction at the tool chip interface due to presence of lubricant layer. It was also reported that high speed machining without lubricants was possible due to multilayer coating technique.

Chen and Tsao (1999) studied the effect of TiN monolayer, TiN multi-layer and TiCN multi-layer coatings on twist drills while machining of JIS SS 400 carbon steel. They observed increase in torque and thrust force with increase in feed rate and decrease within a narrow range with increase in speed for all three coatings.

Benga (2008) studied the effect of PVD coatings on the cutting forces while drilling hardened mold steel. He observed that increase in thrust force is related to increase in tool wear and the TiAlN coating applied with filtered arc deposition with double rotation method on drill significantly improved the tribological behavior of the tool.

Pathak *et al.* (2011) conducted statistically planned experiments for dry drilling of aluminum AA2024 – aircraft grade with HSS and TiAlN coated drills. They reported significant reduction in both the trust force and torque with machining with TiAlN coated drills compared to uncoated HSS drill.

Majerik *et al.* (2012) conducted experimentation with non-coated and PVD TiN coated drills. They considered axial forces and torques in drilling as response variables. They observed that both axial forces as well as torque in TiN coated drills to be significantly lower compared to uncoated HSS drills. They also reported less wear in coated drills compared to un coated drills.

2.2 Delamination study and damage investigation of glass fiber reinforced plastics

Mathew *et al.* (1999) carried out study of de-lamination of fiber reinforced plastics during drilling operation. They observed that the trepanning tool produced de-lamination free holes. In case of conventional drilling the crack propagation about the drilled hole is observed severe while piercing lips passed through the bottom sub layer. As central portion was already cut in conventional drilling, the stiffness of the material decreased and uncut fibers tried to entangle with cutting lips giving rise to twisting effect. Whereas in case of trepanning, fibers were put in the tension and not in the twisting, as cutting phenomenon started at the circumference of the cutting tip of the tool.

Rakesh *et al.* (2011) studied the delamination in the plastics which are reinforced with fiber by using finite element method. They compared the drilling induced damage by a twist drill, a jo-drill and a trepanning tool, keeping the tool diameter and process parameters like speed and feed unchanged. They observed, the damage induced because of drilling in the exit delamination arrangement (represented by the delamination factor) caused by trepanning tool is less in comparision to the twist drill and jo-drill.

Debnath *et al.* (2016) developed trepanning tool for cutting composite material. They measured the tool geometry effect on delamination of composites. They reported improvement in productivity (number of holes per hour). They observed increase in both torque and force with increment in the feed rate. Also overall reduction in torque and thrust over regular twist drill with reduction in exit burr and delamination was reported.

2.3 Trepanning assisted by non-conventional techniques

Jain and Chak (2000) used electrochemical spark machining for drilling of alumina and quartz. They observed that the process was successful for drilling through holes of 1.35 mm depth and 2.35 mm depth in alumina and quartz respectively. They also observed that the constraint of machining depth associated with ECM process was somewhat hassle-free by trepanning action of the tool.

Chak and Rao (2007) carried out trepanning of Al_2O_3 material, using abrasive electrode with supply of pulsed DC in electrochemical discharge machining (ECDM). They observed that ECDM by trepanning method for aluminum oxide can be utilized for drilling holes of comparatively larger size, by somewhat smaller electrodes efficiently. They observed that the cracking tendency was reduced with the use of pulsed DC at high source voltage in comparison to smooth DC and the abrasive electrode's machining ability was better than copper electrode.

Jahns *et al.* (2013) used rotating optics based laser trepanning systems in experimentation. They developed a system which provides a controlled adjustment of movement and inclination of the laser beam at the time of operation, to drill through-holes with arbitrary geometry. It was observed that laser micromachining of straight, positive tapered and negative tapered through holes with an entering diameter in the range of 65 to 1000 μm was possible in stainless steel sheet of 500 μm thickness.

Lotfi *et al.* (2016) conducted experimentation on 8mm thick 1045 steel using minimum quantity lubrication and ultrasonic vibration assisted drilling with 5 mm diameter drill to study its effect of burr produced, the surface roughness of drilled hole and thrust force. They reported decrease in value of surface roughness and thrust force with an increase in cutting speed and increase in surface roughness and thrust force with increase in the feed rate. They also stated about 25% reduction in thrust with application of ultrasonic vibrations in drilling over the conventional drilling process.

2.4 Effect of coating on wear rate / tool life of drills

It is a generally accepted fact that, a thin layer of hard materials on the cutting tip of the tool, enhances the useful life to tool. However, the tool life may vary widely from the coating conditions used, coating batch to batch variation, type of coating unit, the type of substrate and the type of application including the cutting conditions to which it is subjected.

Monaghan and O'Reilly (1992) studied flank and rake face wear of HSS, solid carbide drills and carbide tipped HSS, TiN coated HSS while machining of Al/SiC metal matrix composites. Author's observed, the tool wear of solid carbide drills, carbide tipped drills; TiN

coated HSS drills and uncoated HSS drills was progressively less. They also reported that both HSS drill and TiN coated drills were not suitable for MMCs due to excessive wear observed.

Derflinger *et al.* (1999) reported systematic increase in tool life due to presence of low friction WC/C top layer as the overall stresses and cutting forces are less than conventional drill in dry drilling of alloy steel.

Chen and Tsao (1999) studied the effect of TiN monolayer, TiN multi-layer and TiCN multi-layer coatings on twist drills while machining of JIS SS 400 carbon steel. They reported that TiCN multilayer coating has least flank surface wear compared to other coatings.

Audy *et al.* (2003) carried out experimentation with TiN, TiAlN and TiCN coating for estimating drill life for machining Bisalloy 60 steel material. They observed that life of coated tool was significantly more but no significant advantage of one coating over other was reported.

Talib *et al.* (2007) investigated tool wear of TiCN, TiN and TiAlN coated drills while drilling medium alloy carbon steel material. They observed the wear mechanism to be complex mixture of abrasion, adhesion and thermal wear. Mechanism changes from mix of abrasion and adhesion in the start to mix of abrasion, severe adhesion and thermal wear at the end of drill life.

Danisman *et al.* (2008) experimented with uncoated, TiN and TiAlN coated drills for machining of 1015 and 2080 steels. They observed TiN coating to give better tool life due to low coefficient of friction and their high oxidation resistance.

Kusinski *et al.* (2009) studied the tool life of anti-wear Cr(C,N) coated drills in drilling of annealed steel with 0.18% carbon. The coatings used were deposited by Arc-PVD technique. They reported increased tool life for drills coated with Cr/CrN/CrN+Cr2N/Cr(C,N), than uncoated drills. They observed that the failure mechanism of coated tool involved both sliding and abrasive wear and for uncoated drills, it was adhesion and sticking.

Pathak *et al.* (2011) conducted statistically planned experiments for dry drilling of aluminum AA2024 – aircraft grade with HSS and TiAlN coated drills. They reported a significant reduction in both the trust force and torque with machining with TiAlN coated drills compared to uncoated HSS drill.

Pathak *et al.* (2011) conducted statistically planned experiments for dry drilling of 31 steel with HSS and TiAlN coated drills. They observed a significant improvement of tool life with coated drills over uncoated HSS drills.

2.5 Effect of tool geometry and coating on surface finish

Rao and Shunmugam (1987) studied the surface integrity of En-9 steels using BTA drills. They observed that combined cutting and burnishing action produced superior surface finish

and higher dimensional accuracy compared to conventional drilled hole. Burnishing also increased surface micro hardness by 30 to 40 % and improves corrosion resistance, yield and fatigue strength.

Monaghan (1998) carried out experimentation with HSS, solid carbide drills, TiN coated HSS and carbide tipped HSS drills on machining of Al/SiC metal matrix composites. They observed significant progress in surface finish using carbide and coated drills as compared to HSS drills. Increase in surface roughness with an increase in feed rate for each cutting speed level was reported. They also observed that the carbide tipped drills resulted in overall better surface finish.

Danisman *et al.* (2008) while experimenting with uncoated, TiN coated and TiAlN coated drills observed that surface finish of holes from TiAlN coated drills was better. The coated tools had been used under aggressive machining conditions as well.

Ficici *et al.* (2012) carried out optimization of process parameters for surface roughness of drilled holes for SS 304 steel. They used Taguchi methodology and multiple regression analysis and observed that the lower feed rates and higher cutting speed enabled a reduction in surface roughness of drilled holes with modified HSS drills.

Kivak *et al.* (2012) used Taguchi techniques to optimize process parameters for drilling of AISI 316 steel with HSS twist drills coated at multilayers and PVD mono coated drills. Two feed rates and four speeds were used for 6 mm diameter drill with hole depth 13 mm. TiN / TiAlN, TiN and TiAlN coatings on drills were employed in experimentation. They observed that the feed rate significantly affects the thrust force whereas the tool type affects surface roughness of the produced hole.

Cicck *et al.* (2013) varied out drilling experiment on AISI 304 steel with different drills including conventionally heat treated, cryogenic treated and cryo tempered drills to find the effect of control parameters on hole roundness and surface roughness. They observed that, surface roughness and roundness of the holes produced is considerably affected by cutting speed employed and feed rate of the process.

Amran *et al.* (2013) used response surface methodology (RSM) in order to optimize surface roughness of drilled holes while using high speed steel drills on aluminum alloy. They studied the effects of the feed rate, the spindle speed and the drill diameter on the surface texture and the surface roughness of drilled hole. They observed that spindle speed, drill diameter and feed rate were having significant contribution for surface roughness. They reported decrease in surface roughness with increase in the feed rate, spindle speed and drill diameter.

Siddiquee *et al.* (2014) used L_{18} array for optimizing process parameters of deep drilling for drilling of AISI 321 austenitic stainless steel by using carbide drills. They observed that cutting speed, cutting fluid, feed rate and hole-depth affected the surface roughness in the same order.

Sultan *et al.* (2015) studied the effect of drilling feed rate and speed on surface roughness and other characteristics while drilling AISI 316L steel using uncoated carbide drills of 4 mm diameter. It was reported that feed rate and cutting speed have significant impact on quality of holes. It was reported that the surface roughness decreases with an increase in cutting speed, and increase in the feed rate causes the surface roughness to increase.

2.6 Use of finite element methods for simulation of machining / drilling processes

Espinosa *et al.* (2008) simulated high speed machining of Ti-6Al-4V alloy through ball end milling process. They observed that Smoothed particle hydrodynamics (SPH) model was able to predict both shear localized and also continuous chips. They also observed that the cutting forces predicted through SPH simulation were in close agreement with 3D milling force models. They observed that major advantage of using SPH technique was that there is no need of defining friction parameter at tool chip interface and friction was modeled as particle interaction between tool and work particles. They also noticed that no re-meshing of the deformed work piece was required as the particles rearrange themselves without any topological restrictions.

Petrariu *et al.* (2008) used Advantage, commercially available FEM software for simulating high speed drilling process. They successfully simulated two carbide drill designs of 9.92 mm diameter and different geometries for machining of Ti-6Al-4V. They concluded that FEM methods can be successfully used to simulate drilling process and to predict torque thrust, residual stresses, heat generated and tool wear during drilling.

Abele and Fujara (2010) used simulation approach to design optimized twist drill geometry. They used genetic algorithms to optimize various parameters of a twist drill. The simulation was successfully used to optimize the evacuation of chip, torsional stiffness and strength, torque and coolant delivery.

Gao *et al.* (2010) simulated drilling of stainless steel 1Cr18Ni9Ti using Deform-3D software. The tool and work piece was considered as rigid and deformable body and master and slave respectively. Simulation used adaptive meshing grid (AMG) feature. They reported there is increase in the value of torque and axial force for an increase of diameter, feed and speed of the drill. They also stated that the diameter of drill and feed rate employed have substantial influence on axial force, which increases with increase in parameters.

Bagci (2011) used smooth particle hydrodynamics (SPH) method using LS DYNA to model and analyse orthogonal cutting of AISI H13 steel. Simulations were performed to obtain equivalent plastic strain, equivalent plastic strain rate, shear stress, effective stress and cutting forces. He observed that LS DYNA predicted the values of cutting forces therein close agreement within 8.43% and 11.70% of the values obtained from experiments. He also assigned these variations to chip separations criteria, material modeling, SPH velocity assumption made and friction model while simulating the machining.

Isbilir and Ghassemieh (2011) used Abaqus/Explicit for simulation of drilling of titanium alloy Ti-6Al-4V using TiAlN coated 8 mm carbide drill. They used Lagrangian formulation with explicit integration method and used Johnson-Cook constitutive material model and associated damage model in drilling simulation. They observed that the simulation results for thrust force were in good agreement, whereas torque was overestimated by 20%. They observed that the process simulation was capable to estimate the cutting forces with change in various process parameters.

Maurel-Pantel *et al.* (2012) conducted 3D FEM simulations of shoulder milling tasks on a 304L stainless steel by using LS DYNA. They used Lagrangian formulation with an explicit solution scheme and Johnson Cook material model and a penalty contact algorithm to model the work piece properties. The tool was considered as a stiff body and workpiece to be deformable part. They observed an error ranging from 5% to 35% between the cutting forces experimentally measured with the simulation results.

Hongbing *et al.* (2012) used ALE formulation to compare the cutting forces in drilling a 8 mm thickness titanium Ti-6Al-4V plate with a standard drill of 8 mm diameter, with that of the results of simulation. They used the relationships of the true flow stress with that of true strain of the Ti-6Al-4V titanium alloy between 20℃ and 800℃, at the strain-rates of 0.001/s,1000/s, 5000/s and 10000/s along with Johnson-Cook work material constitutive model. They noted that there was a close agreement between the simulation and experimental results of the cutting forces.

Gyliene *et al.* (2013) successfully used SPH method in LS DYNA to conduct the simulation of drilling with a 10 mm dia. tool on 15 mm thick steel plate. They observed that the chip formation with SPH method is natural and fast compared to other FEM methods. The major focus was on chip separation and material deletion and observations of comparison of experimental and simulated force and thrust values is not recorded.

Su *et al.* (2015) used DFORM 3D software for simulation of drilling of Ti-6Al-4V titanium alloy. They used 6 mm diameter carbide drill and used Johnson Cook classical material

model to model the work piece material. They observed the feed rate to have more influence on the drill force, maximum tool temperature and drilling torque than drilling speed. They also concluded that the combination of high drilling speed (13.19 m/min) and low feed rate (0.08 mm/rev) is recommended for the drilling process of titanium alloys in order to obtain good machining performance and high productivity.

Olleak *et al.* (2015) carried out simulation of orthogonal cutting of AISI 316L steel using five different sets of Johnson-Cook material model to predict the cutting forces with previously known experimental values. They reported that the predicted values of cutting forces with SPH model show good co-relation with experimental values. Since the results for some runs were not on agreement with experimental values, they concluded that the values of Johnson-Cook constants played an important roles in accurate prediction of forces, and experimental values of these constants from split Hopkinson's test must be used.

Patel *et al.* (2016) compared the experimental values of cutting forces in orthogonal machining of Ti-6Al-4V titanium alloy using Arbitrary Lagrangian Eulerian (ALE) formulation using ABAQUS/Explicit. They used ductile damage initiation creation and Johnson-Cook work material constitutive model in machining simulation. They reported that the simulated results of cutting forces was in good agreement with previous experimental results and noted that ALE formulation to be suitable for chip formation and separation.

Nan *et al.* (2016) simulated small hole drilling of AISI 1045 steel with 3 mm diameter solid carbide drill, using Langrangian formulation of Abaqus/Explicit software. Johnson Cook damage law and Johnson Cook plasticity model was used for modeling material behavior and chip separation criterion. They observed that the simulation successfully predicted the torque and thrust force with 23.3 and 31.1 %. They anticipated reduction in prediction error with refined meshing of tool and work piece model.

2.7 Review related to techniques of cutting force measurement

A noteworthy observation to analyse and qualitatively determine the success of any machining process, is the accurate measurement of cutting forces developed. But precise measurement of the cutting forces is difficult due to many considerations involved in it (Shaw 2005). The measurement of the cutting forces directly at the time of cutting is very difficult; hence, generally there are two main techniques of measuring. First method uses piezoelectric crystals. These crystals are quiet sensitive for mechanical forces. When some mechanical load is applied, it produces a potential difference proportional to the applied force. The second method uses strain and deflection produced by force on an elastic mechanical member. An octagonal ring is commonly used mechanical member for force measurement. A strain gauge

affixed on a strain ring transforms the strain produced in the strain ring into the equivalent voltage using a Wheatstone bridge (Shaw 2005). The use of piezoelectric crystals gives the benefit of high sensitivity and bandwidth over 50 KHz; however, they are expensive, need special care for use in harsh environments, and are susceptible to noise from electrical equipment (Shaw 2005).

Some researchers (Kumar 2013, Kumar 2015) have also experimented with square- and hexagonal-shaped strain rings for force measurement. On the other hand, octagonal rings are easy to fabricate of any required size. Strain gauges are easily accessible in a varied range of configurations and characteristics and are relatively inexpensive. Sensing the output with the use of a Wheatstone bridge is easy (Soliman 2015, Karabay 2007).

Yaldiz *et al.* (2007) measured cutting forces in turning operation with a three-component force dynamometer using octagonal ring as sensing element. They used the thin ring theory for designing the rings. The force measuring range was up to 3,500 N. Sensitivity of the system was ±5 N and the cross-sensitivity was approximately 0.17–0.92 %. The used strain gauges of 6 mm length.

Karabay (2007) designed a dynamometer with dissimilar forms of octal strain rings using thin ring theory, to quantify cutting forces in milling and drilling processes. The distribution of strain in the area of strain gauge mounting was not considered in experiments. The measurement of strain signals from Wheatstone bridge was found to be in line with cutting forces.

Korkut (2012) designed octagonal ring type milling and drilling dynamometers. He also used thin ring theory principles to estimate stiffness and strain in octal rings. They reported ±5 N sensitivity and 0.05 % or less cross-sensitivity in measuring cutting force.

Turgut and Korkut (2012) designed and constructed a dynamometer consisting of three 20 KN high-capacity single-point load cells mounted on three mutually perpendicular planes and three isolated strain gauge input modules with a data acquisition system. The load cells were loaded up to 10 KN in various steps from the unloaded condition. The system successfully measured clamping and cutting forces.

Sreejith and Raj (2015) measured thrust force and torque during drilling operation with a strain-gauge based dynamometer using octagonal ring sensing elements. The dynamometer design was then analyzed using ANSYS software to check whether the maximum applied load and torque were within safe limits. They conducted linearity and eccentricity tests to estimate the performance of the dynamometer. The reported percentage errors for the linearity test as 1.3 % and 1.2 %.

Soliman (2015) analyzed the attributes of octal rings as force transducers, using an L_9 array of finite element models of the ring to determine the state of strain upon the load application. He reported decrease in stiffness of rings but increase in sensitiveness of dynamometer on the increase in ring height and decrease in ring thickness. The width of the ring did not have a clear effect of stiffness but increasing width decreased the sensitivity.

2.8 Research gaps

Many researchers (Kusinski *et al*. 2009, Audy *et al.* 2003, Danisman *et al*. 2008, Pathak *et al*. 2011, Monaghan and O'Reilly 1992, Majerik *et al*. 2012, Talib *et al*. 2007, Benga 2008) have studied the effects of various coating materials in drilling on the forces encountered, tool wear etc. However it appears that not much literature is available on effect of forces while using coated multi teeth trepanning tool used in metal drilling.

It is reported that, use of coolant improves performance of cutting tools (Kusinski *et al.* 2009, Audy *et al.* 2003). Various literature is available on performance of drills with use of coolants. However, it appears that almost no literature is available on metal trepanning with the use of coolants.

From the brief review of literature and limitations of trepanning process, it appears that not much literature is available for trepanning tool design methodology, insert geometry selection. There has been not enough literature for provision for path for chip removal from the annular groove. Therefore, it has been planned to design and manufacture multi teeth trepanning tool with provision for multi passage chip removal.

2.9 Proposed research work

On the basis of extensive literature review, the objectives proposed for the research work are:

2.9.1 Objectives of the project

- To design and manufacture multi teeth trepanning tool with provision for multi-passage chip removal.
- To study the effect of tool geometry and tool coatings on response variables like surface roughness of hole and material removal rate (MRR).
- To develop a multi objective function to optimize process variables like cutting speed, feed rate and coating material to minimize surface roughness and maximize MRR.

2.9.2 Proposed methodology

1. To design and manufacture multi teeth trepanning tool with provision for multi-passage chip removal

After the review of literature and study of catalogues of leading cutting tool manufacturers, insert selection was done for size, geometry and coating of the inserts. The experimental levels of process parameters like cutting speed and feed were selected. Different conceptual designs were developed using 3D solid works. Brain storming sessions and discussions were carried out to study the feasibility of the designed tool. The proposed tool design was used for further analysis and simulation of trepanning process. The structural design of tool body was validated by simulating the trepanning process in LS DYNA software.

2. To study the effect of tool geometry and tool coatings on response variables like thrust force, torque, surface roughness of hole and MRR.

There are various process parameters viz the feed rate, cutting speed and the coating type which affect the trepanning process. Thrust force, torque, material removal rate and surface roughness were selected as responses in trepanning process. The influence of several process parameters on to the outcome responses has been studied by using design of experiments (DoE). Statistical models were developed to define the relation between the process parameters and responses. The results were analyzed and explanation has been sought for the obtained behavior.

An octagonal ring type dynamometer using strain gauges was designed and developed to accurately measure the torque and thrust force during the experimentation. Alternately, quartz based KISTLER 4 component dynamometer which was also used for measuring the cutting forces. The surface roughness of the trepanned holes was measured using SURFCOM roughness measuring device. The wear pattern of the used inserts were studied with the help of and LECIA DMiS microscope. It has been proposed to plan and conduct statistically designed experiments using three tools with same geometry with different coatings on the same work material and machining conditions in order to find the effect of coatings on MRR and hole surface finish.

3. To develop a multi objective function to optimize process variables like feed rate, cutting speed and coating material to minimize surface roughness and maximize MRR.

Suitable optimization technique would be used to optimize process parameters to minimize surface roughness and maximize MRR.

Chapter 3

FINITE ELEMENT ANALYSIS AND SIMULATION OF TREPANNING PROCESS

3.1 Introduction

It is evident from the literature review that the cutting forces generated, surface roughness of the drilled hole, material removal rate and tool wear are few of the important indicators of the efficient hole generating processes. It was also observed that assisted trepanning process is useful for certain type of machining applications. The Boring and Trepanning Association drills popularly referred as BTA drills are commonly used for metal trepanning, but they require high pressure coolant system to be employed in process along with special arrangements for tool holding. Another major constraint is that, it requires machines with high rigidity and spindle power. Other efforts of trepanning tool development were mostly concerned with thrust and torque reduction along with improvement in delamination at the exit of holes drilled in GFRP (Mathew *et al.* 1999, Rakesh *et al.* 2011, Debnath *et al.* 2016 and 2017). It was observed that there is no standard design methodology readily available for design of trepanning tool for deep annular groove or through holes in thick stainless steel 304 work pieces. Therefore, it was planned to use the simulation based approach to validate the new tool design and then carry out the development of tool for machining trials.

In this chapter, the design of octagonal ring type dynamometer and trepanning tool, using FEA analysis in its design, fabrication of fixture for work piece holding and design of trepanning tool using FEA simulation is discussed in detail. The design of octagonal ring type dynamometer with strain gauges has been validated with FEA analysis using ANSYS. The design of trepanning tool has been validated using mesh-free method in LS DYNA software.

3.2 Design of octagonal ring type dynamometer using finite element analysis

Measurement of cutting forces is very important in measuring the success of any machining process. The machining process with lower cutting forces is considered to be a better process and vice versa. Lower cutting forces in machining directly means lower tool wear and improved tool life, as well as better surface finish on the machined surface (Shaw 2005). Different techniques are available for measuring the cutting forces in machining processes. Octagonal ring type dynamometer with strain gauge affixed on elastic members is one such widely used technique for cutting force measurement. This method is reasonably accurate and cheaper (Shaw 2005, Parida 2014). Strain rings when used as an elastic member

for force measurement, provide good stability against buckling and have high ratio of sensitivity to stiffness. Manufacturing and assembly of rings in dynamometer assembly is easy. The strain rings provide additional advantage for designing effective Wheatstone bridge circuit as the inside surface of the strain ring is mostly in a contrary state of strain from the outside. Due to symmetry, the rings provide parallel paths for heat flow and equivalent points on opposite sides of a ring remain at the same temperature. By connecting the gauges to form a complete Wheatstone bridge circuit, the problem of drift due to temperature gradient in the vicinity of the dynamometer can be eliminated.

The octagonal ring type dynamometer consisted of four octagonal rings made up of AISI 1040 steel, acting as elastic members for sensing the stresses induced. Strain rings were rigidly secured between a cast iron base plate and mild steel top plate of dimensions 245 mm length and 245 mm width. Base plate and top plate were 38 mm and 75 mm thick respectively. The octagonal rings were secured between top and bottom plate by M16 threaded pins and nuts. The bottom plate had slots to clamp the base on the machine tool table. The top plate had T slots to secure the work piece rigidly through a suitable clamping mechanism. The dynamometer is shown in Fig. 3.1.

Fig. 3-1 Octagonal ring type strain gauge dynamometer

According to thin ring theory used for strain measurement, it is very important to affix the strain gauges at the correct position on strain rings for accurate sensing and measurement of force (Venkatraman *et al.* 1965, Levi 1967, Shaw 2005). The strain gauges, thus located at correct locations are then connected to form active full Whetstone bridge circuit, which measures the strain in elastic members in terms of microvolts (Pandey 2015 and 2018). The

location of strain gauges and their proper bonding with the ring is very important for precise and accurate measurement.

AISI 1040 steel material was considered as material for manufacture of strain rings. This material has high corrosion resistance and heat conductivity and hence vary suitable for manufacturing strain rings. The mechanical properties of AISI 1040 steel are given in table 3.1.

Table 3.1 Mechanical properties of AISI 1040 steel

Modulus of elasticity	210000 N / mm^2	Tensile strength	550 – 570 N / mm^2
Yield strength	280 N / mm^2	Permissible stress	186.66 N / mm^2
Poisson ratio	0.3	Hardness (Brinell)	180
Carbon content	0.37 – 0.44 %		

The octagonal rings were analyzed using finite element analysis to identify the areas with maximum strain and deflections occurring in the strain ring under static loading condition under the application of 2000 Newton load. Simulations using ANSYS software were performed to define the precise position of strain gauges on inside curved surface, outside vertical and inclined faces with maximum sensitivity to strain and at the same time minimum cross sensitivity to strain in opposite direction.

The basic controllable dimensions of an octagonal ring are its diameter (d), thickness (t) and width (b) (Korakut 2003, Yaldiz *et al.* 2007, Hashmi *et al.* 2013, Soliman 2015). Since, the width of rings does not have any effect on strain per unit deflection; it is chosen as 30 mm for the ease of securing the ring and sufficient space for bonding the pair of strain gauges. From the finite element analysis of strain rings, many researchers (Yaldiz *et al.* 2007, Soliman 2015, Korakut 2003) have suggested that the ratio of $\frac{t}{r} > 0.25$ gives excellent sensitivity and rigidity. Considering this, the diameter of the ring was selected as 55 mm for the ease of fixing strain gauges on internal surface. The basic dimensions of the strain ring are shown in Fig. 3.2.

Considering a 2000 N maximum force and basic ring dimensions - width (b) = 30 mm, radius (r) = 27.5 mm and thickness (t) = 7.5 mm, elastic strains produced due to action of thrust and torque is calculated as follows:

$\varepsilon_t = \pm \frac{1.09Ft.r}{Ebt^2}$ =1.6917 x 10^{-4} (3.1) (Milton and Shaw 2005)

$\varepsilon_c = \pm \frac{2.18Fc.r}{Ebt^2}$=3.3834 x 10^{-4} (3.2) (Milton and Shaw 2005)

Where ε_t and ε_c are elastic strains due to tangential and thrust force respectively and F_t and F_r are tangential and thrust forces applied respectively.

This elastic strain is further used to calculate the stress induced in the ring element under torque and thrust force and is compared with the yield strength of the ring material.

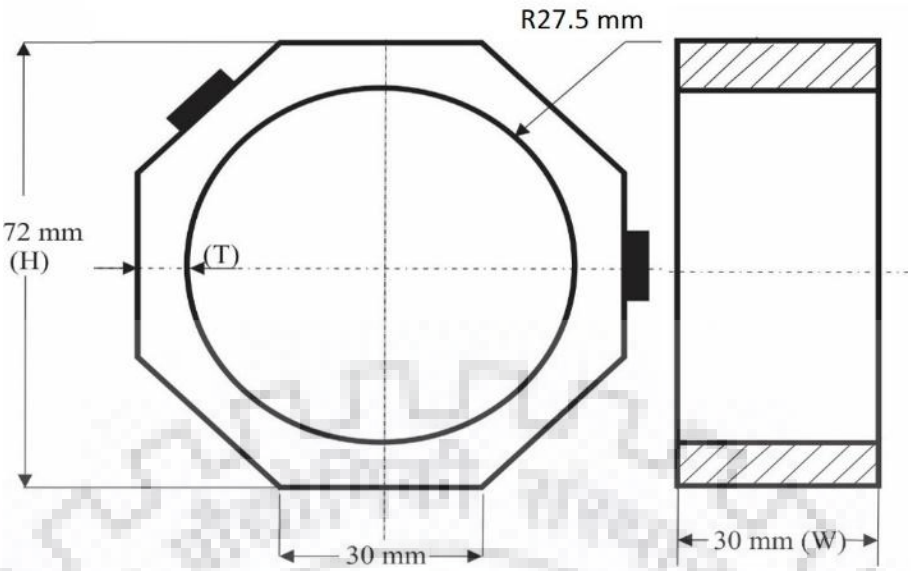

Fig. 3-2 Dimensions of strain ring and strain gauge mounting

Stress induced due to tangential force =$\sigma_t = E\varepsilon_t$ = 35.52 N / mm^2 (3.3)

Stress induced due to thrust force = $\sigma_c = E\varepsilon_c$ = 71.05 N / mm^2 (3.4)

Since, the yield strength of strain ring material AISI 1040 steel is 280 N / mm^2, it is observed that the stress values σ_t and σ_c are within the safety limits. After this design validation under static loading, the dynamic properties of the dynamometer are checked as follows.

It is necessary the natural frequency of the dynamometer is at least four times the natural frequency of the machine with which it is used to avoid resonance (Korakut 2003, Yaldiz *et al.* 2007, Panzera *et al.* 2012, Soliman 2015). The natural frequency of the machine depends upon the spindle speed of the machine and is given by,

$F_m = \frac{n}{60}$ rev / seconds (3.5)

To find the natural frequency of the dynamometer, it is required to determine the ring constant of the dynamometer K_t, which is given by,

$k_t = \frac{Ft}{\delta t} = \frac{Ebt^3}{1.8r^3}$ (3.6) (Milton and Shaw 2005)

$= 210000\ X\ 30\ X \frac{7.5^3}{1.8\ X\ 27.5^3} = \frac{2657812500}{37434.37}$

=70999.25 N / mm

The natural frequency of the dynamometer, considering it to be trivial mass supported by ring elements is attained from the relationship given in equation 3.7. The schematic is shown in Fig. 3.3.

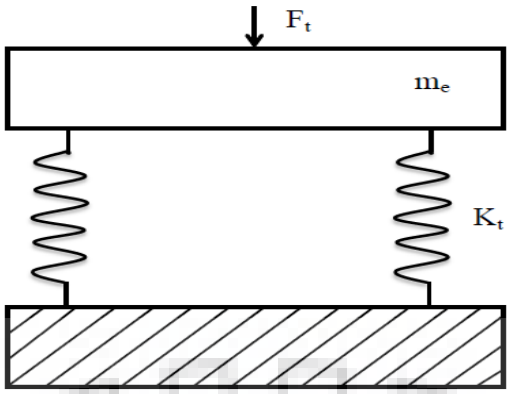

Fig. 3-3 Free body diagram of dynamometer

$$f_d = \frac{1}{2\pi}\sqrt{\frac{Kt}{m}} = \frac{1}{2\ X\ 3.14}\sqrt{\frac{70999.25\ X\ 1000}{50}} \quad (3.7)$$ (Milton and Shaw 2005)

Where K_t is the ring constant dynamometer and m is the mass of the dynamometer.

f_d = 189.75 rev / sec

Considering the maximum spindle speed of the machine to be 2000 rpm, the natural frequency of machine F_m is 33.33 rev / sec. As the natural frequency of dynamometer > 4 times F_m, the design was found to be safe.

Also, maximum strain at y = 0 (center of the ring) is given by,

$$\delta_A = \frac{Ft}{Kt} = \frac{2000}{70999.25} = 0.028$$

It is very important to determine the nature of stresses, level of strains and amount of deflection caused in the octagonal ring under the action of cutting forces. Accurate identification of above factors and proper placement of strain gauges at the correct locations of maximum strains, greatly improves the accuracy and sensitivity of dynamometer (Korakut 2003, Yaldiz *et al.* 2007, Soliman 2015).

The geometrical model of the strain ring was prepared using ANSYS software as shown in Fig. 3.4. The solid 185 (eight noded brick) element was used for modeling. This element had 3 degrees of freedom, viz translation in X, Y and Z direction. The meshed model of the octagonal ring contains 960 elements with total 1530 number of nodes, The boundary condition were same as that of analytical model, i.e. all degrees of freedom at the bottom face were fixed and a vertical load of 2000 N was applied in negative (-) Y direction. The static linear analysis was carried out. The ring material AISI 1040 was considered to be linear elastic.

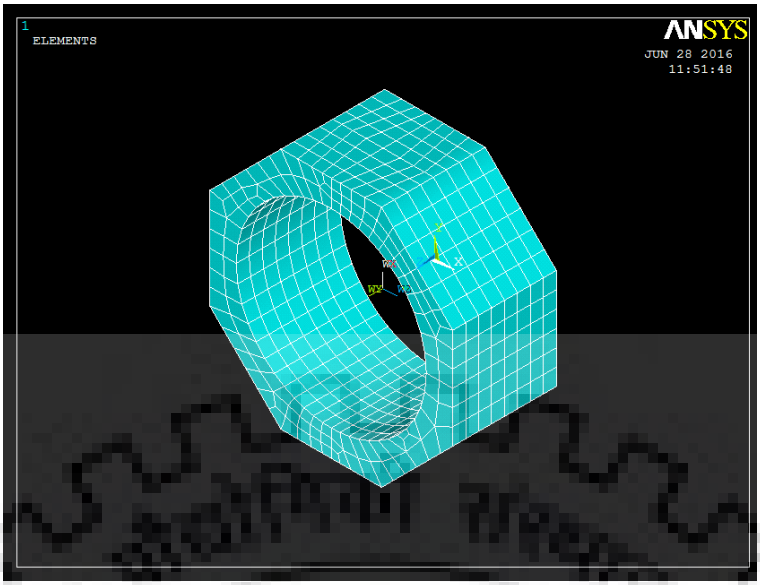

Fig. 3-4 Meshed model of octagonal ring

The important parameters for the analysis were stress distribution across the ring, maximum strain and deflection. According to ring theory, (Karabay 2007, Yaldiz *et al.* 2007, Turgut and Korkut 2012, Uddin 2016) when the vertical force is applied, the external vertical surface is under tension and inside adjacent curved surface undergoes compressive strain. Under such loading the face inclined at 45^0 to vertical axis, experiences minimum strain. The von Mises stress plot in octagonal ring under static loading is shown in fig 3.5.

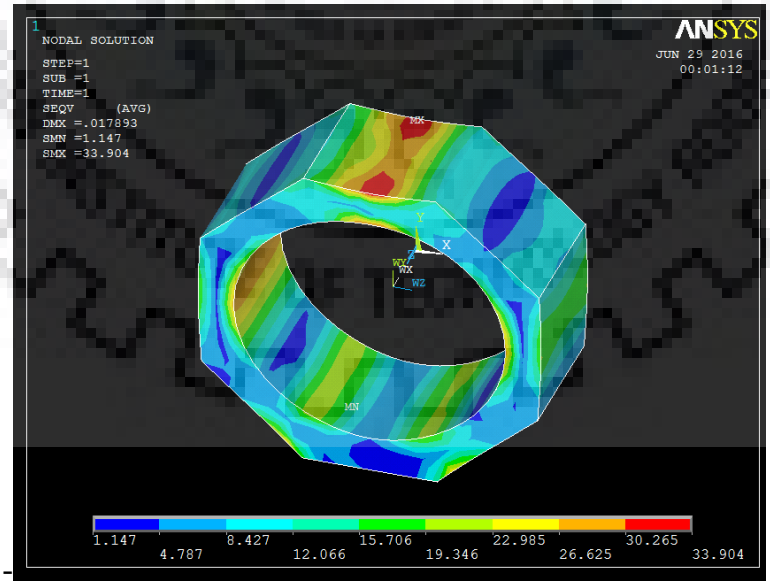

Fig. 3-5 von Mises stress in octagonal ring

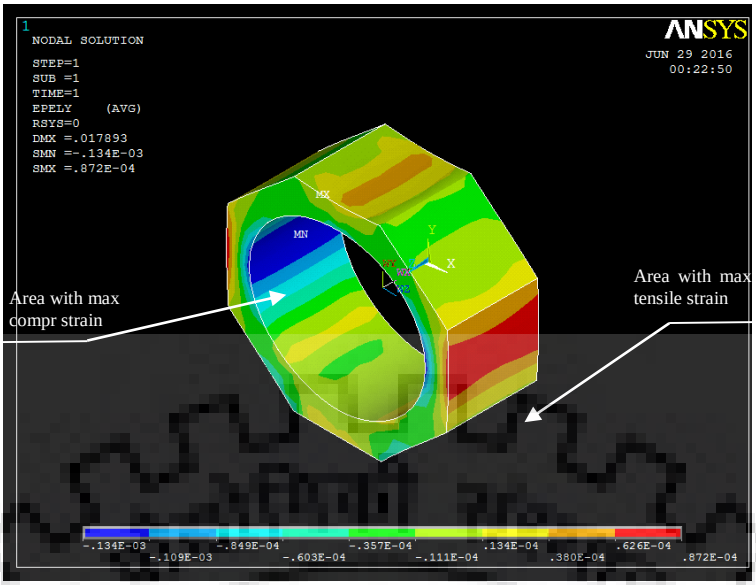

Fig. 3-6 Elastic strain in octagonal ring

The manual strain pick up was used to record the strain at various points on the strain ring. The finite element analysis indicated that the maximum tensile strain of 0.872 x 10^{-4} occurs at the center line of the vertical surface (at Y = 0) and the maximum compressive strain of 0.134 x 10^{-3} of occurs at the inside curved surface near the center line as shown in Fig. 3.6. The strain values registered on the outside and inside surface of the octagonal ring, with corresponding Y position with respect to center of the ring are plotted in Fig. 3.7 and Fig. 3.8. It was observed that, maximum strain occurs at the center line of the octagonal ring. Based on above observation, the strain gauges are affixed at these precise locations to ensure the maximum accuracy of forces to be measured.

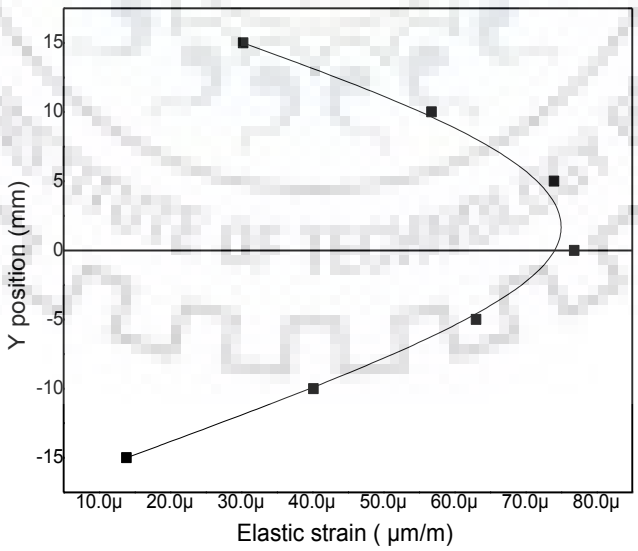

Fig. 3-7 Tensile strain on vertical surface of octagonal ring in Y direction

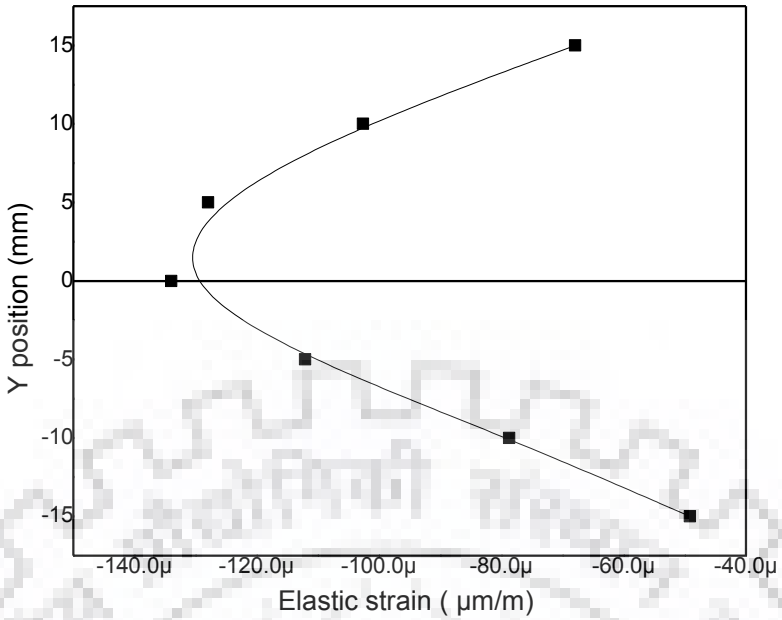

Fig. 3-8 Strain on inside curved surface of octagonal ring in Y direction

The elongation limit on strain gauges used is 5% on gauge length of 10 mm. This amounts to 0.5 mm and the maximum elongation as a result of 2000N load is 0.018 mm which well within the safe limit (Refer Fig. 3.9). Hence, the selected strain gauges can be effectively used in this design. The displacement plot is shown in fig. 3.9.

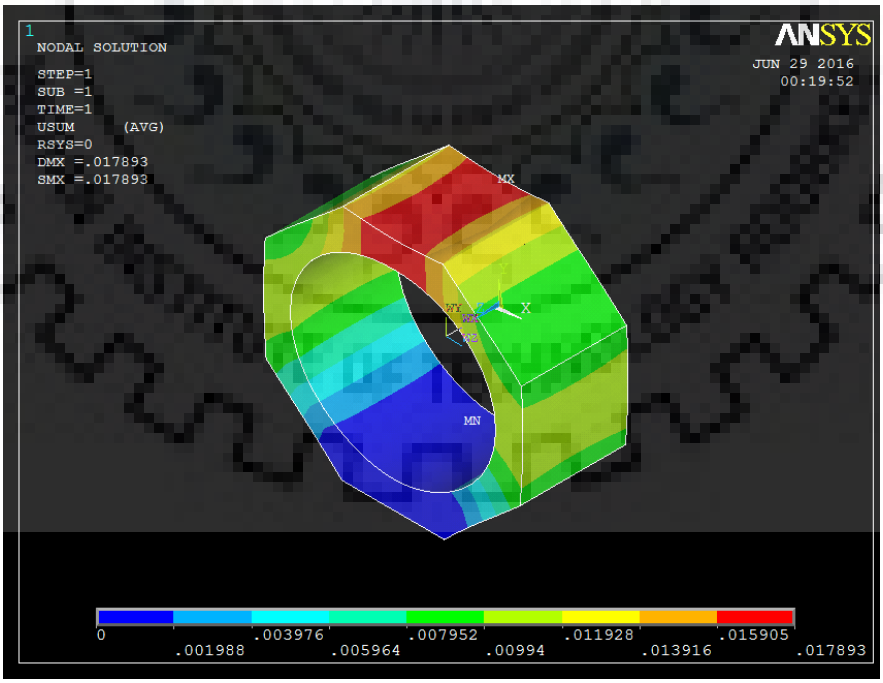

Fig. 3-9 Displacement plot

The deflection of elastic octagonal rings is sensed using bonded strain gauges and suitably amplified for a proper signal of the wheat stone bridge. Out of 16 gauges, eight strain

gauges are used for thrust force (shown in blue color in Fig. 3.10), while other eight are used for torque measurement (shown in red color on Fig. 3.10). Rohit, India make, Bakalite based strain gauge, type BKCT-10, 125.7 +- 0.2 ohms, with gauge factor 2.00 +- 2%, and gauge length 10 mm were used. The schematic of strain gauge arrangement are shown in Fig. 3.10. The strain gauges 3 and 4 were mounted inside the ring B vertically and 11 and 12 were mounted inside the ring D. These strain gauges experience compressive strain due to thrust force. Gauge 1 and 2 were mounted on outside vertical surface of ring A and 9 and 10 were mounted on outside vertical surface of ring C. These strain gauges experience tension due to thrust force.

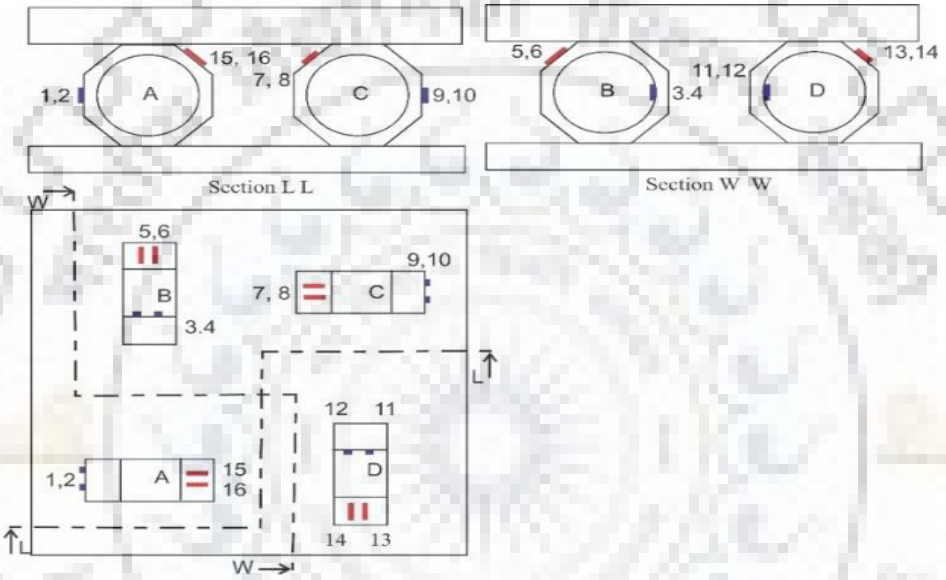

Fig. 3-10 Arrangement of strain gauges on octagonal rings

Gauges 7, 8 and 15, 16 were mounted at 45^0 angle to the horizontal on the outside of rings C and A respectively. These gauges undergo compressive strain due to torque. Gauges 5, 6 and 13, 14 were mounted at 45^0 angle to the horizontal on the outside of rings B and D respectively. These gauges undergo tensile strain due to torque. One full bridge circuit for thrust force and another full bridge circuit for torque were realized as shown in Fig. 3.11 (a) and (b). The bridge output was connected to an eight channel data logger (Make – Digitech, India, model no. MP31C08SM). Data acquisition was realized by connecting data logger to a computer through serial port connection.

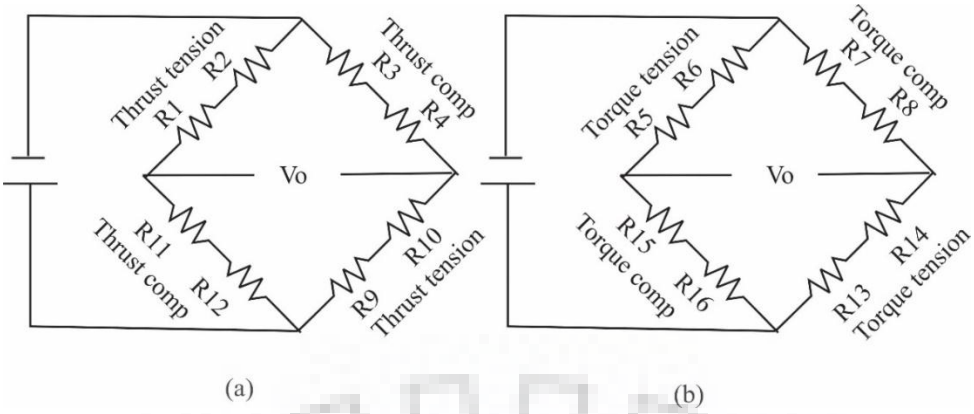

Fig. 3-11 Wheatstone bridge circuit for (a) thrust measurement and (b) torque measurement

The accuracy of cutting force measurement is very important in qualitative analysis of trepanning process. The safe and secure mounting of 100 x 100 x 40 mm work piece on the top plate of the dynamometer was realized by designing a fixture to be clamped on the dynamometer top plate. The work piece was located and secured at the center such that all degree of freedom were locked. Two mild steel plates were machined to create a stepped seat for the work piece. These plates were mounted opposite each other to provide rigid base for the work piece. Due to stepped design, a space 10 mm height was available between the bottom face of the work piece and top plate of the dynamometer. This space was provided for dropping of the trepanned core and for providing exit space for the trepanning tool after completing the trepanning depth. The work piece was kept on the step plates placed 100 mm apart, locking its movement in lateral direction. Two clamps with 12 mm size bolt were used on other two sides to clamp the work piece in its seat.

3.3 Design of trepanning tool

The procedure followed for design and development of trepanning tool suitable for deep annular groove of 40 mm diameter is discussed below.

In many engineering applications, there is a requirement of drilling holes or grooves with diameter greater than 40 mm. In such cases, it is not economical to produce these holes by conventional drilling. As hole size increases, it is also useful to preserve central core by cutting annular grove, rather than converting entire hole volume into chips. Moreover, there are few applications such as such as ‘O’ ring and strain gauge rosette fittings where large size annular rings are required (Giri and Mahapatra 2017). There is no standard tool available to produce these kind of annular rings.

These kind of annual grooves are produced using hole saws in metal sheets of thickness less than 5 mm. This hole saw method is not suitable for thicker plates (Shaw 2005). Few

researchers (Mathew *et.al* 1999, Rakesh *et al.* 2011 and Debnath *et al.* 2016) have successfully developed trepanning tool for cutting composite material. They studied the effect of tool geometry on delamination of composites. Few companies like SANDVIK have developed T-Max family cutters for trepanning process (SANDVIK). This tool recovers lesser material due to minimum 13 mm width of annular ring. Giri and Mahapatra (2017) used a single insert tool to cut 40 mm diameter and 5 mm deep groove in stainless steel work piece as shown in Fig. 3.12. They reported the failure of tool due to high level of vibrations and un-sufficient strength in insert clamping arrangement provided in the tool design as shown in Fig. 3.13. The opening to tool lips under action of cutting forces was observed.

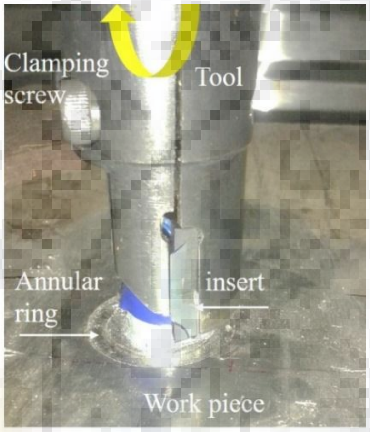

Fig. 3-12 Single insert tool for cutting annular groove (Giri and Mahapatra 2017

Fig. 3-13 Failed of single insert tool

Strain gauge rosette fittings in studies of stress relieving of welded parts, annular grooves required for fabrication of tie rod type cylinders etc. requires annular groves / hole generation of 40 mm or more diameter. Therefore, objective of this work is to design a trepanning tool producing lower cutting forces with high material recovery. The review of studied literature suggests unavailability of well-defined standard procedure for designing a new trepanning tool for cutting deep annular grooves. As there is no standard design procedure available, this work follows the methodology as shown in Fig. 3.14 for design and development of trepanning tool.

This work uses simulation based methodology over experiment based methodology to design trepanning tool. Therefore, CAD model was created for tool and work piece followed by Smoothed Particle Hydrodynamics (SPH) simulation using LS-DYNA under different parametric conditions.

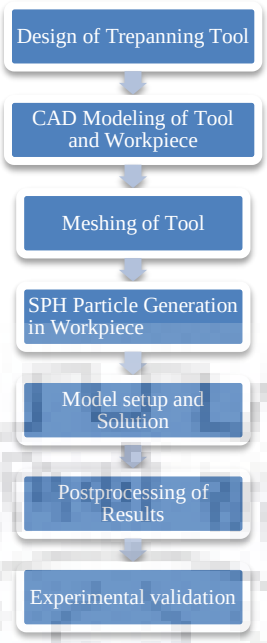

Fig. 3-14 Methodology used in design and development of trepanning tool

3.4 Development of trepanning tool

The important motivation for new trepanning tool design was to have more material saving than commercially available trepanning tools. These tools had a very large lip thickness of 13 mm, meaning the difference in outer and inner radius of tool was 13 mm minimum, thus effectively only a smaller size core could be recovered after trepanning. This material saving is significant, when we consider production of holes of diameter 40 mm and above. If a new trepanning tool, with smaller insert width and less lip thickness is used, lot more materials could be saved in the form of core of larger diameter. For example, for a 40 mm dia hole, effective core retained is of 40-26 i.e. of 14 mm only. However in new proposed design, the saved core diameter could be 40-30 i.e. 20 mm. This is a lot of saving, when quantities to be machined are large and material is costly.

The primary requirement of the trepanning tool was to be able to trepan a hole of 40 mm diameter in 40 mm thick stainless steel 304 plate. In order to design a tool for maximum material recovery, it was necessary, to first choose suitable carbide insert, with width small enough to cut minimum material in the form of annular ring. At the same time, the insert width should be sufficient to withstand cutting forces generated during trepanning. The width of the insert directly defines the amount of material saved as well as amount of material directly converted into chips. On one hand, higher width of insert means less material saving and more material to be removed, higher cutting forces and lower material removal rate. In case a very thin insert is chosen for the tool, the rigidity of the tool would be less and would result in

weaker tool, prone to stress failure. Considering this, few standard insert manufacturers catalogues were referred for selection of insert size, tool geometry and grade of coating used on the insert.

3.5 The selection of insert geometry, sizes and type of coating

3.5.1 Cemented Carbide

Cemented carbide is a popular material for fabricating cutting tools. It includes fine carbide particles which are cemented into a composite by a binder metal. Tungsten carbide (WC), titanium carbide (TiC), or tantalum carbide (TaC) are commonly used aggregates in cemented carbides.

Carbide tools permit faster machining of materials, compared to high speed tool steels and other tool steels. Carbide tools also give better surface finish compared to HSS tools. Carbide tools can be used at high temperatures typically observed at the tool chip interface. This ability results in their faster machining capability. Carbide is a preferred tool material for machining of tough materials viz carbon steels or stainless steel, also in situations where other cutting tools experience higher tool wear rate. They are a preferred choice for mass production of components.

3.5.2 Cemented Carbide Inserts

Carbide inserts find its application in machining wide range of materials such as steels, stainless steels, non-ferrous materials and high temperature alloys. Carbide tools can be designed in the form of indexable bits. Improved surface finish at higher cutting speeds can be obtained with carbide inserts. Cemented carbides are in the form of metal matrix composite (MMC). In MMC, metallic binders binds the carbide particles which acts as the aggregate for making the matrix. During sintering, the binder enters the liquid stage and carbide grains (much higher melting point) remain in the solid state. The properties of this MMC can be varied by altering the composition of aggregate and matrix material. The brittle behavior of carbide ceramic is compensated by naturally ductile metal binder. This increases its durability and toughness. These parameters of carbide may be changed significantly by varying grain size, cobalt and carbon content.

Carbide inserts and tools are more costly than conventional high speed tool steels and other tool materials. Due to their brittleness, they are prone to breaking or chipping when subjected to vibrations and impact loads in machining operations. It is generally not preferred to make the entire tool from cemented carbide. In most tool designs, carbide inserts are brazed or clamped to the tool body or shank, which are made from carbon tool steels like 4140 steels.

This type of tool design where carbide tips do the machining and body is from tougher materials, reduces the cost of the tool as well as imparts shock absorbent capacity to the tooling system.

3.5.3 Coated Cemented Carbide Inserts

Every machining process, to some extent causes the tool to wear and use of worn tools may lead to rejection of components, due to parts produced with wrong dimensions or increased surface roughness. Tool wear also increases vibrations and cutting forces. The process yield also gets reduced due to reduced material removal rate. Providing a thin layer of hard coating materials over carbide tool, is very common practice to increase tool life and reducing wear. A wide variety of coating combinations are commercially available and even custom designed coating layers can also be used to take care of specific machining requirements. Standard popular coating used in machining is titanium nitride, titanium carbide, titanium carbide-nitride and titanium aluminum nitride (TiN, TiC, TiCN and TiAlN). Coating on tools escalates tool's hardness and/or lubricity (Heinemann & Hinduja 2009). A coating disallows the material gall/stick on the cutting edge of a tool by passing smoothly through the material, without having the material gall or stick to it. The coating reduce the temperature at the tool chip interface in cutting zone and helps in improving the life of the tool.

Mainly two main coating processes are used for carbide inserts viz Chemical Vapor Deposition (CVD) and Physical Vapor Deposition (PVD). Each method provides different features and benefits. CVD coatings are highly wear resistant. They are widely used in machining of different grades of steel and cast iron. Usually CVD coating have a typical thickness range of 9 – 20 µm. However, these coatings have disadvantages. They compromise edge toughness (Lacalle *et al.* 2011).

PVD coatings typically have less thickness compared to CVD coatings. Usually PVD coating have a typical thickness range of 2 - 4 µm. PVD coating is tough and smoother compared to CVD coatings. PVD coated tools / inserts are extensively used in machining of super alloys, titanium alloys and difficult-to-machine stainless steels (Lacalle *et al.* 2011).

3.5.3.1 Chemical Vapor Deposition (CVD) Coatings

CVD-coated carbide inserts are preferred in many machining operations. They are very suitable for turning, milling and drilling of ferrous metals.

Chemical vapor deposited coating exhibit following desirable properties.

Titanium Nitride (TiN) Coatings

TiN coatings resist formation of build-up edge while machining and hence are good for machining of gummy materials. They are good for threading and cut-off operations. Identification of used edge / corner is easy. They operate effectively at lower cutting speeds

Titanium Carbide (TiC) Coatings

TiC coatings have excellent wear resistance and are effectiv at medium speeds. They are suitable of machining of abrasive materials

Aluminum oxide (Al_20_3) Coatings

Al_20_3 coatings possess excellent crater resistance and operate effectively at high speeds and high heat conditions.

3.5.3.2 Physical Vapor Deposition (PVD) Coatings

PVD-coated inserts are very suitable for machining of titanium alloys and stainless steel and high-temperature alloys. They can be used effectively used in turning, milling and drilling applications.

Characteristics of PVD Coating Types:

Titanium Nitride (TiN) Coatings

TiN coatings resist formation of build-up edge while machining and hence are good for machining of gummy materials like austenitic stainless steels and high-temperature alloys.

Titanium carbide-nitride (TiCN) Coatings

These coating are harder as compared to TiN coatings. These coatings are popularly used in milling where the work material is abrasive.

Titanium aluminum nitride (TiAlN) Coatings

TiAlN coating are more stable and harder and they are preferred in machining of high temperature alloys and stainless steels.

3.5.4 Advantages and disadvantages of Indexable inserts

Advantages

a) Indexable inserts have more than one cutting edges. The cutting edges can be renewed by unclamping and flipping the insert to bring a new cutting edge into action. Round inserts may have entire periphery as a cutting edge. Inserts in a tool can be replaced without disturbing the machining set ups.

b) Very high production rate can be achieved by using indexable inserts tool

c) Very precise and accurate machining process.

d) Large variety of material can be machined by simply changing coating on the inserts, making them very user friendly.

Limitations

a) Clamping mechanism and screws may get damaged. Tightening torque is relatively low in comparison with the level of force that has to be applied.
b) High stress occurs mainly in tightening or loosening of fasteners which fastens inserts. This develops stresses in tool.
c) Relatively high cost as compared with conventional tooling.

Titanium carbon nitride (TiCN) coating provides harder coating than TiN. This type of coating is effective on turning, drilling and milling. It provides enhanced abrasion resistance with uniform coating, making it good choice for drilling of stainless steels.

Titanium aluminum nitride (TiAlN) coating provides high hardness and oxidation resistance under high temperatures**.** This coating is very effective in easy chip formation and provides better surface finish of work piece. It also provides additional strength to substrate material. TiAlN coated drills are used in drilling of stainless steels owing to its superior properties in terms of adhesion, wear resistance, surface finish and chip formation,

Considering above information, inserts with 4 mm width and 20 mm height were finalized. Three different grades of inserts TT 9080, TT 8020 and TT 7220 were selected for use in the trepanning tool. TT 9080 inserts were AlTiN multilayer coated with physical vapor deposition method. The coating thickness of this coating is 4-6 μm. TT 7220 inserts were monolayer coated with physical vapor deposition method. The TT 8020 inserts have TiCN coating deposited with physical vapor deposition method. Since each coating has some specific positive influence on the performance of trepanning operation, it was expected that the coating materials will have different effect on response variables such as the thrust and torque, surface roughness and material removal rate.

The next step was designing the tool body to properly hold these inserts in place while the tool is given desired cutting speed and feed.

The first design concept was realized by considering use of three equi-spaced parting inserts to ensure that there are no unbalanced forces on the tool while machining. This unbalance of forces and resulting wobbling of the cutter was experienced by single insert cutter (Giri and Mahapatra 2017).

The three insert concept is shown in Fig. 3.15. The tool body was manufactured in die steel. In this design, each insert was clamped in carefully machined insert slots, having the

profile of inserts used. The inserts were fitted with sliding fit in the slot. Holes were provided in the front lip to the insert slot and 3 mm size tapping was done in the hole for fitting of grub screw. Since this threaded hole was drilled on curved surface of the tool body, at most care was taken to ensure that this hole does not tear off the front lip.

Fig. 3-15 Trepanning tool

The inserts were secured in its position with the help of 3 mm diameter, 8 mm long grub screw. The insert slot is designed in such a way that, when the tool is rotating, the inserts upward movement under thrust loading is blocked by the upper face of insert slot. A 3 mm grub screw exerts locking pressure at the middle of the insert length. This combined arrangement ensures that the insert doesn't slip from the seat and remains in its proper cutting position during trepanning operation. This arrangement is shown in Fig. 3.16.

This tool had a shank length of 110 mm and diameter of 32 mm. The shank fits into a standard BT40 adapter suitable for CNC vertical machining center. The length of the body was kept as 90 mm to provide large window in cutter body to provide for easy passage for the chips produced, as shown in Fig. 3.15. Trial experimentation was conducted with this tool. This tool design failed during initial trials due to insufficient strength because of larger overhang of the tool holder in machine spindle. The failed tool is shown in Fig. 3.17.

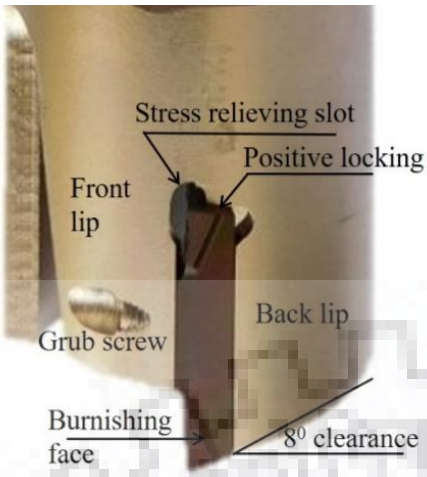

Fig. 3-16 Enlarged view of insert clamping region

Fig. 3-17 Failure of three insert tool

After failure of initial design, another design was proposed with the modifications to overcome failures observed in initial design. During this process, it was planned to use simulation based approach to validate design virtually and minimize number of experiments (Bagci 2011, Pantel *et al.* 2012, Arrazola *et al.*2013). The use of FEA in new tool design provides opportunities to predict the effects of changes in geometry of the designed tool, process parameters, material properties or other machining constraints without conducting costly machining trials. In this work, numerical simulations were performed using Smoothed particle hydrodynamics (SPH) method within LS-DYNA software. In the subsequent design, two modifications were proposed i.e. length of the tool was reduced from 90 mm to 75 mm, reducing the overhang of the tool and secondly, two inserts were used, in place of three equi-spaced inserts. Two insert design increased the strength of the tool body. The inserts were positioned diametrically opposite.

The tool body has 40 mm external diameter and 32 mm internal diameter and has provision for mounting two carbide parting inserts in diametrically opposite position. The mounting of inserts in such fashion helps in balancing of cutting forces and uniform contact with the work piece. The CAD model of trepanning tool is shown in Fig. 3.18 (a) and that of the insert used is shown in Fig. 3.18 (b). Effectively, this tool has 4 mm thick body to hold the inserts in position. The tool uses parting inserts of size 4 x 4 x 20 mm and fitted into slot of the tool body. These insert slot forms a lip just ahead of insert and one behind the insert. The front lip ahead of insert also acts as chip breaker and as a guide for long curly chips, if any.

The front lip also provides support to insert against the resistance offered by work piece. The back lip behind the insert offers support to maintain the proper position. The circular space

between two lips provides chip evacuation passage when the chip gets accumulated during cutting and directs the chips in the inner hollow space in body. A relief angle of 8^0 is provided on the insert and similar profile is given to body lip to avoid fouling of the tool over machined groove. The side faces of the insert do not cut the material but they provide burnishing action on the previously machines side walls of annular grove. This burnishing action improves the surface finish of the hole produced.

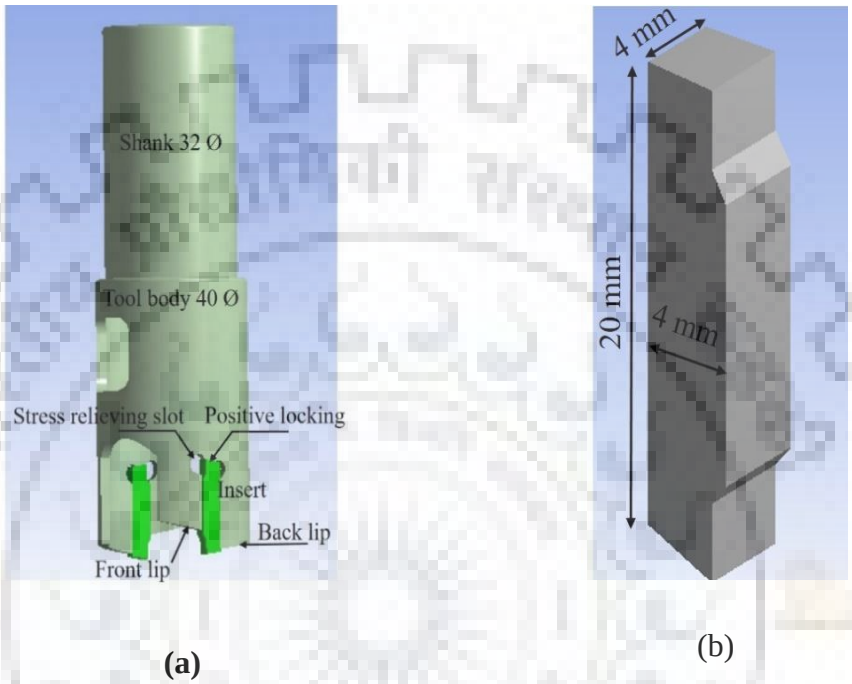

Fig. 3-18 (a) CAD model of trepanning tool with two inserts (b) CAD model of insert

3.6 CAD modeling of the trepanning tool:

The conceptual design of tool was realized in computer aided design using commercially available three dimensional modeling software SOLIDWORKS. The dimensional and geometrical details of the design concept were carefully considered in CAD model of the tool. The solid model of approximate geometry of the insert being used was also prepared. The assembly of the insert and tool body was made considering the required constraints. The upper edge of the tool insert slot was designed without any sharp corners and provision is made for stress relieving where the insert's upper cutting edge rests in the cutter body. When the tool makes initial contact with the stainless steel work-piece, initial impact load acts on the insert which is transferred on the cutter body. When the insert and tool body rotates and is axially fed into the work-piece at feed rate for material removal, the insert and tool body is under continuous compressive load. This loading is likely to cause stress concentration at sharp corners in insert slot. Stress relieving slots in the body absorbs these stresses and helps in avoiding tool body failure under impact loading, as well as fatigue loading

of the tool body. Material for tool body was selected as 4140 steel. This is a low alloy steel containing manganese, chromium and molybdenum. This material is a popular for tool manufacturing due to its useful properties like toughness, high fatigue strength and high abrasion resistance and impact resistance.

3.7 Modeling and simulation of trepanning process:

The use of numerical methods for predicting the outcome of the machining / mechanical deformation including drilling is not new. Many researchers Bagci (2011), Hongbing *et al.* (2012), Pantel *et al.* (2012), Wu *et al.* (2012), El-Bahloul *et al.* (2018), Abdelhafeez *et al.* (2016), Gyliene (2013), Hossainy *et al.* (2001), Wang *et al.* (2012), Gok *et al.* (2013), Bajpai *et al.* (2014) and Lautre *et al.* (2015) used FEA for simulation of their work. Other researchers like Biswas *et al.* (2007, 2011, 2012 and 2016), Li *et al.* (2009, 2016), Pandey *et al.* (2018) have used simulation approach to predict the outcomes of friction stir welding, ultrasonic assisted welding process etc. Literature review reveals that researchers have extensively used Finite Element Method (FEM) based numerical models in metal cutting using commercial softwares such as ANSYS, Abaqus, Marc, Nastran, LS-DYNA, Deform, Forge, Advantage, etc. Review also indicates that there are several methods to simulate machining processes. These approaches include:

- Lagrangian method (Pantel *et al.* 2012, Gok *et al.* 2013, Li *et al.* 2016)
- Eulerian method (Saunders *et al.* 2013)
- Arbitrary Lagrangian and Eulerian (ALE) method (Hongbing *et al.* 2012, Wu *et al.* 2012, El-Bahloul *et al.* 2018)
- Coupled Eulerian-Lagrangian (CEL) method (Abdelhafeez *et al.* 2016)

The material movement in continuum mechanics can be defined by Lagrangian and Eulerian methods. The other two methods, i.e., ALE and CEL are variations of the first two methods where combinations of both the methods are used to overcome the limitations of individual methods. It is also observed that mesh based techniques are widely used in numerical models in simulation of metal cutting process. However, mesh-free methods are also used in simulation of metal cutting processes. Most recent approach is mesh-free methods such as Element-Free Galerkin (EFG) (Yadava and Patil 2007, Yadava *et al.* 2007, Yadava and Judal 2013) method and Smoothed Particle Hydrodynamics (SPH) method (Bagci 2011 and Gyliene 2013). The present work uses SPH method, which does not require a computational grid to perform simulations. Rather, SPH operates by representing the material as a group of Lagrangian particles. Using SPH, a user no longer needs to be wary of mesh (size, smoothing

and tangling) or chip separation criterion, which is essential in other formulations during simulation of metal cutting process.

SPH is a Lagrangian technique that was initially developed in the 1970's as a means to simulate astrophysical phenomena (Bagci 2011). In SPH, a kernel approximation is used to calculate spatial derivatives within randomly distributed interpolation points as indicated in Fig. 3.19. A function f(r) can be thus estimated by the relation:

$$f(r) = \int_{\Omega} f(r')W(r - r', h)d\Omega_{r'} \quad (3.8)$$

Where $W\ (r - r', h)d\Omega_{r'}$= kernel function which can be Gaussian, polynomial, spline, etc.

h = smoothening length which defines a domain containing particles in interaction with particle *i*.

The value of a function at a particle *i is* approximated using the values of the functions at all the particles that interact with particle *i*. The continuous volume integrals are written as sums over discrete particles using Eq. 3.8:

$$f(r_i) = \sum_{j=1}^{N} \frac{m_j}{\rho_j} f(r_i)W(r - r', h) \quad (3.9)$$

Where

m_j and ρ_j are the mass and density of each particle, respectively.

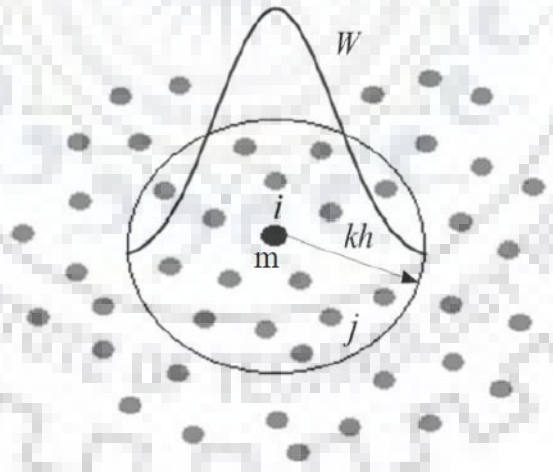

Fig. 3-19 SPH Kernel function

Numerical model used in SPH simulation of trepanning process is shown in Fig. 3.20. Tool is considered as a rigid body and does undergo any deformation. Tool is meshed with hexahedral solid elements. Work piece is meshed with SPH particles. Table 3.2 shows statistics of SPH model. The tool is considered as a rigid body and is not undergoing any stresses and deflection in simulation (Singh *et al.* 2013). There is no point in meshing the entire tool body including the shank. Hence, to reduce the number of elements and thus overall computational

efforts, tool was meshed only in the insert holding region till the chip removal slots, as shown in Fig 3.20.

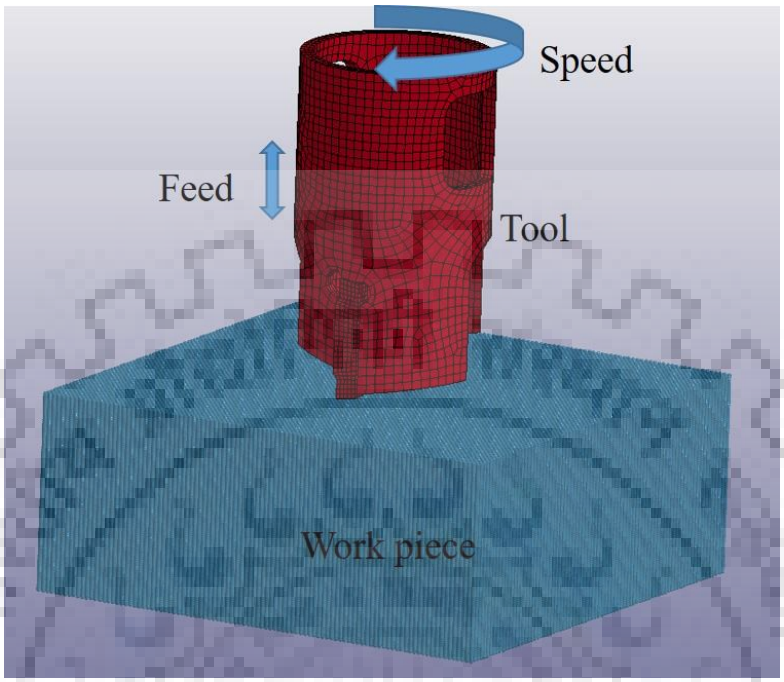

Fig. 3-20 Numerical model used in SPH simulation

Table 3.2 Statistics of SPH model

	Size	**Type of Body**	**Type of Element**	**No. of Elements**	**No. of Nodes**
Tool	ϕ 40 mm	Rigid	SOLID	5638	8580
Workpiece	100 x 100 x 40 mm	Flexible	SPH	800000	800000

Total 800000 SPH particles were created with mass of each particle as 0.000004 kg by keeping mass of work piece as 3.2 kg. Due to closeness of SPH particles, workpiece is appearing as continuum body but it is not. Fig. 3.21 shows the zoomed view of workpiece particles.

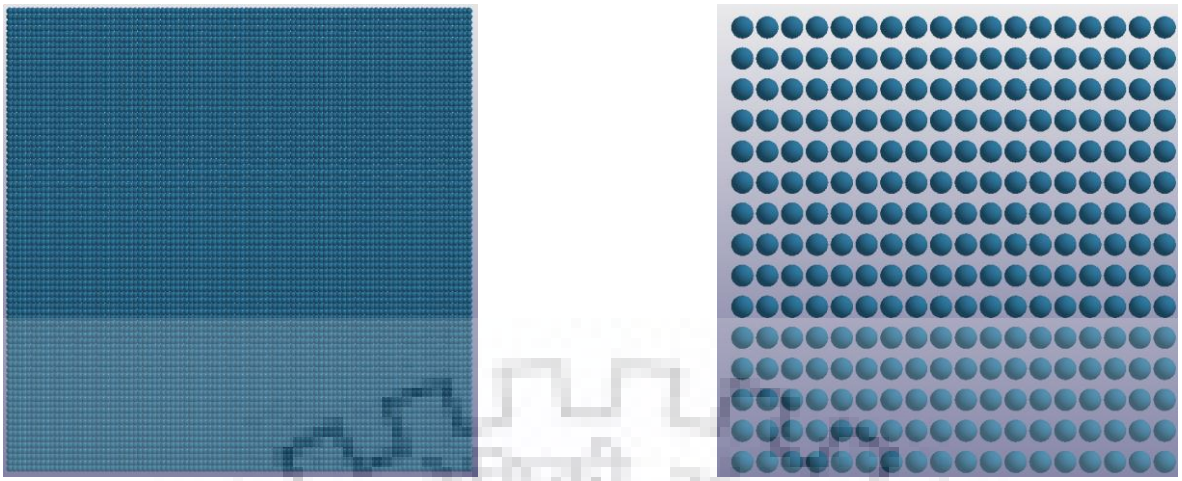

(a) **(b)**

Fig. 3-21 SPH particles in workpiece (a) Top view of complete work piece (b) Zoomed view at corner

Table 3.3 shows tool and work piece material properties used in SPH simulation. Johnson-Cook (J-C) material behavior is widely used by researchers during simulation of metal cutting processes (Nahshon *et al.* 2007, Gupta *et al.* 2013, Krasauskas *et al.* 2014). Therefore, SPH simulations in this work considers work piece material behavior using J-C model. Parameters of J-C model are obtained from literature as given in Table 3.3 (Krasauskas *et al.* 2014). In simulation of trepanning process, work piece is fixed at bottom and tool is given speed and feed.

Table 3.3 Material properties of Work piece and carbide insert (Krasauskas *et al.* 2014)

Parameter	**Work piece (SS 304)**	**Insert (Carbide)**
Density (kg/m^3)	8000	15000
E (GPa)	207.8	800
Possons ratio	0.3	0.2
Material model	Johnson-Cook	Rigid

The Johnson-Cook model is popularly used to describe the stress strain relationships in metals, when material is subjected to large deformations, high strain rates and typically high temperatures as in case of tool chip interface. J-C model is very popular in predicting flow behavior of materials. The flow stress model is expressed as follows:

$$R = [A + B\mathcal{E}^n] + \left[1 + C \ln\left(\frac{\dot{\epsilon}}{\dot{\epsilon_0}}\right)\right]\left[1 - \left(\frac{T - T_0}{T_f - T_0}\right)^m\right] \qquad (3.10)$$

Where σ is the equivalent stress, and ε is the equivalent plastic strain.

A, B, n, C and m are material constants.

A (MPa) - Yield stress of the material under reference conditions

B (MPa) - Strain hardening constant

n - Strain hardening coefficient,

C - Strengthening coefficient of strain rate,

and m - thermal softening coefficient

The first parenthesis in above Equation (3.10) represents the strain hardening effect. The second parenthesis represents, the strain rate strengthening effect and the third parenthesis indicates temperature effect, which influences the flow stress values of the material.

$$\dot{\epsilon^*} = \frac{\dot{\epsilon}}{\dot{\epsilon_{ref}}}, \qquad T^* = \frac{T - T_{ref}}{T_m - T_{ref}}$$

where ε^* is the dimensionless strain rate,

T^* - Homologous temperature,

T_m - Melting temperature of the material,

and T - Deformation temperature.

ε_{ref} and T_{ref} are the reference strain rate and the reference deformation temperature, respectively In the present study, regarding the experimental conditions, the reference strain rate, ε_{ref}, and the reference temperature, T_{ref}, were taken as 1223 K and 1 s−1, respectively.

Table 3.4 Johnson Cook material properties for SS 304 (Krasauskas et al. 2014)

A (MPa)	**B (MPa)**	**n**	**C**	**m**	**ε_0 (s^{-1})**	**T_f (K)**	**T_0 (K)**	**D1**	**D2**	**D3**	**D4**	**D5**
280	802.5	0.622	0.0799	1	1	1873	298	0.69	0	0	0.0546	0

To simulate trepanning process, work piece is fixed at bottom and tool is given speed and feed. Tool speed and feed is defined using *BOUNDARY_PRESCRIBED_MOTION. As tool starts cutting operation, the contact between tool and work piece particles have been defined using automatic node to surface i.e.

*CONTACT_AUTOMATIC_NODES_TO_SURFACE. LS-DYNA input file is divided into following two blocks and input file must begin with *KEYWORD and end with *END:

- Control block: This block is used to define solution control and output parameters.
- Model block: This block is used to define elements, nodes, contact, boundary conditions, material parameters, etc.

For SPH particles, user should define *CONTROL_SPH, *SECTION_SPH and *ELEMENT_SPH whereas all other inputs are similar to Langrangian based simulations.

- *CONTROL_SPH: Used to define controls for computing SPH particles. This also defines space dimensions for SPH particles.
- *SECTION_SPH: Used to define section properties for SPH particles i. e., smoothening length and distance between SPH particles.
- *ELEMENT_SPH: Used to define elements and mass for SPH particles.
- Fig. 3.22 shows von-Mises typical stress contour plot obtained by SPH simulation. The maximum stress is 1.64 GPa for a typical case shown in Fig. 3.22.

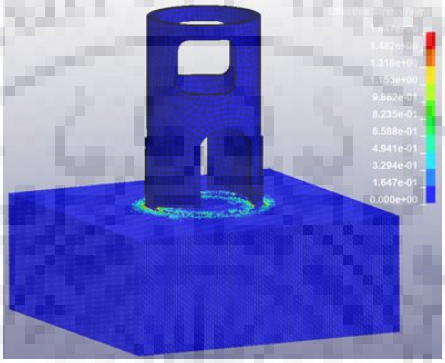

Fig. 3-22 Results of SPH simulation - von-Mises Stress Contours

As the material is fed into the work piece made up of SPH particles, it cuts the annular ring of 40 mm outer diameter and 30 mm inside diameter. The O-ring obtained during SPH simulation of trepanning process is shown in Fig. 3.23.

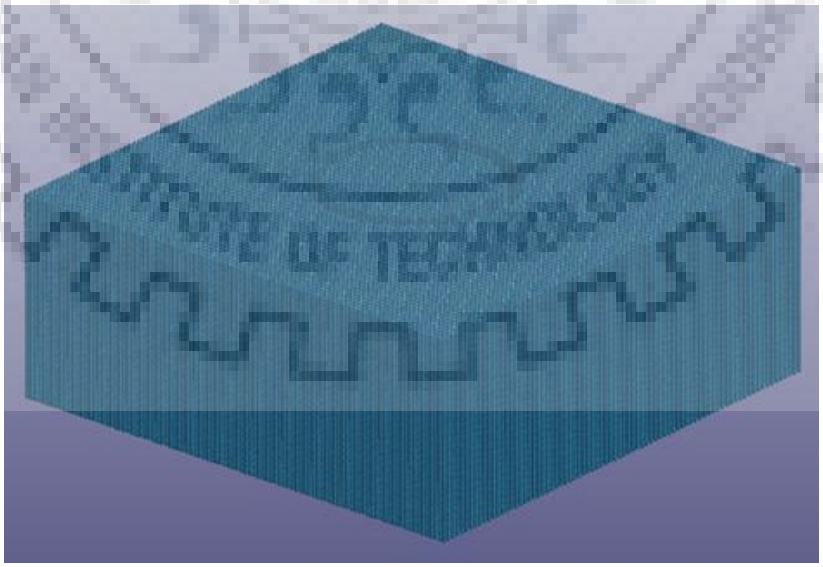

Fig. 3-23 Results of SPH simulation - O-ring formation after trepanning

The cut section taken during the SPH simulation, when the rotating trepanning tool is half way down the thickness of the work piece is shown in Fig. 3.24.

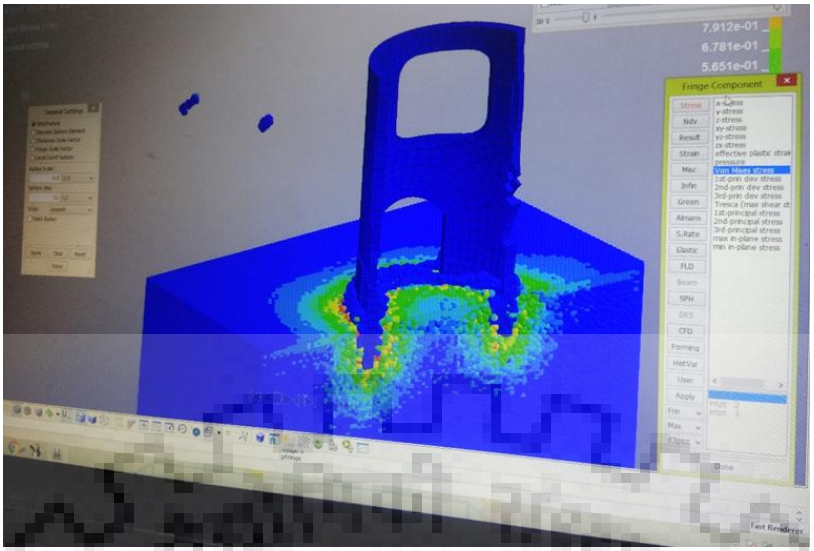

Fig. 3-24 Results of SPH simulation – midway representation

The actual cutting conditions for two set of experiments were implemented in mesh free simulation and the results were obtained. Two extreme cases of machining parameters i.e. the combination of highest level of cutting speed and feed rate as first case and the combination of lowest cutting speed and feed rate is considered for simulation. It was very important that the top surface of the work piece where trepanning tool makes first contact is perfectly horizontal and perpendicular to the machine spindle axis. This was ensured by checking the level with the help of spirit level as well as with filler gauges by just touching the tool insert on the top surface of the work piece. It is essential requirement to ensure that, both the inserts of the trepanning tool engage the work piece at the same time. Any error in this results in material re0moval by only one of the inserts, leading to unbalance in rotating tool as well as errors in the cutting force measurement. The resulting cutting forces namely thrust and torque were recorded through a data logger connected to the dynamometer Wheatstone bridge circuit.

The actual machining of the two cases simulated above were performed with designed trepanning tool. The thrust and torque were measured first using the octagonal ring type dynamometer developed in house for this experimentation. In second repetition of the experiments, the cutting forces were recorded using KISTLER dynamometer.

Table 3.5 Cutting speed and feed

Case	Speed (RPM) (m / min)	Feed mm/min (mm / rev)
Case 1	279 (35)	13.95 (0.05)
Case 2	199 (25)	5.97 (0.03)

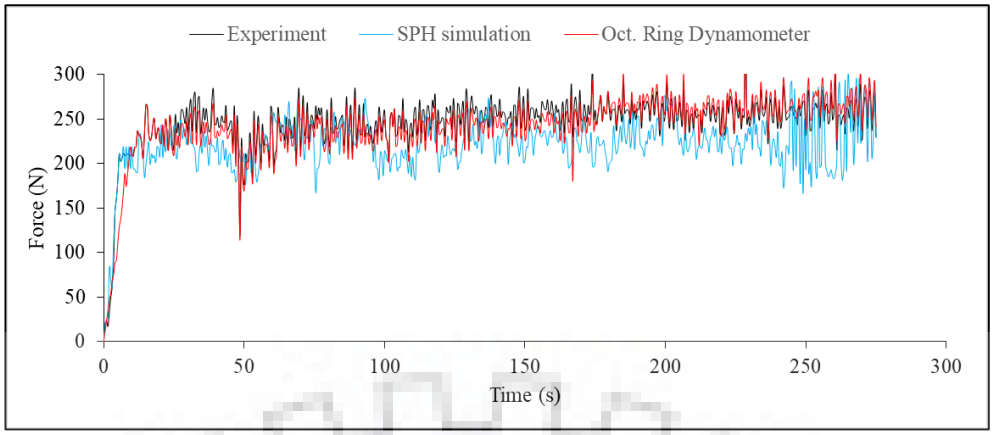

Fig. 3-25 Results comparison of thrust force for case 1

Magnitude of thrust force observed in simulation, as well as recorded values with octagonal ring type dynamometer as well as from that of KISTLER dynamometer are plotted in Fig. 3.25 for case 1. It is observed that, the thrust force was initially zero and gradually attain its average value. Once the continuous contact between the inserts and work piece is established, the thrust force stabilizes for the entire thickness of the work piece. It is observed that, the thrust fluctuates with time, around its mean value. Therefore, average value is used for further discussion. The average cutting force is 225 N for the cutting speed of 35 meters / minute (279 revolutions per minute) and feed rate of 0.05 millimeters / revolutions (13.95 millimeters / minute). The percentage error between simulation and experiments is less than 15%.

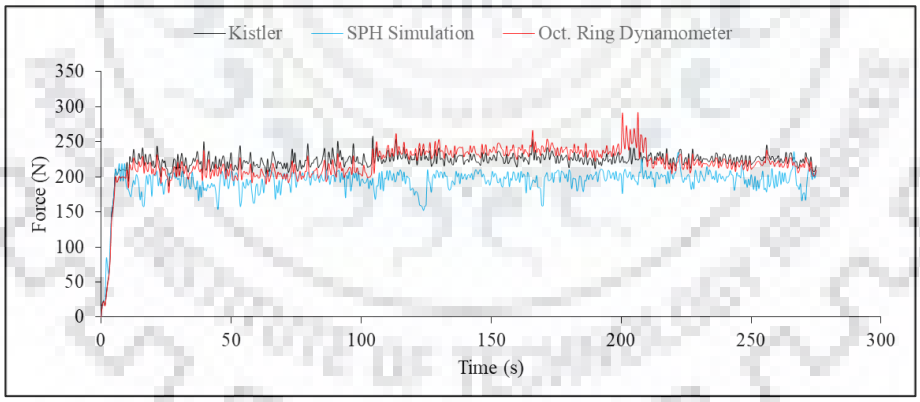

Fig. 3-26 Results comparison of thrust force for case 2

Magnitude of thrust force observed in simulation, as well as recorded values with octagonal ring type dynamometer as well as from that of KISTLER dynamometer are plotted in Fig. 3.26 for case 2. The average cutting force is 196 N was observed for the cutting speed of 25 meters / minute (199 revolutions per minute) and feed rate of 0.03 millimeters / revolutions (5.97 millimeters / minute). It is concluded that the thrust force increases with increase in the feed rate and cutting speed.

Similarly, the magnitude of torque is plotted using simulation results for two cases.

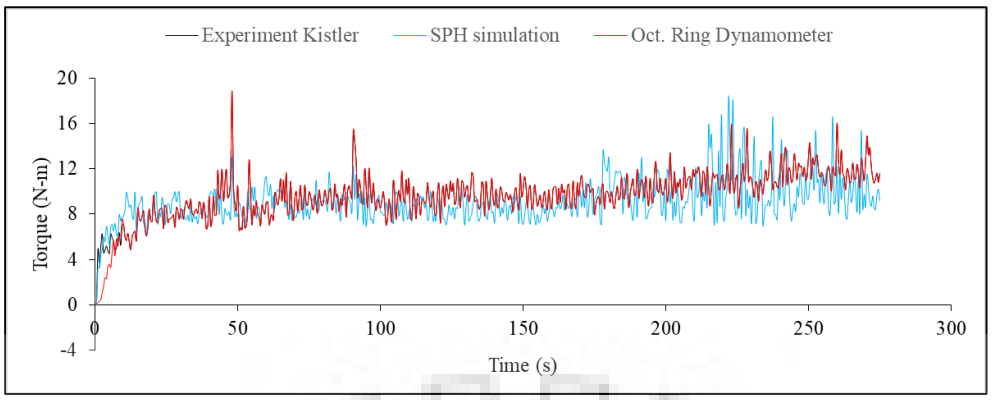

Fig. 3-27 Results comparison of torque for case 1

The Fig. 3.27 shows the comparison of simulated values of torque recorded at 35 m /min cutting speed and 0.05 mm / rev. feed rate, with the torque recorded by octagonal ring type as well as KISTLER dynamometer. The percentage error between simulation and experiments doesn't exceed 7%. The results of simulation as well as experiments are in agreement with fundamentals of machining theory.

It is observed that, the torque was initially zero and gradually attain its average value. Once the continuous contact between the inserts and work piece is established, the torque stabilizes for the entire thickness of the work piece. It is observed that, torque fluctuates with time, around its mean value. Therefore, average value is used for further discussion. The average torque is 9.21 Newton-meter for the cutting speed of 35 meters / minute (279 revolutions per minute) and feed rate of 0.05 millimeters / revolutions (13.95 millimeters / minute).

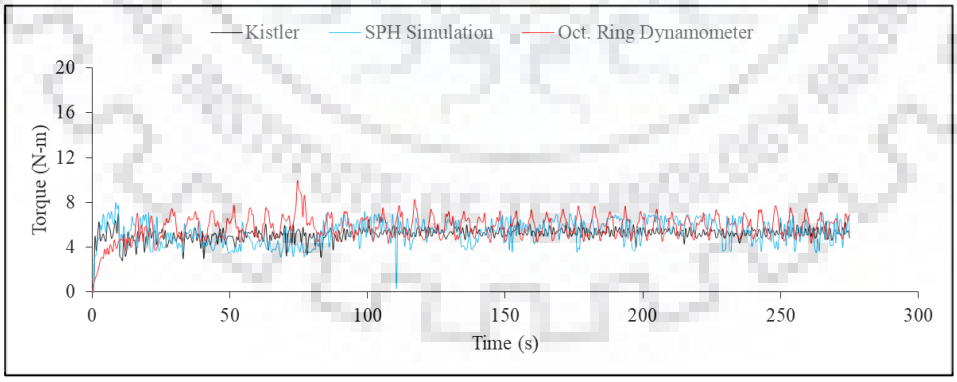

Fig. 3-28 Results comparison of torque for case 2

The comparison of simulated results of torque in N-m for case – 2 i.e. cutting speed of 25 m / min and feed rate of 0.03 mm / rev. are shown in Fig. 3.28. The simulation results are found to be in good agreement with the actual measured values of thrust force. The percentage error between simulation and experiments doesn't exceed 9%. The average torque is 5.34 Newton-meter was observed for the cutting speed of 25 meters / minute (199 revolutions per

minute) and feed rate of 0.03 millimeters / revolutions (5.97 millimeters / minute). It is concluded that the torque increases with increase in the feed rate and cutting speed.

This maximum value of cutting force and torque, obtained from mesh free simulation in LS DYNA software, is further used to study tool deformation using structural analysis in ANSYS. After determining cutting force and torque, structural analysis is performed on tool body to check strength of modified design. To perform structural analysis, detailed CAD model of trepanning tool body is imported in ANAYS as shown in Fig. 3.29 (a). This three dimensional geometry was meshed with BRICK elements as shown in Fig. 3.29 (b). The element size of approximately 1.5 mm was chosen. The meshed model of tool body contains 35094 elements and 129711 nodes. The tool body is made of 4140 steel and structural properties of tool body used in this simulation are given in Table 3.6. After meshing LBC's (Loads and Boundary Conditions) are applied as shown in Fig. 3.29 (c). The load values obtained for Case 1 were considered for this structural analysis as shown in Fig. 3.30.

Table 3.6 Tool body material structural properties

4140 Steel	
Young's Modulus	210 GPa
Poisson's ratio	0.3
Density	7800 kg/m^3
Yield Strength	758 MPa

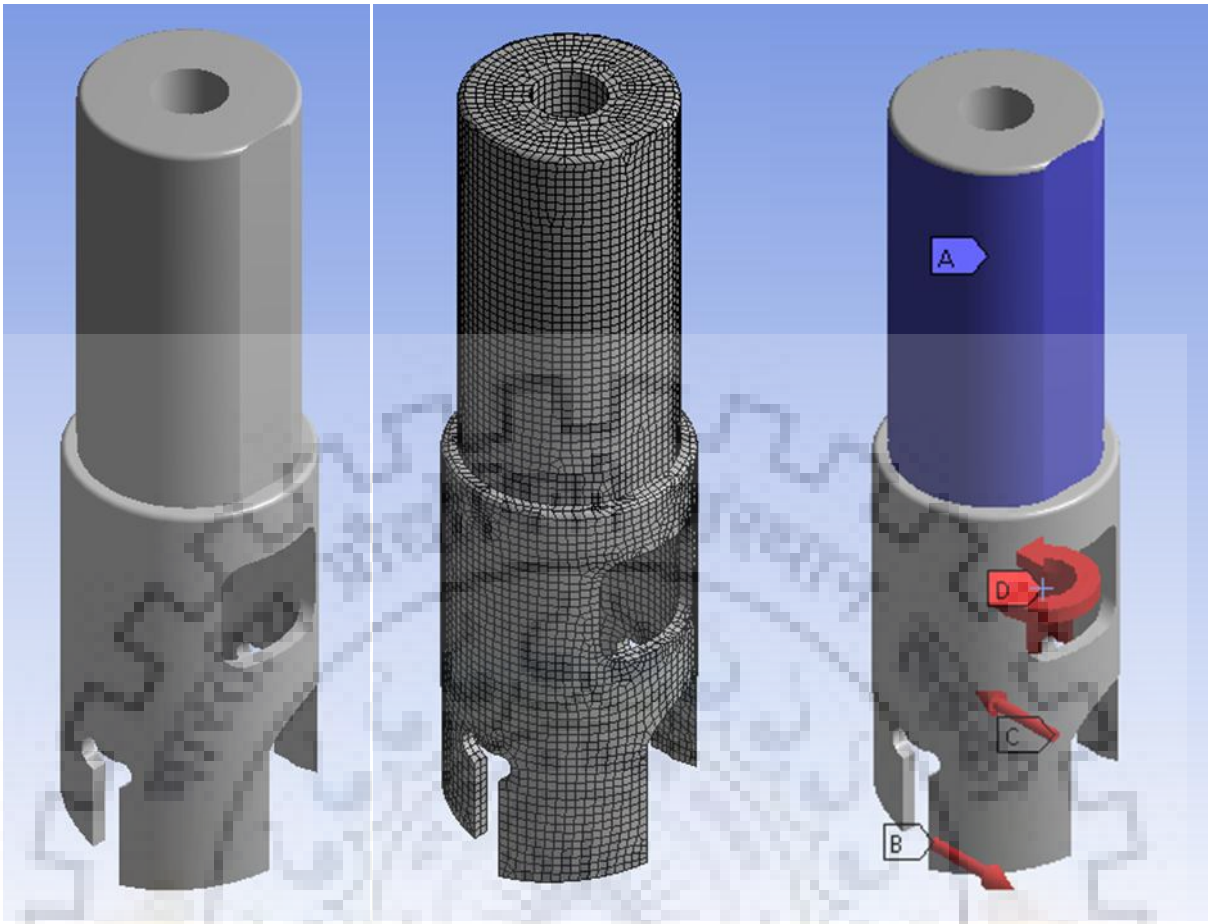

(a) **(b)** **(c)**

Fig. 3-29 Tool body FEA model for structural analysis (a) CAD model (b) Meshed model and (c) Load and boundary conditions

Fig. 3.30 shows the deformation and stresses in tool body. Tool deformation is 0.1136 mm whereas maximum equivalent stress is 268.34 MPa. Tool maximum deformation and stress in tool body is lower than failure limits. Moreover, it was observed that deformation was maximum on back lip of the tool body. The maximum stress was reduced and it was lower than yield limit of tool body material. The resulting factor of safety was 2.8. The maximum stress was observed at stress relieving slot where tool failed typically (Giri and Mahapatra 2017).

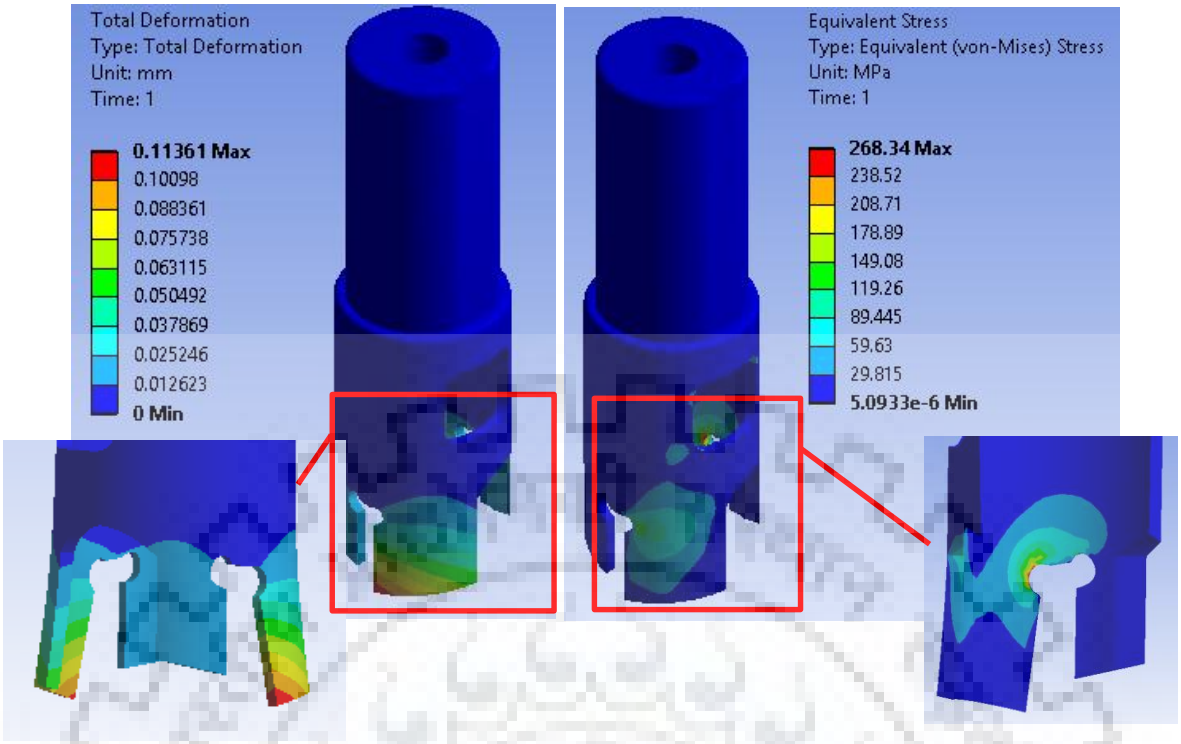

Fig. 3-30 Stress and deformation in tool body

The structural analysis of tool body shows that modified tool design is safe. Since, the deformation and maximum stress developed in tool body at the highest level of cutting speed and feed rate are well within acceptable limits, hence, it can be concluded to proceed with manufacturing of tool from 4140 steel and as per the geometrical specifications of the CAD model analyzed. The tool thus manufactured have undergone experimental trials as per DoE planned for this research work.

Fig. 3-31 Photograph of trepanned work-piece

The Fig.3.31 shows the workpiece machined by using designed trepanning tool. This figure clearly indicates central core saved by trepanning operation and the annular ring cut by the new trepanning tool.

3.8 Summary

- Octagonal ring type strain gauge based dynamometer was designed, manufactured and was successfully used to measure the cutting forces in trepanning.
- The trepanning tool was designed and its structural analysis was carried out to ensure the safe design.
- Simulation of trepanning process was successfully carried out using smoothed particle hydrodynamics (SPH) method in LS DYNA.
- The simulated and actual cutting forces were in close agreement with each other.

Chapter 4

DEVELOPMENT of TREPANNING TOOL and EXPERIMENTAL WORK

After the successful simulation of the trepanning operation using mesh free simulation in LS DYNA and validation of tool design by structural analysis in ANSYS, the next step in this work is to develop the tool and experimental set up. Selection of material for tool body and proper machining as per the geometrical CAD model is very important.

4.1 Development of trepanning tool

After validating trepanning tool design using FEA simulation approach, the tool was manufactured as shown in Fig. 4.1. Various materials available for body material like D2 die steel, tool steel and 4140 alloy steel were studied in detail for their properties and suitability of application. Out of the available material choices, alloy steel 4140 was chosen, as it is commonly used as body or shank material by commercial tool manufacturers. The tool body was machined from 4140 alloy-steel. This material was preferred, due to its high strength, toughness, fatigue strength and wear resistance.

The tool has cylindrical shank of diameter 32 mm and length 90 mm. This shank fits in a standard BT 40 adapter. This adapter, with tool mounted in it, fits in CNC machine spindle as well as automatic tool changer of the CNC machine. The suitable insert geometry and coating grades for inserts was chosen after referring different manufacturers catalogues.

The manufacturing of tool holder, as per the CAD drawing prepared and analyzed for structural strength, is explained in this section. The manufacturing of tool holder was divided into three distinct regions for the sake of different manufacturing set ups involved.

The first region was tool holder shank, which was relatively easy to manufacture. Manufacturing of shank involved turning and milling and cylindrical grinding operations. The bar stock of the material (diameter 45 mm and length 200 mm) was used as a basic raw material stock. The shank was turned from 45 mm diameter to 32 mm diameter and 90 mm length on a center lathe in suitable steps. A very fine final cut was taken to ensure the dimensional accuracy. The shank diameter was finished to a size of $32^{-0.05}$ mm on cylindrical grinding machine. The tool shank has a flat surface machined over its entire 90 mm length. A vertical milling machine was adapted to machine the flat. This flat surface is used for clamping the tool in the standard BT 40 adapter, using two 8 mm Allen bolts. A sliding fit is provided for the shank and adapter. Additionally, a 45^0 chamfer was provided on the top circular edge to facilitate easy insertion of shank and assembly with the BT 40 adapter.

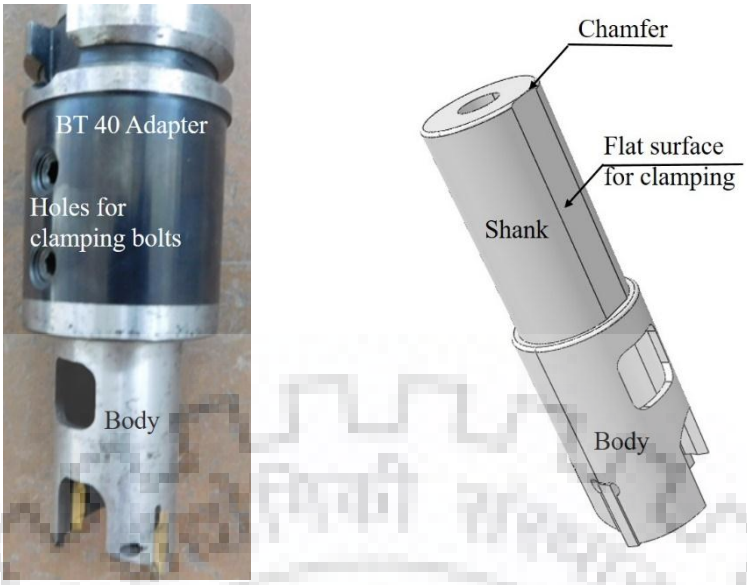

(a) **(b)**

Fig. 4-1 Trepanning tool (a) with BT 40 adapter (b) CAD model of tool

The second region for machining was machining the internal and external diameter as per the CAD model. First, the internal diameter of the body was machined. To begin with, progressive drilling was used to machine the undersized internal diameter. Final sizing of internal diameter was done on lathe machine using boring operation. Final ID size was maintained as 32.8 mm. Later on, external diameter was turned, by holding the shank portion in lathe chuck. The finished external diameter of the tool body was 39.6 mm. The inserts used have 4 mm thickness, slightly more than the wall thickness of the tool body. The tool was designed in such a way that, only side faces of the inserts would be touching the annular ring area machined by the insert cutting edge. These side faces of the inserts cause burnishing action in the annular ring. Hence tool body does not make direct contact with the walls of annular slot. Due to this reason, finishing processes like grinding of the internal or external diameter was not required. The tool fouling was checked during the trial machining. The actual tool and its CAD model is shown in Fig. 4.1.

Machining of the insert slots and insert clamping provision and profile machining of front and back lips on the tool body, is considered as third region for machining. The enlarged view of this area is shown in Fig. 4.2. The marking for the straight insert slots of 4 mm width, placed diametrically opposite to each other were carefully marked. The tool body was carefully clamped in a fixture for machining of insert slots. An end mill cutter was used to machine the insert slots up to exact depth. The slot depth was maintained such that, when insert is fitted, the relief edge of the insert should be just below the starting point of the back lip. Sliding fit was provided for the assembly of insert in the insert slots. Later, the upper corners of the insert slots were further machined for removing the sharp corners and to provide for stress releasing

features, at the top corners of the slot. After careful making of insert slots, the profile of the front lip and back lip was carefully marked on the body for both the slots. These profiles were machined on a vertical milling machine. Drilling of 3 mm diameter holes in the curved body of the tool, for grub screw was carefully carried out. At most care was taken in controlling this hole, as the hole is originated on curved surface of tool body and ends at exact center of the inserts slot. Then 3 mm threads were tapped in the insert mounting holes for clamping the inserts in the insert slots. 3 mm diameter, 6 mm long grub screws were used to tighten the inserts. This assembly was checked to ensure that the screws are exerting sufficient force on the inserts. Thus the inserts are locked in the slot by grub screws as well as the top of the insert slot, where the inserts upper face touches the slot.

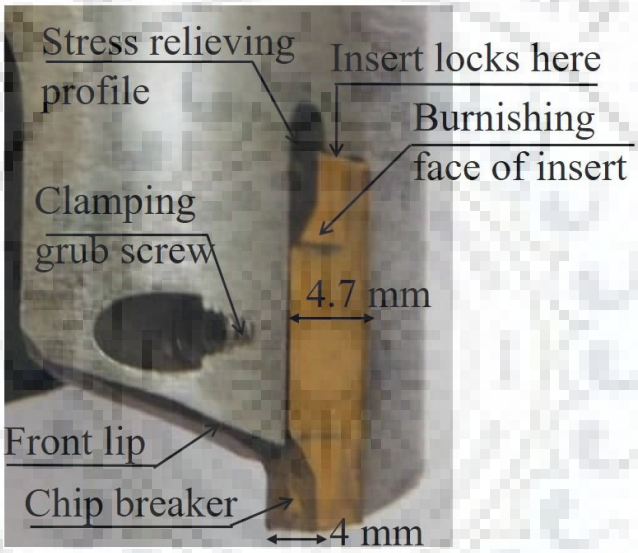

Fig 4-2 Enlarged view of insert area

The profile of front lip was designed in such a way that when insert comes into cutting action, the chips produced first make the contact with face of the insert where chip breakers are provided. After that the chip flows over the front lip of the insert. In case continuous chips are produced, they break down when their flow direction is changed, when they come in contact with the front lip. The chips produced thus are removed from the chip evacuation area near front lip. This is possible up to about 15 mm depth of hole. As the inserts and tool, are further fed into work piece, chip clearance becomes difficult. As the tool is fed further deep, the chips get accumulated in the chip evacuation slots provided in the tool body, above the front lip, with the help of flood coolant spray provided into the cutting zone.

The rear lip of the tool body supports the insert, against the pressure exerted by material resisting its machining near the shear plane. The strength of this lip is very important. The rear lip

has been given profile inclined at 8^0 degrees to the horizontal which is similar to the profile of the insert relief angle. This ensures that the rear lip not to make contact with previously machined annular ring surface. The tool is cleared of the machining area without rubbing on it. The machining of these tool lips was done by first correctly marking the leaves on the tool body. The body was secured in a fixture and lip profile was machined using end mill on vertical milling machine. These two lips are diametrically opposite to each other.

After complete machining of the tool body, the insert were fitted in the slots and clamped by grub screws in place. This tool body with inserts was then fitted in BT 40 adapter by allen bolts. The entire assembly was fitted in CNC machine spindle. The tool was moved in negative (-) Z direction, till it is about to touch the work piece mounted in a fixture, at the center of dynamometer. Leveling and clamping of the insert was checked by filler gauges to ensure that both inserts are making contact with work piece. Now the trepanning tool is ready for use.

As already mentioned, a pair of insert, with exact same geometry and coating grade were used for each machining trial. The inserts with three different grades of coating were used during experimentation. Inserts have 4 mm width at the cutting edge and 20 mm height. Their width at the non-cutting area is 3 mm and insert thickness on the mounting face is 4.7 millimeter. The face relief of 7° is provided near the cutting edge of the insert. This specifically avoids fouling of the insert, on the previously machined surface in the bottom of annular groove. The inserts also have been provided with specifically designed chip breakers, suitable for machining of stronger and gummy materials like stainless steel. Chip breakers ensure that the long curly chips break into smaller segments and help improving machining efficiency of the insert. The below schematic (Fig. 4.3) shows the major dimensions of the insert.

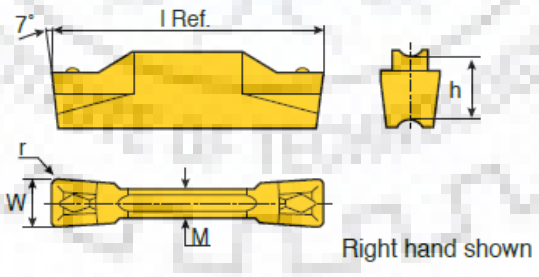

Fig. 4-3 Schematic of the insert used (Taegutec Catalogue 2013)

Fig. 4-4 Insert used in tool (Taegutec Catalogue 2013)

Table 4.1 Dimensions of inserts used (Taegutec Catalogue 2013)

Size	Dimensions (mm)				
	W^{+}.0.05	r	M	l	h
3	3.0	0.4	2.2	20.0	4.7
4	4.0	0.4	3.0	20.0	4.7
6	6.0	0.8	5.0	25.0	5.2

The image of insert is shown in Fig. 4.4 and dimensions corresponding to Fig. 4.3 are shown in table 4.1.

The first grade of coating was AlTiN PVD multilayer coated inserts. These inserts are identified as TT 9080 inserts. These inserts have 0.4 mm corner radius, and very hard submicron-substrate with enough good fracture toughness. The second grade used was TT 8220, with is a mono layer TiCN coated inserts with corner radius of 0.4 mm. They are suitable for medium to low speed machining of low carbon steels, stainless steel, and exotic alloys (TaeguTec 2013). The third grade of coating was TT 7220 TiCN PVD multilayer coated inserts. These insert have corner radius of 0.8 mm insert.

It is absolute necessary that both the inserts used in tool shall have exact same geometry and size. These inserts are rigidly clamped in tool body by 3 mm diameter, 8 mm long grub screws. The locking grub screw touches the insert placed in insert slot at the center of the insert. The grub screws are tightened in threaded holes provided on the curved tool body. However the correct locking torque is to be applied by manual judgment of the operator. This locking pressure on both the inserts needs to be same, to ensure similar performance from both the inserts during machining.

The inserts clamped in the tool-holder, together is recognized as ‘trepanning tool’ or herein after referred simply as a ‘tool’. Similarly, machining response attributed to ‘tool’ is not the mere

effect of cutting-insert(s) but in association with holder that holds the insert. Tool-holder not only supports the inserts to bear machining forces, but also makes the 'tool' capable to carry cutting extremities.

The key performance indicators of trepanning operations are torque and thrust generated during machining of annular ring in the work piece. In this work, the torque and thrust force were recorded using an octagonal ring type dynamometer. Sensitivity of this dynamometer was increased by using total 16 strain gauges. One Wheatstone bridge circuit with 8 strain gauges is used to sense and measure thrust force while another 8 strain gauges are used foe sensing and measurement of torque.

To ensure proper recording of thrust and torque, a top plate, finely ground from both sides was fitted on dynamometer top and a special fixture was mounted on this top plate. The work pieces were properly secured in fixture to minimize vibrations and subsequent variations in measurements as shown in Fig. 4.5. The trepanning process was carried out at the center of the plate for better accuracy of dynamometer measurement.

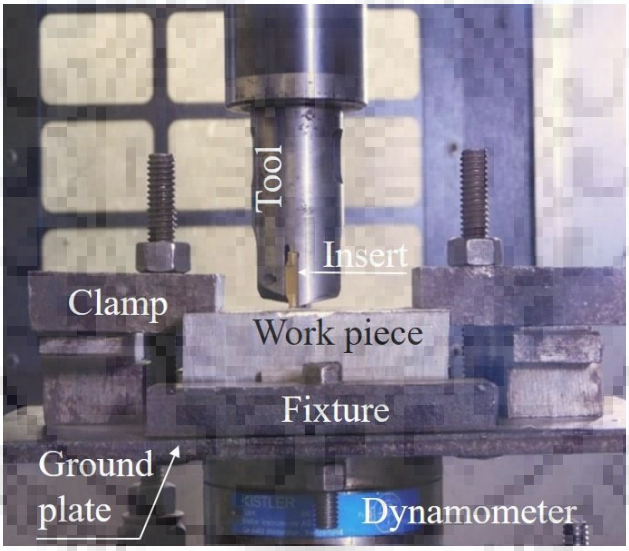

Fig. 4-5 Experimental set up

The complete machining set up includes the trepanning tool, arrangement of securing the work piece on the dynamometer, the octagonal dynamometer with strain gauges and two wheat stone bridges connected for sensing the cutting forces, the force recording arrangement with data logger and a desktop computer to store the results. The strain gauges were connected to data logger by 4 meter long silver conducting cables. The dynamometer was calibrated before trials, to ensure the accuracy of force measurements. The data logger system and desktop computer were kept at a distance from the machining zone. Few measurements were also conducted with Kistler-9272 dynamometer, charge amplifiers, data acquisition (DAQ) system, linked to computer. Few other

researchers (Pandey 2012) have previously used this dynamometer for accurate measurement of forces.

In the present study, a separate electrical connection was provided to CNC machine to reduce electrical disturbance to the system. Proper earthing was ensured to the machine. The CNC machine used was kept on vibration pads. This complete machine set up was made ready and tested before final machining trials as per statistically planned design of experiments. A CNC program for drilling of through holes of entire 40 mm depth of work piece was prepared and used for machining. Water based flush lubricant was used during machining for flushing off the chips produced and to ensure that the temperature at the cutting zone.

4.2 Experimental Work

Literature review (Joshi *et al.* 2007 and 2008, Espinosa *et al. 2008,* Benga *2008)* suggests that the factors such as feed rate, cutting speed, insert geometry, insert coating, tool chip interface temperature etc. contribute to machining response. It is not possible to include all these variables into a single experiment. This work attempts to consider as many variables as possible such as, cutting speed, feed and insert coating in present investigation. All these process variables depend on the work, tool and process related parameters. Feed rate, cutting speed, and insert coating are selected as process related parameters. The reasoning for the selection of machining parameters and their influence on the thrust force, torque and surface quality/integrity, during machining is explained in the following sections, divided into three sub-sections, beginning with design of experiments (DoE), details of experimental set up, equipment used, and experimental procedure followed.

4.3 Design of Experiments and Procedure

4.3.1 Strategies of experimentation

Different strategies of experimentation are available to determine the effect of process parameters on process responses. The most widely used strategies for experimental analysis include:

- **Best-guess approach:** In this approach, investigator guesses the best likely combination of factors to test for the output response, in iterative manner. This is a time-consuming process, and may lead to sub-optimized solution (Montgomery 1996).
- **One-factor-at-a-time:** One-factor-at-a-time is being varied in this approach, over its range for all the factors under study, maintaining other factors constant at pre-selected level. Inferences are drawn by preparing cause and effect diagram as shown in Fig. 4.6.

Though simple, this strategy fails to consider any possible factor interactions (Montgomery 1996).

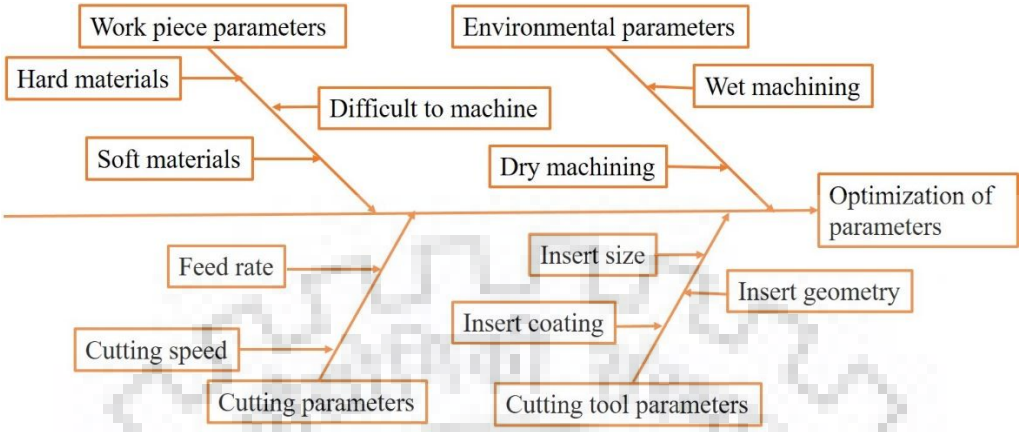

Fig. 4-6 Ishikawa – Cause and Effect Diagram for trepanning Optimization

- **Statistically designed experiments:** This approach considers varying number of factors at a time, to study effect of individual factor as well as interaction of the factors, if any. Various design-of-experiment (DoE) methods are widely used to design the experiment statistically and overcome the issues with earlier mentioned strategies (Montgomery 1996). Taguchi method is most popular and efficient DoE approach.

4.3.2 Taguchi based design of experiments

This technique is commonly used in many fields like new product developments, quality control and process designing. The salient features of this method lead efficient outcomes and optimal solution with simplicity in adaption and least number of experimental runs.

Taguchi defines the term, signal to noise (SN) ratio, formulated for three distinct categories as below (Bagchi 1993, Phadke 1989):

- *Nominal and small are best characteristics*

  These are lower-the-better performance characteristics (e.g. cutting forces, surface roughness/finish, energy consumption etc.), preprocessed following Eq. 4.1 and Eq. 4.2.

$$S/N = -10 \log (\bar{y}/s^2 y) \quad \text{……Equation (4.1)}$$

$$S/N = -10 \log ((l/n)(\Sigma y^2)) \quad \text{...……Equation (4.2)}$$

- *Larger is best characteristics*

  These are higher-the-better performance characteristics (e.g. material removal rate), preprocessed following Eq. 4.3.

$$S/N = -10 \log ((1/n)(\Sigma (1/y^2)) \quad \text{……..……Equation (4.3)}$$

For equations 4.1 to 4.3, *y* is the response variable(s) and *n* is the number of observations in the experiments.

Taguchi method based DoE involves following steps (Bagchi 1993, Phadke 1989).

- Defining research problem
- Identifying noise factors
- Selecting response variables
- Selecting control parameters and their levels
- Identifying interactions of control parameters
- Orthogonal array selection
- Conducting the matrix experiments
- Analyzing data and predicting the optimum level

4.3.2.1 Defining research problem

The problem statement can be defined as *"Performance analysis of trepanning tool for deep annular grooving"*. This is achieved in the current investigation by designing and manufacturing multi teeth trepanning tool with provision for multi-passage chip removal.

4.3.2.2 Identifying noise factors

Sources of noise in this research work could be ambient temperature, vibrations, machine condition and human error in operating the process.

4.3.2.3 Selecting response variables

In any process, the response variables need to be selected to obtain useful information about the performance of the process under study (Joshi et al. 2007). Table 4.2 shows the methodology used for the development of trepanning tool.

Table 4.2 Methodology used for performance analysis of trepanning tool

<table>
<tr><td rowspan="3">Control variables</td><td rowspan="2">Tool related</td><td colspan="2">Tool geometry</td><td>Type</td></tr>
<tr><td colspan="2">Insert thickness = 4 mm, insert length = 20 mm; Manufacturer Taegutec</td><td>Three different coating grades</td></tr>
<tr><td>Process related</td><td>Feed rate (0.03, 0.04 and 0.05 mm / rev)</td><td>Cutting speed (25, 30 and 35 m / min)</td><td>Coating grade 9080, 8020 and 7220</td></tr>
<tr><td>Design of experiments</td><td>Taguchi method</td><td colspan="3">L_{27} (3^{13}) orthogonal array</td></tr>
<tr><td></td><td>Machine</td><td colspan="3">MTAB make Maxmill^{+} vertical milling machine</td></tr>
</table>

Tools and equipment	Inserts	Taegutec make parting inserts TDT 4.00 E-0.4 R turning, grooving and face machining insert
	Adapter	Standard BT 40 adapter
Assessment of response variables	Octagonal ring type dynamometer, Digitech make data logger, LEICA DMi8 Digital microscope, ZEISS SURFCOM Surface meter	
Method of effect analysis	MINITAB 19 software, ANOVA, Grey relation analysis	Qualitative analysis of machined surfaces
Criteria for analysis	Surface roughness	Smaller the better
	Thrust force and torque	Smaller the better
	Material removal rate	Larger the better

Based on the literature review and by considering the parameters mentioned above, the response variables selected for current investigation are surface roughness (R_a values), thrust and torque.

4.3.3 Selection of control parameters and their levels

Selecting control factors, their specific levels, and the range in which these factors are to be varied is very important for drawing meaningful conclusions from the actual experimentation (Pandey et al. 2011, Joshi et al. 2007 and 2008).

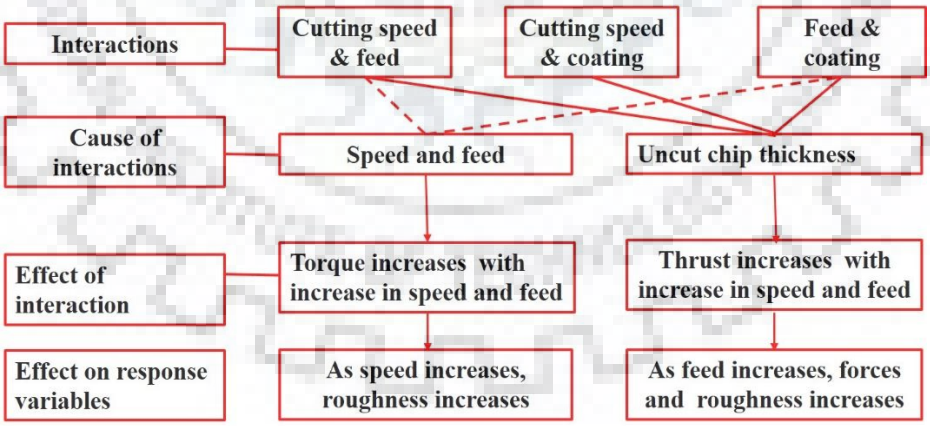

Fig. 4-7 Logic for Selection of Control Parameters and their Interaction

The process parameters affecting the characteristics of machined parts are categorized as: cutting tool parameters- tool geometry, tool material; work piece related parameters- metallography, hardness, etc.; and cutting parameters- cutting speed, feed, dry cutting and wet cutting. The logic selecting control parameters and (their) levels is shown in Fig. 4.7.

- **Selection of cutting speed**

In trepanning, cutting forces and surface roughness varies with the cutting speed (Boothroyd 2006). Nevertheless, so far, the cutting speed influence on surface finish has not been understood clearly. Further, majority of the investigators have reported surface finish deterioration with increase in cutting speed (Cicck *et al* 2013). Besides this, the machine constraint is considered as another reason to select appropriate levels of the cutting speed.

- **Selection of feed**

Feed rate in machining is responsible for the cross sectional area of the chip and thus the resultant cutting forces developed at the tool-chip-interface. It influences the pitch of the machined surface and hence governs its finish, too. The thermal stress developed also influenced by the feed rate. The reinforcement pull-out and fracture also leads deterioration of surface quality/integrity by developing pits and cracks in the machined surface (Boothroyd 2006).

The machine settings and literature review follows consideration of below-mentioned process parameters for the present work:

- Cutting speed
- Feed rate
- Insert geometry and coating
- Other parameters (tool material, work material, presence of coolant)

Preliminary experiments with one-variable-at-a-time approach was carried out to ascertain the ranges of the selected process parameters to be used in final experimentation. During the entire experimentation, the selected parameters were kept fixed.

4.3.4 Experimental procedure and set up

Once the orthogonal-array (OA) is selected, experiments were performed on the selected work piece. Fig. 4.8 shows the methodology followed during performing experiments and experimental set up used.

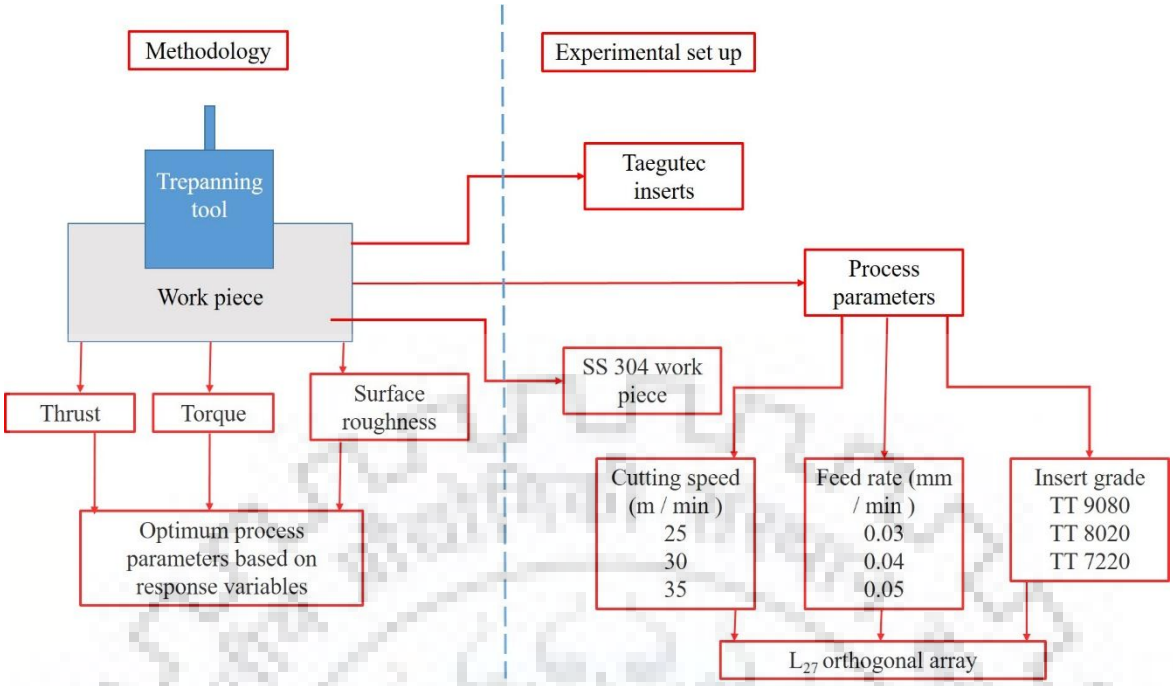

Fig. 4-8 Methodology for experimentation

Experiments were performed as per L_{27} orthogonal array. Trepanning was performed on a work-piece of size 100 mm x 100 mm x 40 mm. Trepanning of work piece was done on MTAB make Maxmill^{+} vertical CNC milling machine available in institute's machine tool laboratory.

Trepanning of each work piece was carried out in a single stretch for the entire thickness. The surface roughness (Ra) was measured at the beginning and the exit of the depth, at two diametrically opposite locations. ZEISS SURFCOM Stylus type Surface meter was used to record Ra values. The 8 mm cut-off length was selected and average value (Ra) of measurements was used as response variables.

Three levels of feed rates, cutting speeds and three different grades of 4 mm wide x 20 mm long inserts were used for trepanning. The cutting parameters and (their) levels are given in table 4.6.

Table 4.3 Process parameters and their levels

Parameter	Level I	Level II	Level III
Cutting speed (m/min)	25	30	35
Feed rate (mm/rev)	0.03	0.04	0.05
Insert grade	TT 9080	TT 8020	TT 7220

The force measurement was carried out using strain gauge based, octagonal ring type dynamometer (Gaikwad *et al.* 2018). The strain data was recorded using Digitech (India) make data logger and stored in a desktop computer. Experimentation was carried out following to

Taguchi orthogonal array L_{27}, and the experimental runs were randomized. For each experimental run a fresh pair of inserts, with same coating and geometry were used and the same pair was inverted for the next run. This means one pair of insert was used for two machining runs.

4.4 Summary

- The experimental set up for trepanning, including the dynamometer and work holding arrangement was developed and tested.
- The trepanning tool was developed as per CAD model.
- Experimental work as per design of experiments was carried out and the response variables were properly recorded.

Chapter 5

RESULTS AND DISCUSSIONS

The trepanning of 40 mm diameter holes was performed using a specially designed trepanning tool on stainless steel 304 work-pieces of size 100 mm x 100 mm x 40 mm, as per the experimental procedure described in earlier sections. The experiments were performed at three distinct levels of the process parameters. The torque, thrust force and surface roughness of trepanned hole were measured and are shown in Table 5.1. The results were analyzed using MINITAB 19 software, by analysis-of-variance (ANOVA), linear regression analysis, and grey relation analysis. Each response variable was analyzed with process parameters, and main effect plots were plotted (Singh and Kumar 2004, 2006 and 2014, Joshi *et al.* 2007).

Criterion selected for the analysis was "smaller the better" for all the response variables. Smaller the thrust force and torque observed during trepanning, better will be the machining process, leading to use of less rigid machines, fewer vibrations, less heat generation, less tool wear, prolonged tool-life and improved surface finish (Heinemann and Hinduja 2007). Smaller the surface roughness better will be the integrity of surface, leading to better fatigue strength of the work piece.

Analysis-of-variance (ANOVA) helps testing significance of all main factors and their interactions. For this, ANOVA compares the mean square against the estimate of experimental errors at specific confidence levels. Here, F ratio is the ratio of mean square error to residual, which is used to determine significance of a factor.

The thrust force, torque, average surface roughness of trepanned hole and average inside diameter of trepanned hole are shown in Table 5.1 given below. The statistical inferences drawn from this data are discussed in details below. This experimental data recorded was further analyzed for finding the optimum setting of process parameters that gives the optimum response in terms of minimum thrust force, torque and surface roughness. Different statistical techniques like analysis of variance (ANOVA), regression analysis and Grey relation analysis (GRA) were used to draw meaningful conclusions from the recorded data.

Table 5.1 Experimental results of trepanning process

Run No.	Speed (m / min)	Feed (mm / rev)	Insert grade	Thrust (N)	Torque (Nm)	Roughness Ra (μm)
1	25	0.03	9080	152.02	3.72	1.713
2	25	0.03	8020	181.36	4.27	1.956
3	25	0.03	7220	193.91	5.62	1.926
4	25	0.04	9080	201.34	4.67	2.562
5	25	0.04	8020	209	4.87	2.915
6	25	0.04	7220	245.71	5.96	2.518
7	25	0.05	9080	236.46	5.01	2.873
8	25	0.05	8020	239.58	6.77	2.306
9	25	0.05	7220	295.52	7.65	2.304
10	30	0.03	9080	196.13	5.36	1.953
11	30	0.03	8020	222.65	6.02	3.140
12	30	0.03	7220	232.38	4.92	1.869
13	30	0.04	9080	238.72	6.38	2.375
14	30	0.04	8020	242.33	6.92	3.149
15	30	0.04	7220	256.66	7.01	2.835
16	30	0.05	9080	248.58	6.32	2.531
17	30	0.05	8020	278.23	7.78	3.246
18	30	0.05	7220	296.11	7.02	2.945
19	35	0.03	9080	222.56	6.78	1.783
20	35	0.03	8020	235.74	7.03	2.013
21	35	0.03	7220	287.48	7.78	2.035
22	35	0.04	9080	234.44	7.73	2.742
23	35	0.04	8020	258.94	8.96	2.278
24	35	0.04	7220	325.53	9.89	2.905
25	35	0.05	9080	286.51	9.63	3.014
26	35	0.05	8020	311.2	10.454	3.145
27	35	0.05	7220	353.6	11.34	3.515

5.1 Statistical results and discussions (thrust force)

The thrust in trepanning is the force exerted by the tool along the spindle axis, when the rotating tool is fed in the work piece for trepanning. Presence of minimum thrust force in trepanning operation, is an indication of better cutting. Less thrust force indicates that the tool is piercing the work piece material with ease and with minimum resistance. The thrust force in trepanning depends on many parameters such as the tool geometry, material and coating used on the tool, mechanical properties and homogeneity of work piece material. It is also affected by other machining parameters like cutting speed and feed rate employed for the trepanning process. The thrust force was measured with the help of strain gauge based, octagonal ring type dynamometer specially developed for this measurement. The ANOVA reveled that all three factors i.e. cutting speed, feed rate and the coating of the insert were statistically significant factors at 95% confidence level. ANOVA results are shown in table 5.2 and Fig. 5.1.

Table 5.2 Analysis of variance (ANOVA) for thrust in trepanning

Parameter	DoF	Seq. SS	MS	F	P	Contribution (%)
Speed	2	17532.2	8766.1	86.26	0.000	31.86%
Feed	2	21500.1	10750.1	105.78	0.000	39.07%
Coating	2	12672.1	6336.1	62.35	0.000	23.03%
Speed*Feed	4	606.9	151.7	1.49	0.291	1.10%
Speed*Coating	4	1658.1	414.5	4.08	0.043	3.01%
Feed*Coating	4	253.8	63.4	0.62	0.658	0.46
Error	8	813.0	101.6	R^2 = 98.52%		1.48
Total	26	55036.2		R^2 (Adj)=95.20%		100.00%

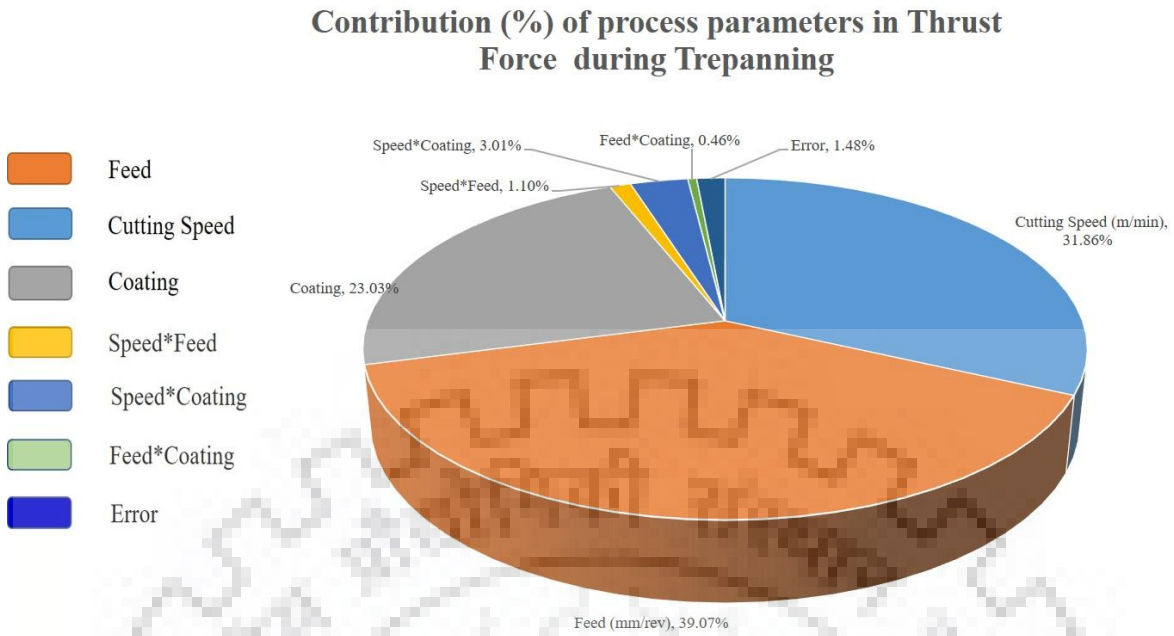

Fig. 5-1 Plot indicating % contribution of process parameters in thrust force

As shown in table 5.1, it was observed the feed rate employed, cutting speed, insert coating and interaction of speed and coating were statistically significant factors affecting the thrust force produced. This observation is valid for the specific set of input range of parameters for the trepanning tool described in previous chapters during trepanning of stainless steel 304. The feed rate has a contribution of 39.07 %, cutting speed contributes 31.86 %, the coating contributes 23.03 % and interaction of speed and coating contributes 3.01 % in the trust force generated.

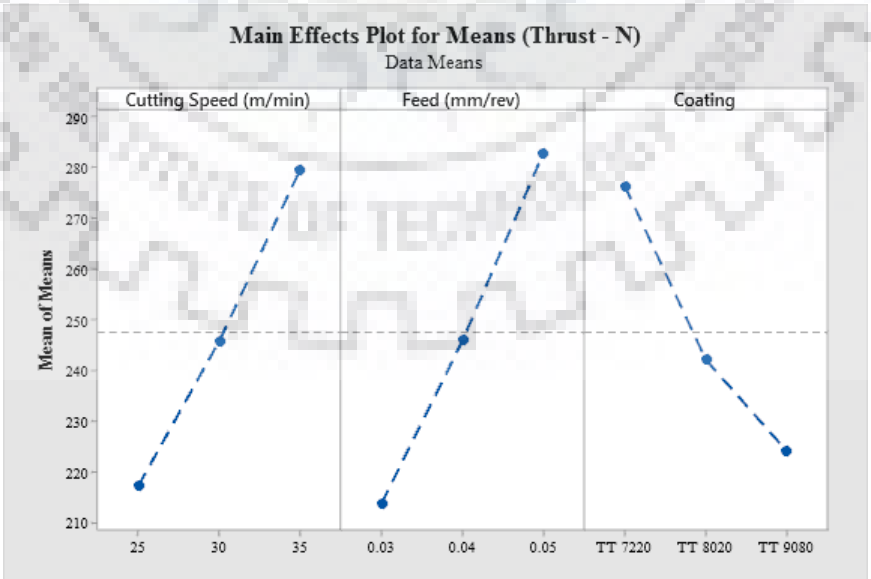

Fig. 5-2 Main effects plot for means for thrust force

Main effects plots for means for thrust force are shown in Fig. 5.2. It was observed that, as the cutting speed increases from 25 m / min to 30 m / min and from 30 m / min to 35 m / min, thrust force increased proportionately. Generally thrust force was expected to remain steady or decrease with increase in cutting speed, due to the temperature rise at the tool chip interface. This increased temperature would have thermal softening effect on the work piece, reducing the force required for plastic deformation and shearing of the metal. However due to use of coolant and difficulty in chip removal after 20 mm depth, causes the thrust force to rise when speed increases from 30 m / min to 35 m / min.

As the feed rate increase from 0.03 mm / rev. to 0.05 mm / rev., increase in thrust force was observed. Increase in the uncut chip thickness with increases in feed rate causes the tool to encounter more resistance from material for shearing. The increase in thickness of shear zone thickness leads to increase in thrust force.

PVD TiCN coated TT 7220 insert produces higher thrust. PVD TiCN coated TT 8020 insert produces lower thrust and lowest values of thrust were obtained with PVD AlTiN multilayer coated TT 9080 inserts. This lower level of thrust was due to the low thermal conductivity, high hardness and high adhesion strength of Nano TiAlN coating. There is no conclusive evidence that a particular type of coating performs better in terms of cutting forces while drilling or any other machining operation. However, it has been reported by researchers that the hard coating layer improves cutting performance of the tool (Audy *et al.* 2003, Talib *et al.* 2007, Kusinski *et al.* 2009).

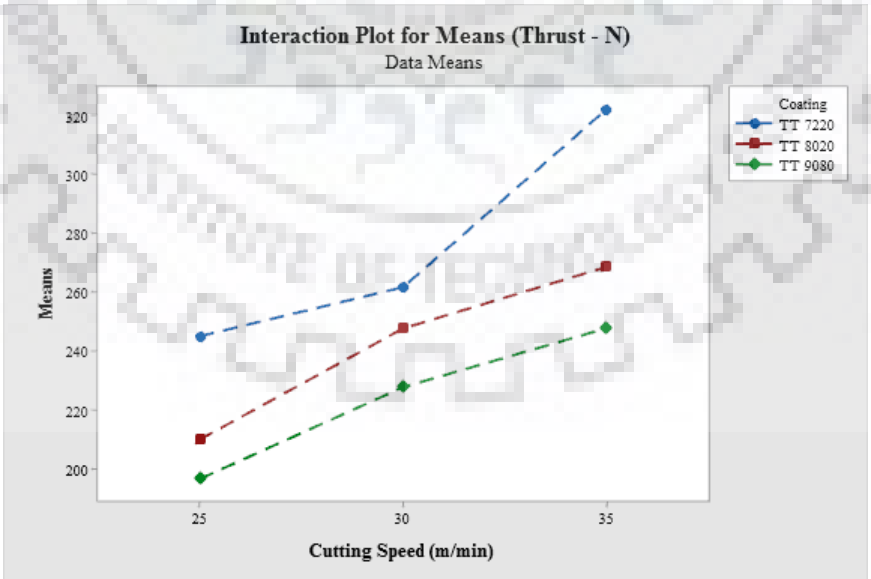

Fig. 5-3 Interaction plot between cutting speed and coating for thrust force

The interaction amongst all the factors was considered in ANOVA. As given in ANOVA table 5.2, only the interaction of cutting speed with coating was observed to be

statistically significant. The interaction plot between cutting speed and insert coating is shown in Fig. 5.3.

It was observed that for the TT 9080 insert, the increase in thrust with increase in cutting speed is uniform. However, for insert TT 7220, the thrust significantly rises when speed is increased from 30 m / min to 35 m /min. It can be concluded that, the rate of increase in thrust force with increase in cutting speed is affected by the properties of the insert coating material. Lower amount of thrust while using 9080 inserts can be attributed to high strength, hardness and low thermal conductivity of TiAlN coating.

5.2 Statistical results and discussions (torque)

The torque in trepanning is the force created by tangential force components, opposing the rotation of trepanning tool, when the tool is rotated and fed in the work piece for cutting operation. Presence of minimum torque in trepanning is an indication of better cutting. Less torque indicates that the tool is able shear the work piece at the shear plane with ease and with minimum resistance. The torque in trepanning depends on many parameters such as the geometry, material and coating used on the tool, sharpness and strength of cutting edge. Torque is also affected by mechanical properties and homogeneity of work piece material. Also machining parameters like cutting speed and feed rate employed for the trepanning process influences the torque generated. All three factors i.e. cutting speed, feed rate and the coating of the insert were statistically significant factors at 95% confidence level. ANOVA results are shown in table 5.3 and Fig. 5.4.

Table 5.3 Analysis of Variance (ANOVA) of Torque in Trepanning

Parameter	DoF	Seq. SS	MS	F	P	Contribution (%)
Speed	2	56.550	28.2748	229.48	0.000	59.07%
Feed	2	23.320	11.6598	94.63	0.000	24.36%
Coating	2	7.671	3.8357	31.13	0.001	8.01%
Speed*Feed	4	3.117	0.7793	6.32	0.013	3.26%
Speed*Coating	4	3.209	0.8022	6.51	0.012	3.35%
Feed*Coating	4	0.887	0.2219	1.80	0.222	0.93%
Error	20	0.986	0.1232	R^2 = 98.97%		1.03%
Total	26	95.740		R^2 (Adj)=96.65%		100.00%

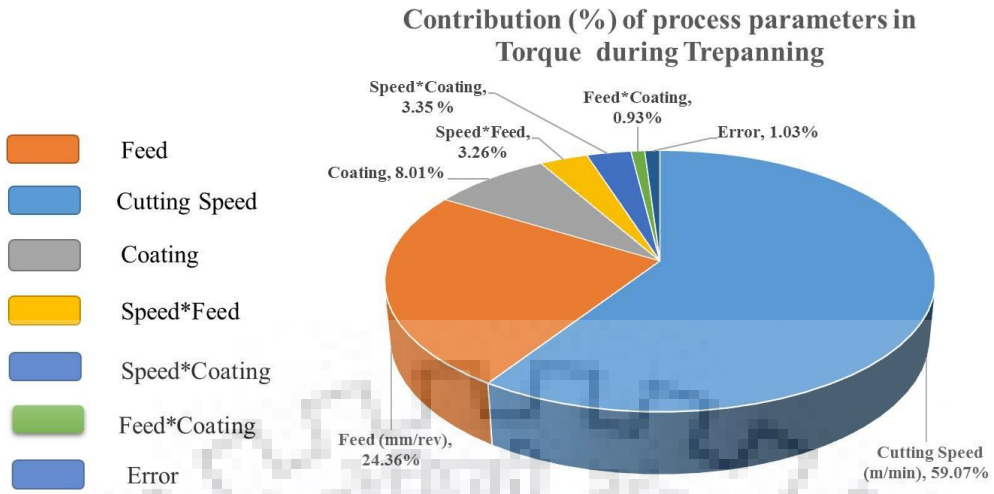

Fig. 5-4 Plot indicating % contribution of process parameters in torque force

As shown in Table 5.3, it was observed that the cutting speed, feed rate employed, coating and interaction of speed x feed and speed x coating are statistically significant factors affecting the torque produced. The cutting speed has highest contribution of 59.07 %, followed by feed rate with 24.36 %, coating with 8.01 %, interaction of speed x feed 3.26 % and speed x coating at 3.35 % contribution in the torque generated.

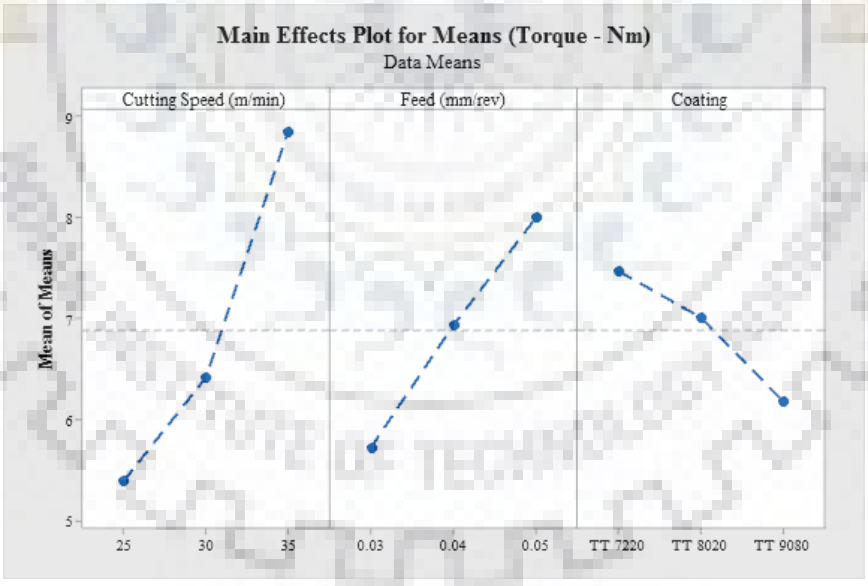

Fig. 5-5 Main effects plot for means for torque

As shown in Fig. 5.5, it was observed that, increase in cutting speed causes the torque to increase. But this increase is less when speed changes from 25 m / min to 30 m / min and torque increases rapidly when speed is further increased from 30 to 35 m / min. It was observed that, discontinuous chips were produced at low cutting speed of 25 m / min, and at higher level of speeds, longer continuous chips were produced. These chips get accumulated in the already

produced annular ring, especially as the depth of ring increases. This causes undue loads on the insert and causes the torque to increase at higher levels of cutting speed.

From the main effects plot, it can be seen that, torque increases with feed rate. As the feed rate increase from 0.03 mm/rev to 0.05 mm/rev, the uncut chip thickness increases and increases chip volume removed per unit time. Thus requires more machine power to cut the material, increasing the torque. Monolayer coated TT 7220 insert produces higher torque. PVD TiCN coated TT 8020 insert produces lower torque and lowest values of torque were obtained with PVD AlTiN multilayer inserts TT 9080. This lower torque produced can be associated with the low thermal conductivity, high hardness and high adhesion strength of nano TiAlN coating.

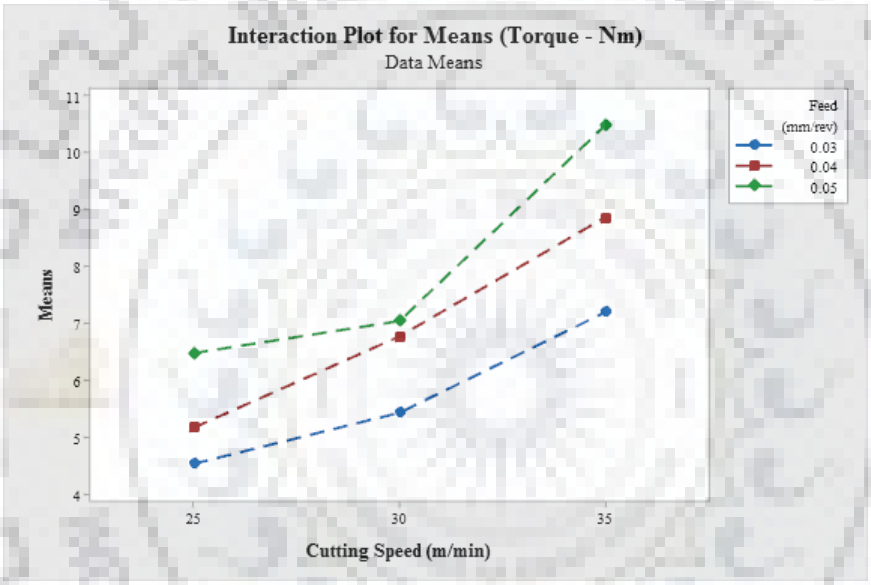

Fig. 5-6 Interaction plot between speed and feed for torque

As given in ANOVA table 5.3, the interaction of cutting speed with feed and speed with coating was observed to be statistically significant. The interaction plot between cutting speed and feed rate is shown in Fig. 5.6. As the cutting speed increases, feed rate per revolution of tool also increases, Increase in torque was observed as there is increase in cutting speed from 25 m/min to 35 m/min. However this increase is predominantly observed at higher feed rates. At higher feed rates, more amount of material is presented at the tool chip interface, as the feed rate increases proportionately increases with speed. Thus more material is converted into chips and this increases torque in trepanning. Higher feed rate in trepanning means more uncut chip thickness and more material removal rate.

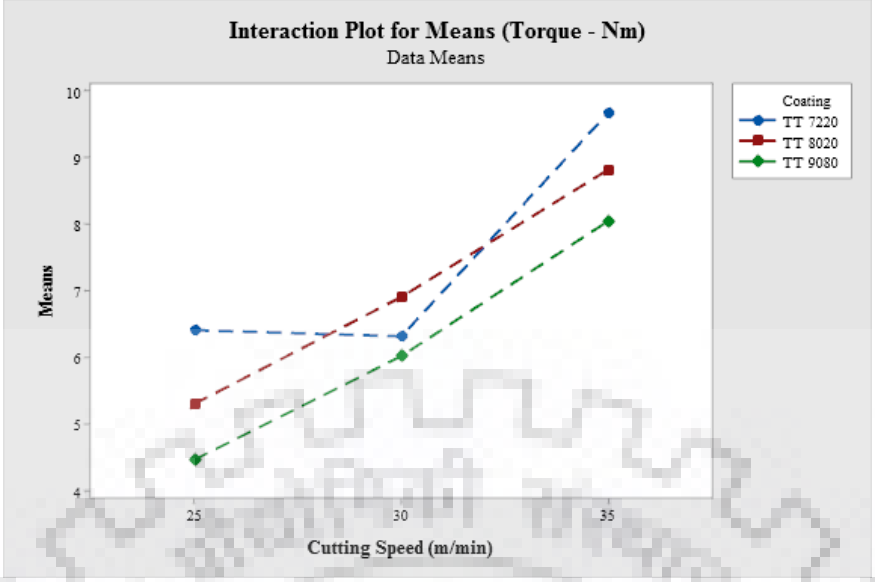

Fig 5-7 Interaction plot between Speed and Coating for torque

The interaction plot between cutting speed and insert coating is shown in Fig. 5.7 It is observed that for insert coating TT 9080 and TT 8020, there is uniform increase in torque with increase in cutting speed from 25 m/min to 35 m / min. However the behavior of single layer coated TT 7220 insert was different. For this insert, the torque did not change when cutting speed was increased from 25 to 30 m/min, but an increase in torque was observed when cutting speed was further increased from 30 to 35 m / min. This increase can be associated to poor strength of coating on the cutting edge as this grade of coating is monolayer and has poor strength compared to other grades of coatings used. The more wear on the insert cutting edge and breaking off of the edge was observed for TT 7220 insert, which has resulted in higher torque at higher level of cutting speed.

5.3 Statistical results and discussions (surface roughness)

The surface roughness of holes produced by trepanning operation is very important criterion for analyzing the tool performance. Lower surface roughness of hole, avoids need of further finishing and sizing operations in some cases. Also better surface finish means more surface integrity and better fatigue life for the component. Like thrust and torque in trepanning, the surface roughness also depends on many parameters such as the geometry, material and coating used on the tool, sharpness and strength of cutting edge, mechanical properties and homogeneity of work piece material. Also machining parameters like cutting speed and feed rate employed for the trepanning process also affects the surface roughness generated. However the feed rate employed is always most responsible parameter for surface roughness. The surface roughness was measured with the help ZEISS SURFCOM stylus type surface meter.

Roughness was measured in diametrically opposite locations at the beginning of the hole, at mid position and near the exit of the hole. Average of these six values was considered for calculation. ANOVA results for surface roughness are shown in table 5.4 and Fig. 5.8.

Table 5.4 Analysis of Variance (ANOVA) of Surface roughness in Trepanning

Parameter	DoF	Seq. SS	MS	F	P	Contribution (%)
Speed	2	0.5465	0.27324	3.93	0.065	7.85%
Feed	2	3.4585	1.72926	24.86	0.000	49.71%
Coating	2	0.3761	0.18806	2.70	0.127	5.41%
Speed*Feed	4	0.6507	0.16268	2.34	0.143	9.35%
Speed*Coating	4	1.1321	0.28304	4.07	0.043	16.27%
Feed*Coating	4	0.2372	0.05931	0.85	0.531	3.41%
Error	20	0.5565	0.06956	R2 = 92.00%		8.00%
Total	26	6.9577		R2 (Adj)=74.01%		100.00%

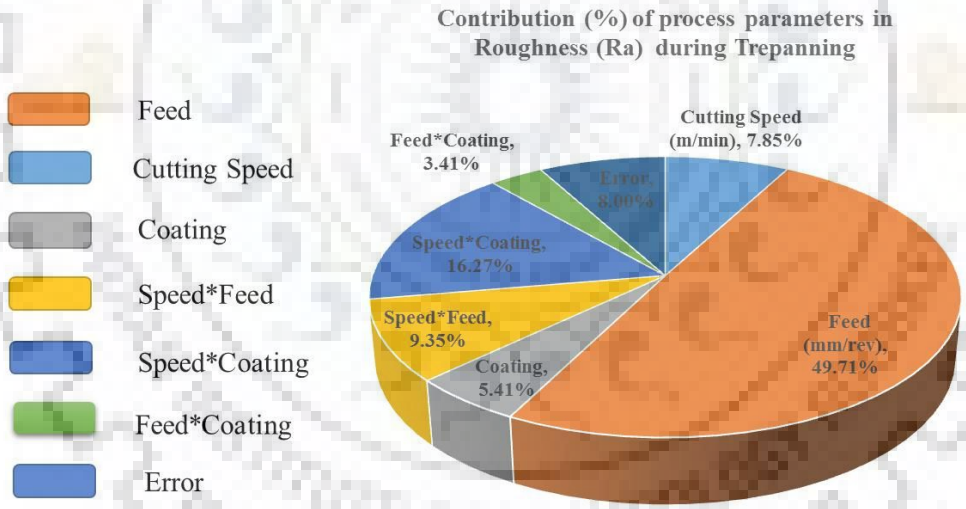

Fig. 5-8 Plot indicating % contribution of process parameters in surface roughness

As shown in Table 5.4 and Fig. 5.8, it was observed the feed rate employed and interaction of speed and coating were statistically significant with contribution of 49.71 % and 16.27 % respectively in the surface roughness produced.

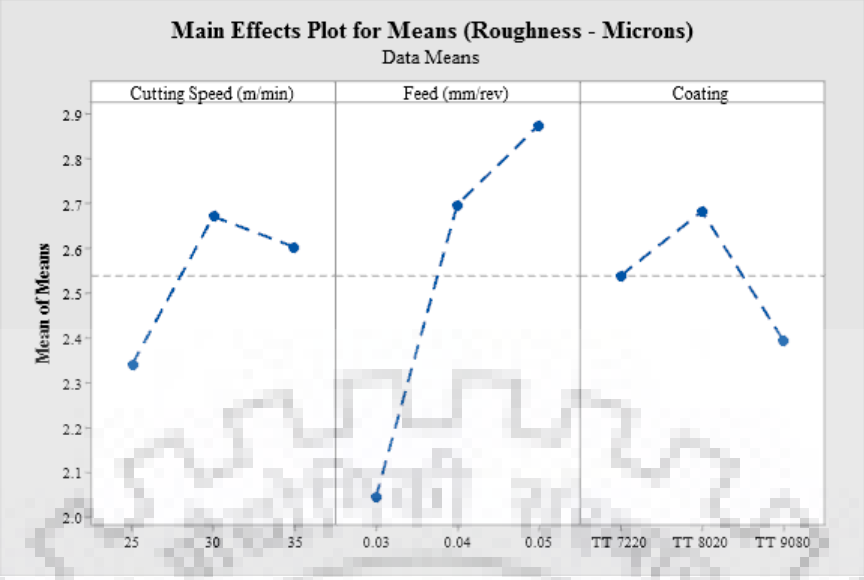

Fig. 5-9 Main effects plot for surface roughness during Trepanning

It was observed that the cutting speed and type of coating does not significantly affect the surface roughness of the trepanned hole. However the feed rate was statistically significant factor at 95% confidence level. Increase in surface roughness with increase in cutting speed from 25 to 30 m/min was observed, and with further increase in speed from 30 to 35 m / min, a reduction in surface roughness was observed. The thermal softening of work piece material due to increased chip tool interface temperature makes the machining easier. As the machining becomes easier, this results in less thrust, torque and vibrations. Also, stainless steel being sticky material, it is prone to form built up edge. At higher cutting speed, this built up edge breaks out, improving the surface finish.

The change in feed rate from 0.03 mm / rev. to 0.04 mm / rev. causes a large increase in surface roughness. When the feed rate is further increased from 0.04 mm / rev to 0.05 mm / rev., comparatively less increase in surface roughness was observed. The increase in surface roughness with increase in feed rate can be associated with increase in uncut chip thickness causing more thrust and torque. This increases load on machine and vibrations and chatter associated. However, at higher feed rates, tool chip interface temperature increases and makes machining easy. Thus comparatively less increase in surface roughness is observed when feed rate increases from 0.04 to 0.05 mm/rev.

The strong and hard nano coating on TT 9080 inserts works better even at higher speeds and feed rates and thus produces lower surface roughness compared to other coating grades used in experimentation. PVD TiCN coated TT 8020 inserts produced more surface roughness from among the three inserts used.

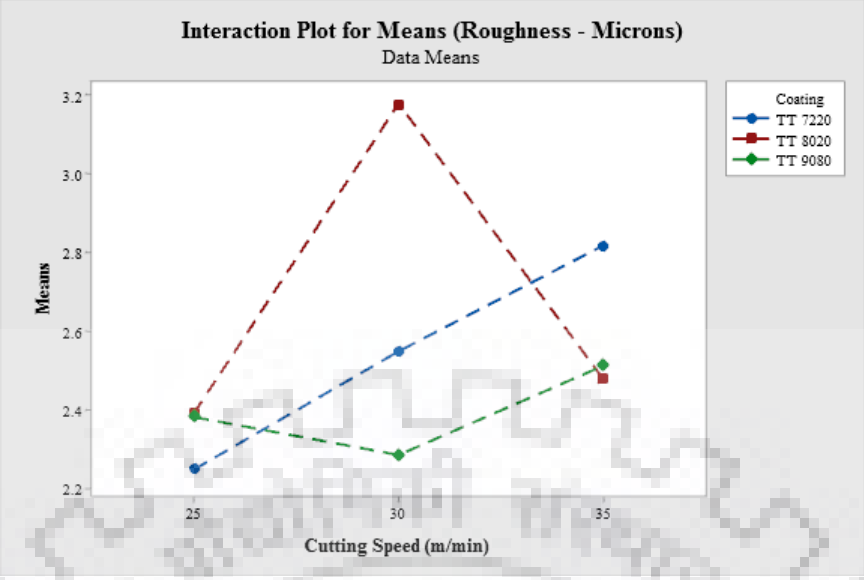

Fig. 5-10 Interaction plot between speed and coating for surface roughness

The interaction plot between cutting speed and insert coating for surface roughness is shown in Fig. 5.10. It is observed that for insert coating TT 9080, there is not much variation in surface roughness produced at all three levels of speed. For TiCN coated TT 8020 insert, increase in roughness was observed for increase in speed from 25 to 30 m / min and roughness decreases when speed is further increased from 30 to 35 m / min. The decrease in surface roughness with increase in cutting speed from 30 to 35 m / min can be attributed to breaking of built up edges formed at higher cutting speeds. This make the insert edge to rub on the machined surface and improves the surface finish. An uniform increase in roughness with increase in cutting speed from 25 m/min to 35 m/min was observed for TT 7220 insert.

Taguchi experimental design is a useful tool in design of experiments for a single factor design problem. However our current research problem under study has three response variables namely –thrust force, torque generated and surface roughness during trepanning. There are also three process parameters involved, namely cutting speed, feed rate and coating grade of insert, all at three different levels. Optimization of such a problem is not possible with Taguchi methods. Grey relation analysis is a very handy optimization tool in such situations. Following section briefly discusses the application of GRA to current research problem.

5.4 Grey relation analysis

When system model is unsure or data set is small or incomplete, classical statistical methods of analysis are not able to give reliable solutions. Classical statistical methods require large data set and need to satisfy certain mathematical criteria. In such cases grey theory proves to be very useful. It uses small data sets and does not demand strict compliance to certain statistical laws.

The Grey theory established by Dr. Deng includes grey relational analysis (GRA), grey modeling, prediction and decision making of a system in which the model is unsure or the information is incomplete. GRA can be used when there are multiple inputs with uncertainty and data is in discrete form (Chang *et al.* 2003).

This theory is adopted for solving complicated interrelationships among multiple response variables. The grey relation coefficient can express the relationships between desired and actual experimental results. A grey relational grade is obtained to evaluate multiple responses. Optimization of complicated multi response can be converted into optimization of a single grey relational grade (Chang *et al.* 2003).

The major advantage of grey theory is that it can handle both the incomplete information and unclear problems very precisely. It serves as an analysis tool, especially in cases when there is no enough data is available. There are several aspects for the theory of Grey system.

1. Grey generation: This is data processing to supplement information. It is aimed at processing complicated and tedious data to gain a clear rule, which is the whitening of a sequence of numbers.
2. Grey modeling: This is done by step 1 to establish a set of Grey variation equations and Grey differential equations, which is the whitening of the model.
3. Grey prediction: By using the Grey model to conduct a qualitative prediction, this is called the whitening of development.
4. Grey decision: A decision is made under imperfect countermeasure and unclear situation, which is called the whitening of status.
5. Grey relational analysis: Quantify all influences of various factors and their relation, which is called the whitening of factor relation.
6. Grey control: Work on the data of system behavior and look for any rules of behavior development to predict future behavior, the prediction.

5.4.1 Grey Relational Generation

In grey relational analysis, when the range of sequence is large or the standard value is enormous, the function of factors is neglected. However, if the factor goals and directions are different, the grey relational analysis might also produce incorrect results. Therefore, one has to preprocess the data which are related to a group of sequences, which is called “grey theory relational generation”.

Data pre-processing is the first stage in grey analysis since the range and unit in one data sequence may differ from others. Data pre-processing is a means of transferring the

original sequence. Depending on the characteristics of a data sequence, there are various methodologies of data pre-processing available for this analysis (Chang *et al.* 2003).

Larger the better

$$X_{ij} = \frac{Y_{ij} - min_i\, Y_{ij}}{max_i\, Y_{ij} - min_i\, Y_{ij}} \quad \ldots\ldots\ldots\ldots\ldots\ldots\ldots \text{Equation (5.1)}$$

Smaller the better

$$X_{ij} = \frac{max_i\, y_{ij} - y_{ij}}{max_i\, y_{ij} - min_i\, y_{ij}} \quad \ldots\ldots\ldots\ldots\ldots\ldots\ldots \text{Equation (5.2)}$$

Where

- y_{ij} is the i^{th} performance characteristic in the j^{th} experiment (i=1,2,3…..27; k= 1,2,3)
- $max_i\, y_{ij}$ and $min_i\, y_{ij}$ are the maximum and minimum values of i^{th} performance characteristics for alternate j, respectively.

5.4.2 Grey Relational Grade (GRG)

In the grey relational analysis, the grey relational grade is used to show the relationship among series. Let (X, Γ) be a grey relational space, X stand for the collection of grey relational factors, xi be the compared series (Eq. 5.3), and x_0 be the reference series (Eq. 6.4) (Chang et al. 2003).

$$x_i = (x_i(1), x_i(2), \ldots., x_i(n)), \quad x_i \in X, i = 1, 2, \ldots, m \quad \ldots\ldots\ldots\ldots\ldots\ldots\ldots\ldots \text{Equation (5.3)}$$

$$x_o = (x_o(1), x_o(2), \ldots., x_o(n)), \quad x_o \in Xo \quad \ldots\ldots\ldots\ldots\ldots\ldots \text{Equation (5.4)}$$

The grey relational coefficient (GRC) (Eq. 5.5) is calculated as

$$\gamma\big(x_0(k), x_i(k)\big) = \frac{\Delta min + \zeta \Delta max}{\Delta_{0i}(k) + \zeta \Delta max},$$

$$\zeta \in [0,1] \quad \ldots\ldots\ldots\ldots\ldots\ldots\ldots\ldots \text{Equation (6.5)}$$

Where

- i = 1, 2……27; k =1, 2, 3,4
- $\Delta min = min_i\, min_j \parallel x_0(k) - x_i(k) \parallel$
- $\Delta max = max_i\, max_j \parallel x_0(k) - x_i(k) \parallel$

The Grey Relational Grade (GRG) (Eq. 5.6) is obtained as

$$\gamma(x_0, x_i) = \frac{1}{m}\sum_{k=1}^{m} \gamma\big(x_o(k), x_i(K)\big) \quad \ldots\ldots \text{Equation (5.6)}$$

Table 5.5 shows the experimental data considered for calculation of grey relational coefficient and grey relational grade for experiments performed. The grey relational co-efficient and grey grade for L27 experiments performed is depicted in Table 5.5.

Table 5.5 Data for Grey Relation Analysis

Orthogonal Array (k)	Response variables			
	Thrust (N) (1)	Torque (Nm) (2)	Roughness (μm)(3)	Material removal rate (mm^3/min) (4)
1	152.02	3.72	1.713	7500
2	181.36	4.27	1.956	7500
3	193.91	5.62	1.926	7500
4	201.34	4.67	2.562	10000
5	209	4.87	2.915	10000
6	245.71	5.96	2.518	10000
7	236.46	5.01	2.873	12500
8	239.58	6.77	2.306	12500
9	295.52	7.65	2.304	12500
10	196.13	5.36	1.953	9000
11	222.65	6.02	3.140	9000
12	232.38	4.92	1.869	9000
13	238.72	6.38	2.375	12000
14	242.33	6.92	3.149	12000
15	256.66	7.01	2.835	12000
16	248.58	6.32	2.531	15000
17	278.23	7.78	3.246	15000
18	296.11	7.02	2.945	15000
19	222.56	6.78	1.783	10500
20	235.74	7.03	2.013	10500
21	287.48	7.78	2.035	10500
22	234.44	7.73	2.742	14000
23	258.94	8.96	2.278	14000
24	325.53	9.89	2.905	14000
25	286.51	9.63	3.014	17500
26	311.2	10.454	3.145	17500
27	353.6	11.34	3.515	17500

Table 5.6 Processed Data with Grey Relation Analysis

	Response variables				Normalization				Deviations				GRA co efficient				GRG
	Thrust	Torque	Roughness	MRR	Thrust	Torque	Roug.	MRR	Thrust	Torque	Roug.	MRR	Thrust	Torque	Roug.	MRR	
1	152.02	3.72	1.713	7500	1	1	1	0	0	0	0	1	1	1	1	0.333	0.833
2	181.36	4.27	1.956	7500	0.8544	0.9278	0.865	0	0.1455	0.0721	0.135	1	0.774	0.873	0.787	0.333	0.692
3	193.91	5.62	1.926	7500	0.7921	0.7506	0.8816	0	0.2078	0.2493	0.1183	1	0.706	0.667	0.808	0.333	0.628
4	201.34	4.67	2.562	10000	0.7553	0.8753	0.5283	0.25	0.2446	0.1246	0.4716	0.75	0.671	0.800	0.514	0.4	0.596
5	209	4.87	2.915	10000	0.7173	0.8490	0.3322	0.25	0.2826	0.1509	0.6677	0.75	0.638	0.768	0.428	0.4	0.558
6	245.71	5.96	2.518	10000	0.5352	0.7060	0.5527	0.25	0.4647	0.2939	0.4472	0.75	0.518	0.629	0.528	0.4	0.519
7	236.46	5.01	2.873	12500	0.5811	0.8307	0.3555	0.5	0.4188	0.1692	0.6444	0.5	0.544	0.747	0.437	0.5	0.557
8	239.58	6.77	2.306	12500	0.5656	0.5997	0.6706	0.5	0.4343	0.4002	0.3293	0.5	0.53	0.555	0.603	0.5	0.548
9	295.52	7.65	2.304	12500	0.2881	0.4842	0.6716	0.5	0.7118	0.5157	0.3283	0.5	0.412	0.492	0.603	0.5	0.502
10	196.13	5.36	1.953	9000	0.7811	0.7847	0.8666	0.15	0.2188	0.2152	0.1333	0.85	0.695	0.699	0.789	0.370	0.638
11	222.65	6.02	3.140	9000	0.6496	0.6981	0.2072	0.15	0.3503	0.3018	0.7927	0.85	0.587	0.623	0.387	0.370	0.492
12	232.38	4.92	1.869	9000	0.6013	0.8425	0.9133	0.15	0.3986	0.1574	0.0866	0.85	0.556	0.760	0.852	0.370	0.634
13	238.72	6.38	2.375	12000	0.5698	0.6509	0.6322	0.45	0.4301	0.3490	0.3677	0.55	0.537	0.588	0.57	0.476	0.544
14	242.33	6.92	3.149	12000	0.5519	0.5800	0.2022	0.45	0.4480	0.4199	0.7977	0.55	0.527	0.543	0.385	0.476	0.483
15	256.66	7.01	2.835	12000	0.4809	0.5682	0.3766	0.45	0.5190	0.4317	0.6233	0.55	0.490	0.536	0.445	0.476	0.487
16	248.58	6.32	2.531	15000	0.5209	0.6587	0.5455	0.75	0.4790	0.3412	0.4544	0.25	0.510	0.594	0.524	0.666	0.573
17	278.23	7.78	3.246	15000	0.3738	0.4671	0.1483	0.75	0.6261	0.5328	0.8516	0.25	0.444	0.484	0.370	0.666	0.491
18	296.11	7.02	2.945	15000	0.2851	0.5669	0.3155	0.75	0.7148	0.4330	0.6844	0.25	0.411	0.535	0.422	0.666	0.509

	Response variables				Normalization				Deviations				GRA co efficient				GRG
	Thrust	Torque	Roughness	MRR	Thrust	Torque	Roug.	MRR	Thrust	Torque	Roug.	MRR	Thrust	Torque	Roug.	MRR	
19	222.56	6.78	1.783	10500	0.6500	0.5985	0.9611	0.3	0.3499	0.4015	0.0388	0.7	0.588	0.554	0.927	0.416	0.621
20	235.74	7.03	2.013	10500	0.5846	0.5656	0.8333	0.3	0.4153	0.4343	0.1666	0.7	0.546	0.535	0.750	0.416	0.562
21	287.48	7.78	2.035	10500	0.3280	0.4671	0.8211	0.3	0.6719	0.5328	0.1788	0.7	0.426	0.484	0.736	0.416	0.516
22	234.44	7.73	2.742	14000	0.5911	0.4737	0.4283	0.65	0.4088	0.5262	0.5716	0.35	0.550	0.487	0.466	0.588	0.523
23	258.94	8.96	2.278	14000	0.4695	0.3123	0.6862	0.65	0.5304	0.6876	0.3137	0.35	0.485	0.420	0.614	0.588	0.527
24	325.53	9.89	2.905	14000	0.1392	0.1902	0.3377	0.65	0.8607	0.8097	0.6622	0.35	0.367	0.381	0.430	0.588	0.441
25	286.51	9.63	3.014	17500	0.3328	0.2244	0.2772	1	0.6671	0.7755	0.7227	0	0.428	0.391	0.409	1	0.557
26	311.2	10.454	3.145	17500	0.2103	0.1162	0.2042	1	0.7896	0.8837	0.7957	0	0.387	0.361	0.386	1	0.533
27	353.6	11.34	3.515	17500	0	0	0.0011	1	1	1	1.0011	0	0.333	0.333	0.333	1	0.5

The last column of the table 5.6 indicates the Grey relation grades. Higher the numerical value of grade, better is the result optimized and indicates optimum parameter setting in relation to the multiple objective optimization requirement. Experimental run numbers 1,2 and 10 have the top three Grey relation grades. This indicates that the corresponding cutting speed, feed rate and insert grade combination gives the bset optimization for minimum values of thrust force, torque and surface roughness and maximum value of material removal rate. This exercise combines all the response variables in a single grade.

5.5 Test for finding the significance of individual parameter

Grey relation grade for all set of same values of experimental observations was averaged i.e. Grey grades for all the experiments with speed level of 25 m / min is averaged in first column, for 30 m / min in second column and then 35 m / min in third column. Similarly, average values for Grey grades for parameter feed rate are calculated in second row and average values of grades for same coating in third row.

The minimum and maximum values of these are recorded in next column and finally, the difference of minimum and maximum values of these gray grades is calculated. Higher the difference is considered as single most significant individual factor affecting the response variables. From table 5.7, it is observed that, feed rate has highest influence on maximizing the MRR and minimizing the thrust torque and roughness values. After feed rate, insert coating and cutting speed affect the response variables. This conclusion is in line with previous research findings.

Table 5.7 Significance of parameters based on GRA

Parameter	1	2	3	Max	Min	Significance (max-min)	Rank
Speed	0.604096	0.539479	0.5315	0.604096	0.5315	0.072596	**3**
Feed	0.624487	0.520232	0.530358	0.624487	0.520232	0.104255	**1**
Insert coating	0.605208	0.543265	0.526603	0.605208	0.526603	0.078606	**2**

5.6 Confirmatory experiments as per GRA

The grey relational analysis (GRA) was carried out to find the optimum process parameters. After analysis, the best parameters were listed according to hierarchy. Based on this hierarchy, corresponding process parameters for first three ranks were considered to carry out validation experiments. Experiment number 1, 2 and 10, which give optimum results were performed for validation of grey relation analysis, using same experimental set up and the same

insert coating grade and the response variables like thrust, torque and surface roughness was measured.

Table 5.8 Comparison of Taguchi and GRA responses

Expt. No.	Thrust	Torque	Roughness	MRR
1	152.02	3.72	1.71	2793.66
GRA	158.34	3.32	2.13	2723.03
2	181.36	4.27	1.96	2714.04
GRA	176.44	4.15	2.31	2640.54
10	196.13	5.36	1.953	3232.71
GRA	241.81	5.04	2.39	3246.52

The results of thrust, torque and surface roughness in comparison with original experiments performed using Taguchi method are given in Table 5.8.

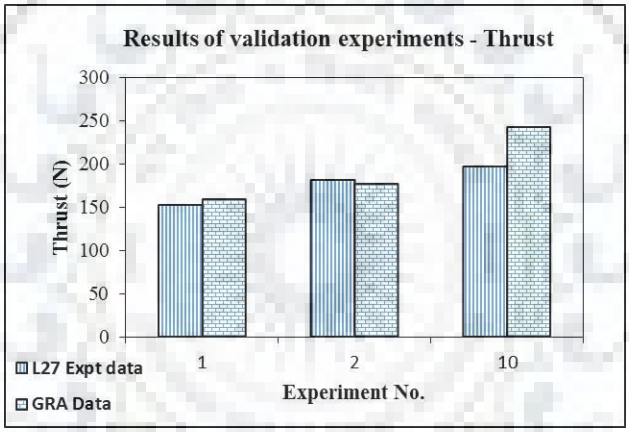

Fig. 5-11 Plot for validation experiments - Thrust

The comparisons of thrust force for top 3 ranks as identified by GRA and corresponding L_{27} experiments of are shown in Fig. 5.11. The results were observed to be in close agreement with each other. Third rank experiment (no. 10) shows slightly more variation.

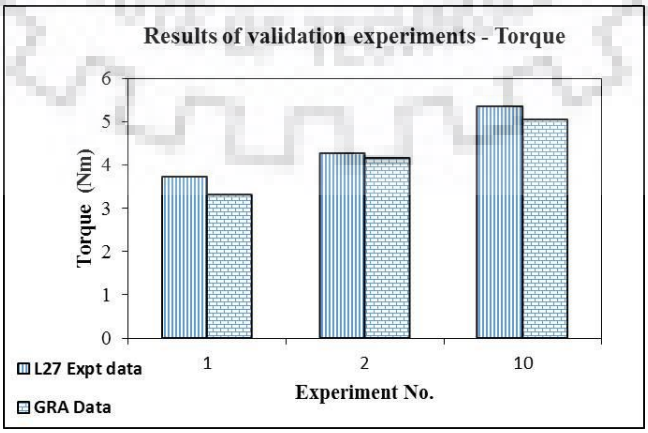

Fig. 5-12 Plot for validation experiments – Torque

The comparisons of torque for top 3 ranks as identified by GRA and corresponding L_{27} experiments of are shown in Fig. 5.12 (Expt. Nos. 1, 2 and 10). The results were observed to be in close agreement with each other.

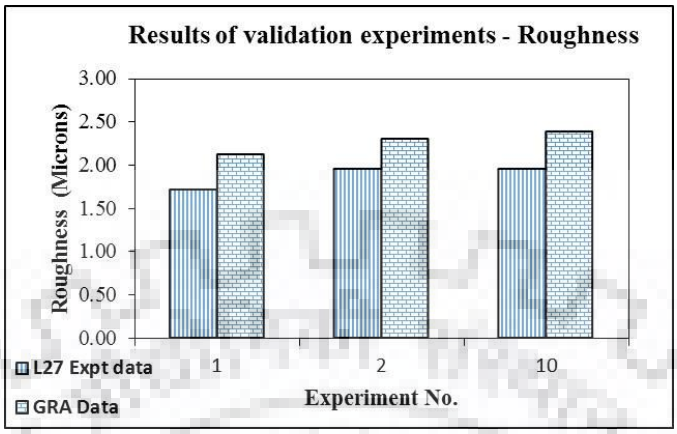

Fig. 5-13 Plot for validation experiments – Surface roughness

The comparisons of surface roughness for top 3 ranks as identified by GRA and corresponding L_{27} experiments of are shown in Fig. 5.13 (Expt. Nos. 1, 2 and 10). The results were observed to be in close agreement with each other.

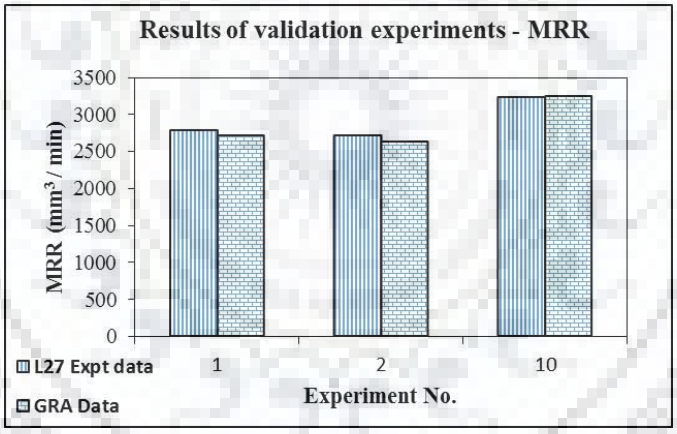

Fig. 5-14 Plot for validation experiments – MRR

The comparisons of material removal rate for top 3 ranks as identified by GRA and corresponding L_{27} experiments of are shown in Fig. 5.14 (Expt. Nos. 1, 2 and 10). The results were observed to be in close agreement with each other.

5.7 Observations on tool wear

Surface quality of the machined surface and cutting forces developed, are important indicators quality of cutting tool and its performance. However the tool life obtained while machining is most important quality indicator. The tool life directly affects the cost and economics of the process. For the machining method and tool selection to be economically viable, cutting tool must be able to give desired surface quality, with minimum cutting forces for a longer period of time. Tool life in general can be expressed in time units. It is total time accumulated before the tool

fails. It can be defined as period during which the tool cuts satisfactory. Also it can be expressed as time for which the tool can be used without re-grinding the cutting edge or replacing the cutting edge in case of indexable tools.

The cutting edge of the all the three types of inserts used in the experimentation were studied under LECIA DMiS digital microscope for the analysis and study of tool wear pattern. A crater wear of 206 μm depth and 472 μm width was observed as shown in Fig. 5.15 (a) and (b). This depth was less than the failure criteria of 0.5 millimeter depth for considering the tool to have failed (Talib *et al* 2007). It was observed that, AlTiN coated TT 9080 inserts have proven to be better, producing lowest mean thrust force, mean torque and mean surface roughness values. It was observed that these inserts have performed better compared to other inserts used in this work. The better performance of this grade can be associated to its nano multi-layer coating of 4 – 6 μm thickness and its strong cutting edge. Bonding of this coating with substrate material is very strong.

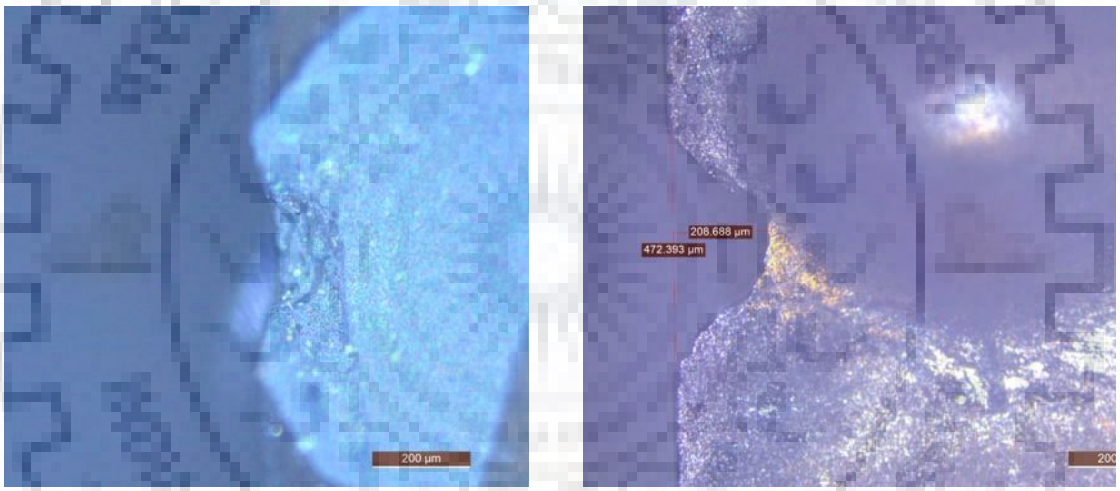

(a) **(b)**

Fig. 5-15 Crater wear on TT 9080 insert

The second grade of insert used in experimentation was titanium carbide nitride (TiCN) coated TT 8020. The cutting edge studied under the microscope revealed uniform wear of the cutting edge. The average depth of edge of chipping was reported to be 68 μm for entire width of the insert. Some pits were also observed on cutting edge with maximum pit depth of around 25 μm at the center. This TT 8020 insert provided intermediate values of thrust and torque but it also produce the highest surface roughness value amongst all the three insert used. The uniform edge wear and pits are shown in Fig. 5.16 (a) and (b).

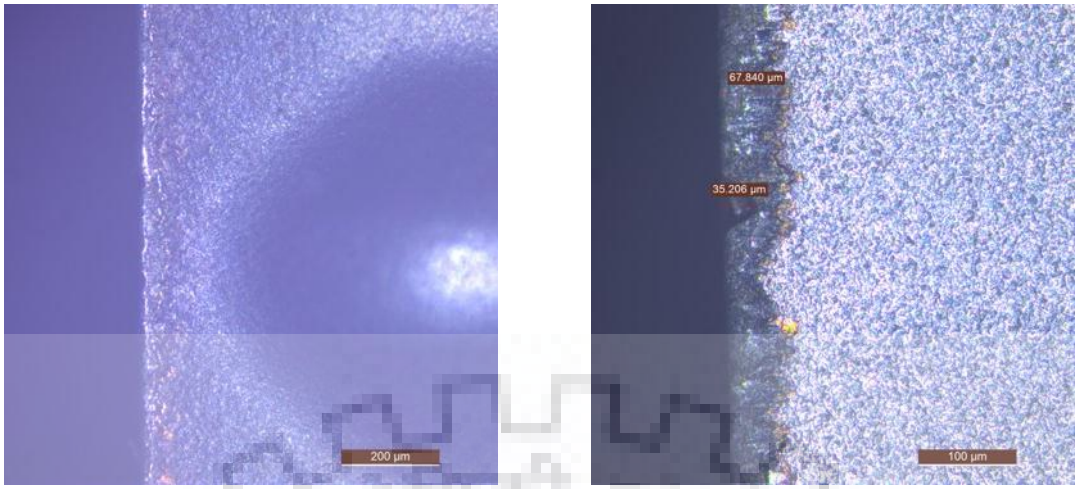

(a) **(b)**

Fig. 5-16 TT 8020 insert (a) Uniform edge wear (b)Pitting on insert

The third grade of insert used in experimentation was PVD TiCN coated TT 7220 mono layer coated inserts. When this insert was observed under microscope, uneven wear on the relief face of the insert was observed. Edge chipping up to 725 µm of length was observed. One corner of the insert was broken as shown in Fig. 5.17 (b). This TT 7220 insert produced the highest value of mean thrust and torque and intermediate values of surface roughness.

(a) **(b)**

Fig. 5-17 TT 7220 insert (a)Edge wear of the insert (b) Broken edge

The study of wear pattern of the inserts indicates that, TT 9080 AlTiN insert has proven to be a better insert as compared to other to grades of the insert coating used in this experimentation. This AlTiN coating has multilayer nano coating, gives very high edge strength had coating has very strong bonding with the substrate. Due to these reasons, this coating has produced minimum thrust force and mid-range of torque and surface roughness.

5.8 Observations on the chips produced

In machining, materials get converted into chips. The chips thus produced give us an insight on the nature of machining. The size, shape, length, colour and texture of chips produced tells us about the success of machining process. It was observed that size, shape and other parameters of chips varied with the insert used and the levels of machining parameters. The Fig. 5.18 (a) (b) and (c) shows photographs of chips produced 25 m /min cutting speed and at varying feed rate of 0.03, 0.04 and 0.05 mm / rev. respectively, while using TiCN coated TT 8020 inserts in trepanning. These are for run numbers 2, 5 and 8 as per L_{27} orthogonal array.

Fig. 5-18 Chips (a) at 0.03 mm / rev (b) at 0.04 mm / rev and (c) at 0.05 mm / rev

As shown in Fig. 5.18 (a) the chips produced at 0.03 mm / rev. feed rate have very small cross section and are dis-continuous chips. They have very smooth surface.

The Fig. 5.18 (b) shows chips produced at a higher feed rate of 0.04 mm / rev. It was observed that chips were continuous and there was no indication of burning or overheating at tool chip interface. These chips did not break properly and posed some problems in chip evacuation at increased cutting speed.

The Fig. 5.18 (c) shows the chips produced at cutting speed of 30 m / min but at highest feed rate of 0.05 mm / rev. Increase in feed rate increases the uncut chip thickness. This causes formation of continuous chips. As the continuous chips rubs on the chip breaker and front lip of the tool, its bottom surface experiences more friction. Thus the serrations on chip surface are produced. Higher amount of thrust and torque was recorded at higher feed rates. With continuous chips, chip clearance from machining area after reaching depth of insert length becomes difficult. The chips gets clogged in annular area. This increases the torque on the tool. Excessive heat and burnt chips were observed at higher feed rate of 0.05 mm / revolution.

5.9 Observations on hole diameter

Along with the other quality parameters, the diameter of trepanned holes is one of the important quality parameters. It is very important to ensure that hole produced has circularity and

straightness. Diameter of the hole at the entrance and at the exit of the hole was measured by micrometer at two different positions. In conventional drilling, some amount of burr is produced at exit of the hole. The height of the burr is also one of the quality criterions. It was observed that the diameter of holes produced at the beginning and at the exit was almost same. The diameter of the hole produced varied between 39.350 and 39.750 mm with a mean value of 39.570 mm. Similarly the external diameter of the central core removed was also measured and it was observed to very between a maximum values of 31.550 mm to a minimum value of 31.275 mm. The mean diameter of central core was reported to be 31.46 mm. Based on these observations, it was concluded that the performance of the newly designed trepanning tool was satisfactory.

Table 5.9 Measurement of hole and core diameter

Run no.	Inner dia. of hole (1) in mm	Inner dia. of hole (2) in mm	Outer dia. of core (1) in mm	Outer dia. of core (1) in mm	Avg. Inner dia. of hole (mm)	Avg. outer dia. of core (mm)
1	39.65	39.70	31.05	31.50	39.67	31.27
2	39.70	39.30	31.40	31.25	39.50	31.32
3	39.75	39.40	31.40	31.40	39.57	31.40
4	39.75	39.40	31.50	31.60	39.57	31.55
5	39.75	39.40	31.40	31.50	39.57	31.45
6	39.70	39.30	31.40	31.30	39.50	31.35
7	39.75	39.40	31.50	31.60	39.57	31.55
8	39.60	39.40	31.40	31.30	39.50	31.35
9	39.75	39.70	31.50	31.40	39.72	31.45
10	39.65	39.44	31.50	31.40	39.54	31.45
11	39.65	39.45	31.60	31.40	39.55	31.50
12	39.30	39.45	31.50	31.45	39.37	31.47
13	39.70	39.70	31.50	31.60	39.70	31.55
14	39.70	39.50	31.45	31.20	39.60	31.32
15	39.66	39.40	31.50	31.40	39.53	31.45
16	39.66	39.50	31.50	31.50	39.58	31.50
17	39.64	39.42	31.50	31.40	39.53	31.45
18	39.75	39.75	31.60	31.50	39.75	31.55
19	39.71	39.35	31.50	31.40	39.53	31.45
20	39.72	39.40	31.50	31.45	39.56	31.47
21	39.67	39.38	31.50	31.60	39.52	31.55
22	39.45	39.25	31.50	31.50	39.35	31.50
23	39.75	39.60	31.50	31.60	39.67	31.55
24	39.75	39.40	31.50	31.45	39.57	31.47
25	39.75	39.70	31.50	31.50	39.72	31.50
26	39.70	39.40	31.45	31.45	39.55	31.45
27	39.75	39.30	31.45	31.51	39.52	31.48
				Avg. Size	39.57	31.46

5.10 Multi objective optimization using Minitab R19

In performance analysis of trepanning tool, four different response variables are considered. They are thrust force generated, torque, surface roughness of the trepanned hole and material removal rate. Out of which the material removal rate is considered to be maximum to be better whereas cutting forces that is thrust force, torque and the surface roughness generated on the trepanned hole are smaller the better. All these four response variables depend on the three input variables that is cutting speed mentioned in meters per minute, feed rate in mm per revolution and type of coating used on the inserts and the interaction between them. We have three different grades of insert coatings.

First of all regression model for individual response variables were generated. For developing regression model, the parameters cutting speed and feed rate, which have numerical values, are considered as continuous predictor variables. Whereas the parameter insert coating has three different grades and which is not expressed in numerical value is considered as categorical predictor variable.

This selection of insert coating as a categorical variable gives a set of three regression equations for predicting the thrust force for each setting of insert coating as given below.

For insert coating TT9080, Thrust = -101.1 + 6.234 Speed+3453 Feed

For insert coating TT8020 Thrust = -83.0 + 6.234 Speed + 3453 Feed

For insert coating TT7220 Thrust = -48.8 + 6.234 Speed + 3453 Feed.

Thus the experimental data set is analyzed separately for each setting of continuous variable.

Similarly, the regression equation for torque also gives three different regression equations for each setting of insert coating as given below.

For insert coating TT9080, Torque = -8.72+ 0.3450 Speed+ 113.7 Feed

For insert coating TT8020 Torque = -7.89+ 0.3450 Speed+ 113.7 Feed

For insert coating TT7220 Torque =-7.44+ 0.3450 Speed+ 113.7 Feed

The regression equation for the surface roughness is given below.

Roughness = 0.874+ 41.62 Feed

The regression equation for the material removal rate is given below.

MRR = 451 - 16.8 Speed - 8516 Feed+ 3930 Speed*Feed

In this work, optimization of conflicting response variables is required. Three response variables need to be minimized while simultaneously one response variable needs maximization. For this type of multi-objective optimization, a utility called “response

Optimizer" in Minitab 19 software was used. This utility can optimize up to 25 independent responses at a time. This utility has a provision to define the criterion for optimization such as smaller the better, target value or larger the better. In present work, one parameter i.e. material removal rate is "maximum the better" and other three variables i.e. thrust, torque and surface roughness are "minimum the better".

Considering the above optimization requirements and data set of experimental observations, the optimal parameter setting recommended by the utility response optimizer is as given below:

Table 5.10 Optimized parameter setting through Minitab 19

Cutting speed (m/min)	Feed rate (mm/rev)	Coating grade	MRR (mm^3/min)	Roughness (μm)	Torque (Nm)	Thrust (N)
29.1414	0.0378788	TT9080	3976.77	2.45046	5.64025	211.407
Validation experiment results			3989.79	2.497	5.76	215.23

The graph indicating the optimized parameter setting and corresponding response variables is shown in Fig. 5.19 below.

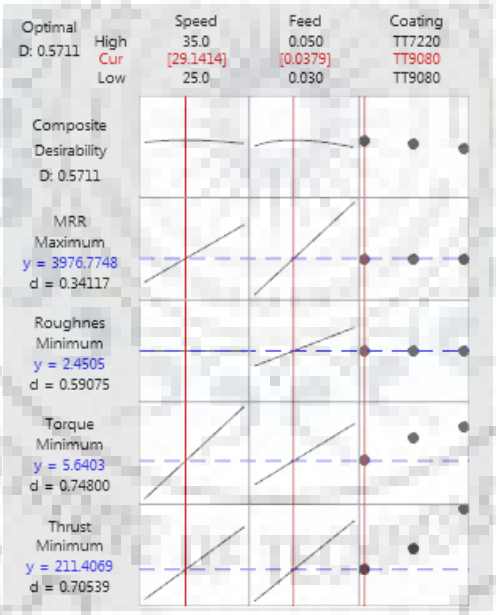

Fig. 5-19 Multi objective optimization of response variables

The response optimization utility in Minitab has given optimized parameter settings as shown in Table 5.10. Validation experiment was conducted using fresh TT 9080 insert at cutting speed of 29.1414 m/min and feed rate at 0.038 mm/revolution. The octagonal ring type dynamometer was used for recording the thrust and torque forces during machining.

Chapter 6

SUMMARY, CONCLUSIONS and FUTURE SCOPE

6.1 Summary

Increasing the productivity and efficiency of any machining process along with the overall cost reduction is a very important consideration in manufacturing industry. In conventional drilling operations, the entire volume of drilled hole is converted into chips. This wastage is very large if the hole diameter is more than 30 mm and if these holes are required in large quantities.

Since drilling is most commonly used machining process of all machining processes, material recycling or any other form of improvement in drilling techniques has a very positive impact on the economics of machining. Trepanning process produces holes by removing material in the annular ring form and saving the central core for any other further use. The motivation for this work was to design a tool which would save central core from a 40 mm diameter drilled hole efficiently. The designed tool saves more material than commercially available alternatives for the same size. Engineering design methodology has been followed for this toll development. The summary of the present work is given below.

Chapter 1 presented an introduction, the drilling processes and their different variations. Basic principle and advantages and limitations of trepanning process were discussed. At the last of this chapter, motivation of the present research work with thesis overview has been discussed.

Chapter 2 involved discussions on various aspects of drilling, trepanning and its advancements. The literature review was divided in different categories like effect of tool geometry on thrust and torque forces, delamination studies in GFRP machining, non-conventional trepanning processes, effect of tool coating on tool life, effect of tool geometry and coating on surface finish and latest trends in finite element methods in simulation of machining processes. The methodology of the proposed research work was also discussed in the end of this chapter.

Chapter 3 discussed about design and manufacturing of octagonal ring type strain gauge based dynamometer for the measurement of cutting forces. The detailed methodology and process followed for new trepanning tool designed is discussed in details. The application of smoothed particle hydrodynamics (SPH) method in LS DYNA used for simulation and validation of new tool design is discussed in this chapter. The results of simulation and actual force measurement is also discussed in this chapter.

Chapter 4 discussed the manufacturing of trepanning tool, machining set up and experimental work carried out. The strategy of experimentation, selection of control parameters and their level is also discussed in this chapter. The Taguchi method was followed for experimental work and the same has been reported.

Chapter 5 discussed the effect of the various input process parameters on the response variables. Four response variables were considered in this work. The thrust, torque and surface roughness were considered as smaller the better. The material removal rate was considered as larger the better. Statistical results for each of the response variable, the Grey relation analysis for optimization are also discussed in details in this chapter. The other important criterions like tool wear, analysis of hole diameter and multi objective optimization strategy using response optimizer utility in Minitab software is discussed in this chapter.

6.2 Conclusions

Based on the results presented in the chapter 3 to 5 following major conclusions have been drawn.

- The octagonal ring type strain gauge based dynamometer was designed and manufactured for the accurate measurement of thrust force and torque in trepanning of stainless steel (SS 304) work pieces.
- The validation of structural design of dynamometer was carried out using finite element method with the help of ANSYS software.
- The maximum sensitivity, minimum cross sensitivity and high accuracy of force measurement was ensured by placing strain gauges at accurate locations on strain sensing members i.e. octagonal rings using FEA analysis with ANSYS software.
- The trial experimentation of trepanning was carried out with a three insert tool concept for trepanning of 40 mm diameter holes.
- New tool design concept using two inserts was realized in CAD modeling using SOLIDWORKS software.
- The simulation of trepanning operation on 40 mm thick stainless steel 304 was conducted using mesh free simulation feature of LS DYNA software, smoothed particle hydrodynamics (SPH).
- Structural analysis of the proposed trepanning tool body was carried out using mesh free simulation feature of LS DYNA software.
- The trepanning tool was developed as per the geometry specifications in CAD model.
- The simulation results for the thrust force and torque were cross checked by conducting

actual trepanning of work piece. Simulation and actual results were found to be in good agreement with each other.

- It has been found that the tool successfully drills 40 mm depth and 40 mm diameter holes in stainless steel 304 material.
- The effect of the process parameters on the thrust force and torque developed, and the surface roughness of trepanned hole have been studied using design of experiments and ANOVA analysis. The thrust and torque were predicted using Finite element analysis and it is evident that the simulation results and experimentation results are in close agreement with each other.
- The measurement of surface roughness of trepanned hole reveled that, the developed tool produces good surface finish of the holes. Average surface roughness (Ra) values in a range of 1.783 μm to 3.246 μm were obtained.

6.3 Scope for future work

The work presented in this thesis may be extended further in the following ways:

- In the present work, a trepanning tool for trepanning of 40 millimeter diameter holes in 40 millimeter thick stainless steel 304 material is developed successfully. This tool can be used for other difficult to machine / aerospace materials by selecting proper insert coating grades.
- The current tool does not have facility for centering the tool at proper location. This facility can be added in the tool design to ensure accurate positioning of the tool at desired location.
- A provision for super finishing of the trepanned hole, by providing some suitable arrangement like an abrasive layer on the tool body, up stream of the insert can be tried upon.
- Comparison between trepanning and other similar operations in which the tool is guided (drilling or drilling like) in annular way can be corroborated for future extension of this study.

REFERENCES

[1] Abdelhafeej *et al*., "A coupled Eulerian Lagrangian finite element model of drilling titanium and aluminium alloys", SAE International Journal of Aerospace 9(1), Pp 198-207, 2016, https://DOI.org/10.4271/2016-01-2126

[2] Abele and Fujara, "Simulation-based twist drill design and geometry optimization", CIRP Annals, Volume 59, Issue 1, 2010, Pp 145-150, https://DOI.org/10.1016/j.cirp.2010.03.063

[3] Amran *et al.,* "Effects of machine parameters on surface roughness using response surface method in drilling process", The Malaysian International Tribology Conference 2013, MITC2013, DOI: 10.1016/j.proeng.2013.12.142

[4] Arrazola *et al.,* "Recent advances in modeling of metal machining processes", CIRP Annals - Manufacturing Technology 62, 2013, Pp 695–718

[5] Ashkenasi *et al.,* "Advanced laser micro machining using a novel trepanning system", Journal of Laser Micro/Nanoengineering Vol. 6, No. 1, 2011, DOI:10.2961/jlmn.2011.01.0001

[6] Audy *et al.,* "The effect of PVD coatings on the cutting forces and friction when orthogonal cutting 316 stainless steel," Proceedings of the Third Asia Pacific Forum on Precision Surface Engineering and Deburring Technology, 2003, The Swinburne University of Technology, Melbourne, Pp 336–345

[7] Bagchi, "Taguchi methods explained: Practical steps to robust design", 1993, Prentice-Hall

[8] Bagci, "3-D numerical analysis of orthogonal cutting process via mesh-free method", International Journal of the Physical Sciences Vol. 6(6), Pp 1267-1282, 2011, DOI: 10.5897/IJPS10.600

[9] Bajpai *et al.,* "Finite element modeling of three-dimensional milling process of Ti–6Al–4V", Materials and manufacturing processes, Vol. 29, 2014, Issue - 5, Pp 564-571, DOI: 10.1080/10426914.2014.892618

[10] Benga, "The influence of different PVD coatings techniques on cutting forces in a drilling process", 6th International DAAAM Baltic Conference, Industrial engineering - 24-26 April 2008, Tallinn, Estonia

[11] Biswas *et al.,* "Three-dimensional finite element prediction of transient thermal history and residual deformation due to line heating", Proceedings of the Institution of Mechanical Engineers Vol. 221 Part M: Journal of Engineering for the Maritime Environment, 2007

[12] Biswas *et al.,* "Prediction of welding deformations of large stiffened panels using average plastic strain method", Science and Technology of Welding and Joining, 16:3, Pp-227-231, 2011, DOI: 10.1179/1362171811Y.0000000004

[13] Biswas *et al.,* "Study on the effect of tool profiles on temperature distribution and material flow characteristics in friction stir welding", Proceedings of the Institution of Mechanical Engineers Part B: Journal of Engineering Manufacture 226(9), 2012, DOI: 10.1177/0954405412451811

[14] Biswas *et al.,* "Prediction of weld-induced distortion of large structure using equivalent load technique", Proceedings of the Institution of Mechanical Engineers Part B Journal of Engineering Manufacture · March 2016, DOI: 10.1177/0954405416646309

[15] Boothroyd and Knight, "Fundamentals of metal machining and machine tools", 2006, Marcel Dekker Inc

[16] Chak and Rao, "Trepanning of Al_2O_3 by electro-chemical discharge machining (ECDM) process using abrasive electrode with pulsed DC supply", International Journal of Machine Tools & Manufacture 47, 2007, Pp 2061-2070

[17] Chang et al., "Applying grey relational analysis to the vendor evaluation method", International Journal of Computer, The Internet and Management, Vol. 11, No. 3, 2003, Pp 45-53

[18] Chen and Tsao, "Cutting performance of different coated twist drills", Journal of Materials Processing Technology, Volume 88, Issues 1–3, April 1999, Pp 203-207, https://DOI.org/10.1016/S0924-0136(98)00396-3

[19] Cicek *et al.,* "Performance of cryogenically treated M35 HSS drills in drilling of austenitic stainless steels", International Journal of Advanced Manufacturing Technology, 60 (1–4), 2012, Pp 65-73

[20] Danisman *et al.,* "Comparison of wear behaviors of cathodic arc TiN, TiAlN coated and uncoated twist drills under aggressive machining conditions", Tribology in industry Volume 30, No. 1& 2, 2008

[21] Debnath *et al.*, "Damage-free hole making in fiber-reinforced composites: an innovative tool design approach", Materials and manufacturing processes, Vol. 31, 2016, Issue - 10, Pp 1400-1408, DOI: 10.1080/10426914.2016.1140191

[22] Debnath *et al.,* "An innovative tool for engineering good-quality holes in composite laminates", Materials and manufacturing processes, Vol. 32, 2017, Issue - 9, Pp 952-957, DOI: 10.1080/10426914.2016.1221084

[23] Derflinger *et al.,* "New hard/lubricant coating for dry machining", Surface and Coatings Technology, Volume 113, Issue 3, March 1999, Pp 286-292, https://DOI.org/10.1016/S0257-8972(99)00004-3

[24] DeGarmo's, "Materials and processes in manufacturing", John Wiley, 10th edition; Pp 627, 638, 646-651

[25] Drake and McGEOUGH. "Aspects of drilling by electrochemical arc machining", Proceedings of the 22nd International Machine Tool Design and Research Conference, Macmillan Publishers Limited, 1982

[26] El-Bahloul *et al.,* "Experimental and thermo-mechanical modeling optimization of thermal friction drilling for AISI 304 stainless steel", CIRP Journal of Manufacturing Science and Technology 20, 2018, Pp 84-92

[27] Espinosa *et al.,* "High Speed machining with the SPH method", 10th International LS-DYNA Users Conference, 8 June 2008 - 10 June 2008, Dearborn, United States

[28] Ficici *et al.*, "Optimization of cutting parameters for surface roughness of stainless steel in drilling process", International Journal of Science and Advanced Technology, 2 (3), 2012, Pp 114-121

[29] Gaikwad et al., "Design, development, and calibration of octagonal ring type dynamometer with FEA for measurement of drilling thrust and torque", Journal of Testing and Evaluation, Nov. 2018, https://DOI.org/10.1520/JTE20170791

[30] Gao *et al.,* "Simulation of stainless steel drilling mechanism based on Deform-3D", Advanced Materials Research Online: 2010-11-11, DOI:10.4028/www.scientific.net/AMR.160-162.1685

[31] Giri and Mahapatra, "On the measurement of sub-surface residual stresses in SS 304L welds by dry ring core technique", Measurement 106, 2017, Pp 152-160, DOI: dx.DOI.org/10.1016/j.measurement.2017.04.043

[32] Gök *et al.,* "The validation as experimental and numerical of the values of thrust force and torque in drilling process", Journal of Engineering Science and Technology Review 6 (3), 2013, Pp 93 - 99, DOI: 10.25103/jestr.063.17

[33] Gupta *et al.,* "Development of constitutive models for dynamic strain aging regime in Austenitic stainless steel 304", Materials and Design 45, 2013, Pp 616–627

[34] Gyliene and Eidukynas, "The numerical analysis of cutting forces in high feed face milling, assuming the milling tool geometry", 2013

[35] Gyliene, "Drilling process modelling using SPH", 9th European LS-DYNA Conference 2013

[36] Hashmi *et al.,* "Measurement and analysis of forces during high speed milling of EN-30b alloy steel", Journal of Basic Applied Science Res., 3(2), 2013, Pp 888-895

[37] Heinemann & Hinduja, "Investigating the feasibility of DLC-coated twist drills in deep-hole drilling", International Journal of Advanced Manufacturing Technology, 2009, 44, Pp 862-869, DOI 10.1007/s00170-008-1912-8

[38] Heinemann and Hinduja, "Effect of tool coatings on the performance of small-diameter drills in drilling deep holes with higher cutting speed", Proceedings of the 35th International MATADOR Conference, Formerly The International Machine Tool Design and Research Conference 2007

[39] Hongbing *et al.,* "Study on simulation and experiment of drilling for titanium alloys", Materials Science Forum Vols. 704-705, 2012, Pp 657-663

[40] Hossainy *et al.,* "Finite element simulation of metal cutting considering chip behavior and temperature distribution", Materials and manufacturing processes, Vol. 16, 2001, Issue -6, Pp 803-814, DOI:10.1081/AMP-100108700

[41] Isbilir and Ghassemieh, "Finite element analysis of drilling of carbon fiber reinforced composites", Applications of Composite Materials 19(3–4), Pp 637–656, 2012, DOI: 10.1007/s10443-011-9224-9

[42] Jain and Chak, "Electrochemical spark trepanning of alumina and quartz", Machining Science and Technology, Volume 4, 2000 - Issue 2, Pp 277-290, https://DOI.org/10.1080/10940340008945710

[43] Jahns *et al.,* "Laser trepanning of stainless steel", Lasers in Manufacturing Conference, 2013

[44] Joshi *et al.,* "An investigation of cutting forces and surface damage in high-speed turning of Inconel 718", Journal of Materials Processing Technology 192–193, 2007, Pp 139-146

[45] Joshi *et al.,* "Surface finish and integrity of machined surfaces on Al/SiCp composites", Journal of Materials Processing Technology 192–193, 2007, Pp 166-174

[46] Joshi *et al.,* "Effect of machining parameters and cutting edge geometry on surface integrity of high-speed turned Inconel 718", International Journal of Machine Tools & Manufacture 48, 2008, Pp 15-28

[47] Kalpakjian & Schmid, "Manufacturing engineering & technology", Prentice Hall, 6th Edition, 2009, pp 647

[48] Karabay, "Performance testing of a constructed drilling dynamometer by deriving empirical equations for drill torque and thrust on SAE 1020 steel", Materials and Design 28, 2007, Pp 1780-1793

[49] Karabay, "Analysis of drill dynamometer with octagonal ring type transducers for monitoring of cutting forces in drilling and allied process", Materials and Design 28, 2007, Pp 673-685

[50] Kivak *et al.,* "Taguchi method based optimization of drilling parameters in drilling of AISI 316 steel with PVD monolayer and multilayer coated HSS drills", Measurement 45, 2012, Pp 1547-1557, http://dx.DOI.org/10.1016/j.measurement.2012.02.022

[51] Korkut, "A dynamometer design and its construction for milling operation", Materials and Design 24, 2003, Pp 631-637

[52] Krasauskas *et al.,* "Experimental analysis and numerical simulation of the stainless AISI 304 steel friction drilling process", ISSN 1392−1207, MECHANIKA, 2014, Volume 20(6), Pp 590-595

[53] Kumar *et al.,* "The development and characterization of a square ring shaped force transducer", Measurement Science and Technology, 24, 2013,

[54] Kumar *et al.,* "Development and characterization of a modified ring shaped force transducer", MAPAN-Journal of Metrology Society of India, 2015, 30(1), Pp 37-47

[55] Kusinski *et al.,* "Investigation of the life-time of drills covered with the anti-wear Cr(C,N) complex coatings, deposited by means of Arc-PVD technique", Journal of Achievements in Materials and Manufacturing Engineering 33/1, 2009, Pp 86-93

[56] Lacalle et al., "Advanced Cutting Tools", Chapter 2, J.P.Davim (Eds.), Machining of hard materials,Springer-Verlag, London, 2011

[57] Lautre et al., "A simulation approach to material removal in microwave drilling of soda lime glass at 2.45 GHz", Applied Physics - A Material science and processing, 2015, 120: Pp 1261-1274, DOI 10.1007/s00339-015-9370-2

[58] Lautre *et al.,* "Performance of different drill bits in microwave assisted drilling", Int. Journal of Mech. Eng. & Rob. Res. Special Issue, Vol. 1, No. 1, January 2014

[59] Levi, "Drill press dynamometers", International journal of machine tool design and research, Vol. 7, 1967, Pp 269-287

[60] Li and Chunbo, "A Coupled Thermal-Mechanical Analysis of Ultrasonic Bonding Mechanism", The Minerals, Metals & Materials Society and ASM International, 2009, DOI: 10.1007/s11663-008-9224-9

[61] Li *et al.,* "An integrated welding and damage model for practical prediction of creep Life in welded p91 alloy", Proceedings of the Pressure Vessel & Piping Conference ASME 2016 PVP, July 17-21, 2016, Vancouver, BC, Canada

[62] Lotfi *et al.,* "Built-up edge reduction in drilling of AISI 1045 steel", Materials and Manufacturing Processes, 2016, DOI:10.1080/10426914.2016.1221104

[63] Mathew *et al.,* "Investigations into the effect of geometry of a trepanning tool on thrust and torque during drilling of GFRP composites", Journal of Materials Processing Technology 91, 1999, Pp 1-11

[64] Majerik *et al.,* "The verification of axial forces and torques in drilling by the non-coated cutting tools and drills with PVD TiN coating", Annals of DAAAM for 2012 & Proceedings of the 23rd International DAAAM Symposium, Volume 23, No.1, ISSN 2304-1382

[65] Monaghan and O'Reilly, "The drilling of an Al/SiC metal-matrix composite", Journal of Materials Processing Technology, Volume 33, Issue 4, September 1992, Pp 469-480, https://DOI.org/10.1016/0924-0136(92)90280-6

[66] Montgomery, "Design and Analysis of Experiments", Wiley, 2006

[67] Nahshon *et al.,* "Dynamic shear rupture of steel plates", Journal of Mechanics of Materials and Structures, Volume 2, No 10, December 2007

[68] Nan *et al.,* "On the application of 3D finite element modeling for small-diameter hole drilling of AISI 1045 steel", Int J Adv Manuf Technol, 2016, 84: Pp 1927-1939

[69] Noh *et al.,* "Trepanning Optical System Using Tilting Focus Lens for Laser Drilling Process", Journal of Laser Micro/Nanoengineering Vol. 4, No. 3, 2009, DOI: 10.2961/jlmn.2009.03.0019

[70] Olleak *et al.,* "The influence of Johnson-Cook parameters on SPH modeling of orthogonal cutting of AISI 316L", 10th European LS-DYNA conference 2015, Germany

[71] Pandey and Mulik, "Experimental investigations and modeling of finishing force and torque in ultrasonic assisted magnetic abrasive finishing", Journal of Manufacturing Science and Engineering October 2012, Vol. 134 / 051008-1, DOI: 10.1115/1.4007131

[72] Pandey *et al.,* "Study on machinability of al2o3 ceramic composite in EDM using response surface methodology", Journal of Engineering Materials and Technology April 2011, Vol. 133 / 021004-1, DOI: 10.1115/1.4003100

[73] Pandey *et al.*, "On the estimation of error in measuring the residual stress by strain gauge rosette", Measurement, Vol. 65, 2015, Pp 41-49

[74]Pandey *et al.*, "Effect of weld consumable conditioning on the diffusible hydrogen and subsequent residual stress and flexural strength of multi pass welded P 91 steels", Metallurgical and materials transactions B, Vol. 49, Issue 5, 2018, Pp 2881 -2895

[75] Pantel *et al.*, "3D FEM simulations of shoulder milling operations on a 304L stainless steel", Simulation Modelling Practice and Theory, Volume 22, 2012, Pp 13-27

[76] Panzera *et al.*, "Development of a three-component dynamometer to measure turning force", International Journal of Advance Manufacturing Technology, 2012, 62: Pp 913-922

[77] Parida *et al.*, "Design and development of fixture and force measuring system for friction stir welding process using strain gauges", Journal of Mechanical Science and Technology 29 (2), 2015, Pp 739-749

[78] Patel et al., "Force determination during orthogonal machining of titanium alloy using ABAQUS/explicit", 2016, DOI 10.1007/s00170-015-7782-y

[79] Pathak *et al.*, "Experimental analysis of coated and uncoated twist drill: Review", International Journal of Mechanical & Industrial Engineering, Volume-1 Issue 1, 2011

[80] Petrariu *et al.*, "Study about finite element analysis of high speed drilling", ANNALS of the Oradea University, Fascicle of Management and Technological Engineering, Volume VII (XVII), 2008

[81] Phadke, "Quality engineering using robust design", Prentice-Hall, Englewood Cliffs, NJ

[82] Rakesh *et al.*, "Delamination in fiber reinforced plastics: a finite element approach". Engineering, 2011, 3, 549-554 DOI:10.4236/eng., 2011

[83] Rao and Shunmugam, "Analysis of axial and transverse profiles of holes obtained in B.T.A. machining", International Journal of Machine Tools and Manufacture, Volume 27, Issue 4, 1987, Pp 505-515

[84] SANDVIK catalogue

[85] Saunders and Lauderbaugh, "A finite element model of exit burrs for drilling of metals", Finite Elements in Analysis and Design 40, 2003, Pp 139-158

[86] Saunders, "A finite element model of exit burrs for drilling of metals", Finite Elements in Analysis and Design, Volume 40, Issue 2, December 2003, Pp 139-158, https://DOI.org/10.1016/S0168-874X(02)00194-4 2013

[87] Shaw, "Metal cutting principles", 2nd Edition, Oxford University Press, 2005

[88] Siddiquee *et al.*, "Optimization of deep drilling process parameters of AISI 321 steel using Taguchi method", Procedia Materials Science 6, 2014, Pp 1217-1225

[89] Singh *et al.,* "Finite Element Modeling of Laser-Assisted Machining of AISI D2 Tool Steel", Materials and Manufacturing Processes, 28:4, Pp 443-448, 2013, DOI: 10.1080/10426914.2012.700160

[90] Singh and Kumar, "Tool wear optimization in turning operation by Taguchi method", Indian Journal of engineering and materials sciences, Vol 11, February 2004, Pp 19-24

[91] Singh and Kumar "Optimizing multi-machining characteristics through Taguchi's approach and utility concept", Journal of Manufacturing Technology Management, Vol. 17 Issue: 2, Pp 255-274, https://DOI.org/10.1108/17410380610642304

[92] Singh and Kumar, "Multi-response optimization in dry turning process using Taguchi's approach and utility concept", Procedia Materials Science 5, 2014, Pp 2142-2151

[93] Soliman, "Performance analysis of octal rings as mechanical force transducers", Alexandria Engineering Journal, 2015, 54, Pp 155-162

[94] Sreejith and Manu Raj, "Design and development of a dynamometer for measuring thrust and torque in drilling application", International Journal of Engineering Research-Online Vol.3., Issue.5, 2015

[95] Stephonson and Agapiou, "Metal cutting theory and practice", CRC press, 3rd Edition, Pp 2, 34-35, 233

[96] Su *et al*., "3D Finite element analysis of drilling of ti-6al-4v alloy", International Conference on Computer Information Systems and Industrial Applications, June 2015, https://DOI.org/10.2991/cisia-15.2015.245

[97] Sultan *et al.,* "Effect of machining parameters on tool wear and hole quality of AISI 316L stainless steel in conventional drilling" Procardia Manufacturing 2, 2015, Pp 202-207, 2nd International Materials, Industrial, and Manufacturing Engineering Conference, MIMEC2015, Indonesia

[98] Talib *et al.*, "Wear mechanism of TiN, TiAlN and TiCN coated drills during drilling of carbon steel", Journal of Physical Science, Vol. 18(1), 2007, Pp 75-85

[99] Taegutec Catalogue No: 6121504, English Version: CT 07/2013 (3rd Imp.)

[100] Turgut and Korkut, "High capacity three-component dynamometer design, construction and its calibration", Scientific Research and Essays Vol. 7(30), 2012, Pp 2699-2707

[101] Uddin and Songyi, "On the design and analysis of an octagonal–ellipse ring based cutting force measuring transducer", Measurement 90, 2016, Pp168-177

[102] Venkatraman *et al*., "An analysis and performance testing of a dynamometer for use in drilling and allied processes", International machine tool design research, Vol. 5, 1965, Pp 233-261

[103] Wang *et al.,* "Prediction of milling force based on numerical simulation of oblique cutting", Materials and manufacturing processes, Vol. 27, 2012, Issue -10, 1011-1016, DOI: 10.1080/10426914.2011.654150

[104] Wu *et al.,* "Study on simulation and experiment of drilling for titanium alloys", Materials Science Forum, Vols. 704-705, 2012, Pp 657-663, https://DOI.org/10.4028/www.scientific.net/MSF.704-705.657

[105] Yadava and Patil, "Finite element analysis of temperature distribution in single metallic powder layer during metal laser sintering", International Journal of Machine Tools & Manufacture 47, 2007, Pp 1069-1080

[106] Yadava *et al.,* "Simulation for the prediction of surface roughness in magnetic abrasive flow finishing (MAFF), Journal of Materials Processing Technology 190, 2007, Pp 282-290

[107] Yadava and Judal, "Modeling and simulation of cylindrical electro-chemical magnetic abrasive machining of AISI-420 magnetic steel", Journal of Materials Processing Technology 213, 2013, Pp 2089- 2100

[108] Yaldız *et al.,* "Design, development and testing of a four-component milling dynamometer for the measurement of cutting force and torque", Mechanical Systems and Signal Processing 21, 2007, Pp 1499-1511

Research Publications

- Title:" Design, Development, and Calibration of Octagonal Ring Type Dynamometer with FEA for Measurement of Drilling Thrust and Torque"
  Authors: Sharad V. Gaikwad, M.M. Mahapatra, and Rahul S. Mulik.
  Journal: Journal of Testing and Evaluation, DOI:10.1520/JTE20170791,
  Impact factor: 0.72

- Title: "Design and Development of a Trepanning Tool for Machining of Stainless Steel"
  Authors: Sharad V. Gaikwad and Rahul S. Mulik
  Journal: Journal of the Brazillian Society of Mechanical Sciences and Engineering (Springer), Under review
  Impact Factor: 1.743

- Title: "Performance Analysis of Trepanning Tool for Machining of SS 304"
  Authors: Sharad V. Gaikwad and Rahul S. Mulik
  Under preparation